SELÇUK ÜNİVERSİTESİ

SELÇUK ÜNİVERSİTESİ MÜHENDİSLİK - BİLİM VE TEKNOLOJİ DERGİSİ

SELCUK UNIVERSITY JOURNAL OF ENGINEERING SCIENCE AND TECHNOLOGY (SUJEST)

EISSN 2147-9364

SELCUK UNIVERSITY JOURNAL OF ENGINEERING, SCIENCE AND TECHNOLOGY (SUJEST)
SELÇUK ÜNİVERSİTESİ MÜHENDİSLİK, BİLİM VE TEKNOLOJİ DERGİSİ

HAKEMLİ DERGİDİR

Correspondance Address/ Yazışma Adresi
Selçuk Üniversitesi Muhendislik Fakültesi Dekanlığı
42075-Kampüs, Selçuklu, Konya-TURKEY

Tel : 0 332 241 0 634
Fax : 0 332 241 0 635
E-mail : sujest@selcuk.edu.tr
Web : http://sujest.selcuk.edu.tr

SELÇUK ÜNİVERSİTESİ MÜHENDİSLİK, BİLİM VE TEKNOLOJİ DERGİSİ
Selcuk University Journal of Engineering, Science and Technology
(SUJEST)

ISSN 2147 – 9364 (Elektronik)

Cilt	5	Mart	2017	Sayı	1
Volume	5	March	2017	Number	1

İÇİNDEKİLER (CONTENTS)

Araştırma Makalesi (Research Article)

SELÇUK ÜNİVERSİTESİ MÜHENDİSLİK FAKÜLTESİ

SUJEST, c.5, s.1, 2017
SUJEST, v.5, n.1, 2017
ISSN: 2147-9364 (Electronic)

DIFFERENTIAL DRIVE MOBILE ROBOT TRAJECTORY TRACKING WITH USING PID AND KINEMATIC BASED BACKSTEPPING CONTROLLER

[1]Faik DEMİRBAŞ, [2]Mete KALYONCU

[1,2]Selcuk University, Faculty of Engineering, Department of Mechanical Engineering, 42079 Alaaddin Keykubad Campus, Selcuklu, Konya, TURKEY
[1] demirbasfaik@gmail.com, [2] mkalyoncu@selcuk.edu.tr

(Geliş/Received: 30.11.2016; Kabul/Accepted in Revised Form: 28.12.2016)

ABSTRACT: In this study, the mathematical model of a nonholonomic vehicle was derived. A PID and kinematic based backstepping controller (KBBC) was designed for a differential drive mobile robot to be able to track a desired trajectory. The KBBC was used to overcome the nonlinearity of the trajectory tracking and the PID controllers was used for the DC motors' speeds adjustments. Responses of the vehicle's controller in the square shaped trajectory had obtained and results were graphically presented. The effectiveness of the designed controller has been discussed.

Key Words: *Differential drive, Trajectory tracking, Nonholonomic mobile robot, Kinematic based backstepping control.*

PID ve Kinematik Tabanlı Geri Adımlamalı Kontrolcü Kullanılarak Diferansiyel Sürüşlü Robotun Yörünge Takibi

ÖZ: Bu çalışmada, holonomik olmayan bir aracın matematiksel modeli elde edilmiştir. Diferansiyel sürüşlü mobil robotun arzu edilen yörüngeyi takip edebilmesi için PID ve kinematik tabanlı geri adımlamalı kontrolcü tasarımı yapılmıştır. Geri adımlamalı kontrolcü yörünge takibinin doğrusal olmama durumunun üstesinden gelebilmek, PID kontrolcü ise DC motorların hız ayarlamaları için kullanılmıştır. Kare şekilli bir yörüngeni takibi için aracın kontrolcüsünün cevabı elde edilmiş ve sonuçlar grafiksel olarak sunulmuştur. Tasarlanan kontrolcünün etkinliği tartışılmıştır.

Anahtar Kelimeler: *Diferansiyel sürüş, Yörünge izleme, Holonomik olamayan mobil robot, Kinematik tabanlı geri adımlamalı kontrol.*

INTRODUCTION

Ground mobile robots may be separated into several groups that are wheeled mobile robots, legged mobile robots and tracked mobile robots. In these groups, wheeled mobile robots are mostly used in consequence of low energy consumption, low mechanical complexity and fast motion capability.

Navigaition of wheeled mobile robots and their controls have been studied in recent years much more than the past years due to their applicability to the wide range of challenging situations with developing control techniques. A differential drive mobile robot is a common type that has an application area in the robotic research often. Despite the apparent simplicity of the mathematical model of this robot, the existence of nonholomic constrains make difficult to control this system. Because of Brockett's conditions, a smooth, time-invariant, static state feedback control law cannot be used. To

DOI: 10.15317/Scitech.2017.65

overcome this drawback, most studies use non-smooth and time-variant control laws. On the other side, this drawback can be eliminated by tracking of a predefined trajectory. First, this was carried out by Kanayama (Kanayama et al., 1990) through the using kinematic based backstepping controller. After his study, this controller has been used by other researchers (Fierro and Lewis, 1995; Oubbati, et al., 2005; Hwang, et al., 2013).

Backstepping is a controller design method for many groups of nonlinear dynamical systems. The main idea of this technique is to design globally asymptotically stabilizing controllers from known globally stabilizing controllers for certain subsystems.

MATHEMATICAL MODELLING OF THE DIFFERENTIAL DRIVE MOBILE ROBOT

The dynamics model of the nonholonomic mobile robot was derived by Langrange method. The mathematical model and the controllers of the nonholonomic mobile robot was implemented in the Matlab/Simulink environment. The kinematic based backstepping controller was designed based on Lyapunov Theorem that the stability of the system is proved by. The PID controller was used for each DC motor. A square shaped trajectory was chosen to perform simulation.

Kinematics of the Differential Drive Mobile Robot

At first, two different coordinate systems were designated as the Inertial Coordinate System $[X_\iota \quad Y_\iota]$ and Robot Coordinate System $[X_R \quad Y_R]$. Robot position matrices in the robot coordinate system and inertial coordinate system respectively and orthogonal rotation matrix were defined as below;

$$q^r = \begin{bmatrix} x^r \\ y^r \\ \theta^r \end{bmatrix}, \quad q^\iota = \begin{bmatrix} x^\iota \\ y^\iota \\ \theta^\iota \end{bmatrix}, \quad R(\theta) = \begin{bmatrix} \cos\theta & \sin\theta & 0 \\ -\sin\theta & \cos\theta & 0 \\ 0 & 0 & 1 \end{bmatrix} \tag{1}$$

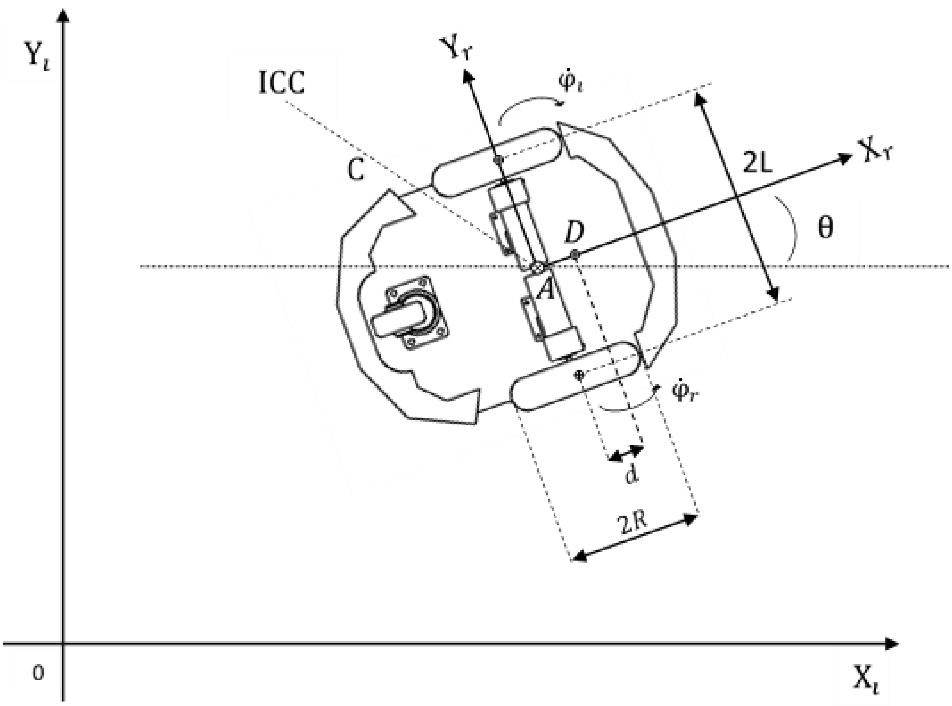

Figure 1. Coordinate systems

In the Figure 1, R is the radius of each wheel, d is the distance between the center of mass (point D) and mid point of the axis center of driving wheels (point A), L is each wheel distance to point A, $\dot{\varphi}_R$ and $\dot{\varphi}_L$ is the right and left wheel angular speed respectively, θ is the degree between the robot frame (front direction) and the inertial frame, C is the distance between point A and instantaneous centre of curvature (ICC).

The orthogonal axis (Y_r) skidding constraint:

$$\dot{y}_a^r = 0 \tag{2}$$

The longitudinal axis (X_r) slipping constraint for the right and left wheel, respectively:

$$v_{pR} = R\dot{\varphi}_R, \qquad v_{pL} = R\dot{\varphi}_L \tag{3}$$

Using the rotation matrix $R(\theta)$ (1), Equations (2) and (3), three constraint Equations can be obtained and these Equations are written in the matrix form below (Solea et al., 2015):

$$A(q) = \begin{bmatrix} -sin\theta & cos\theta & -d & 0 & 0 \\ cos\theta & sin\theta & L & -R & 0 \\ cos\theta & sin\theta & -L & 0 & -R \end{bmatrix} \tag{4}$$

In this Equation (4), A is the constraints matrix and q are generalized coordinates.

Kinematic is the study of the motion without considering the forces. The purpose of the kinematic modelling is to derive robot velocities as a function of the driving wheels' velocities in predefined constraints. Robot's wheels have same angular speed according to the instantaneous curvature centre. So the right wheel and the left wheel velocity relation can be obtained as below (Mac et al., 2016);

$$\omega(C + L) = v_L, \ \ \omega(C - L) = v_R \quad \rightarrow \quad C = L\,(v_R + v_L)/(v_R - v_L) \tag{5}$$

The linear and the angular velocity of the robot as follow, respectively;

$$v = \omega * C = {}^{v_R + v_L}/_{2} = R\ {}^{(\dot{\varphi}_R + \dot{\varphi}_L)}/_{2L}, \ \ \omega = {}^{v_R - v_L}/_{2L} = R\ {}^{(\dot{\varphi}_R - \dot{\varphi}_L)}/_{2L} \tag{6}$$

In order to find velocities and the final position following Equations (7), (8) can be used;

$$v_x = v(t)\cos\big(\theta(t)\big), v_y = v(t)\sin\big(\theta(t)\big) \tag{7}$$

$$x(t) = \int v(t)\cos\big(\theta(t)\big)dt, \ y(t) = \int v(t)\sin\big(\theta(t)\big)dt, \quad \theta(t) = \int \omega(t)\,dt \tag{8}$$

In robot coordinate system and inertial coordinate system, Robot's velocity according to point A for the robot coordinate system and inertial coordinate system respectively:

$$\begin{bmatrix} \dot{x}_a^r \\ \dot{y}_a^r \\ \dot{\theta} \end{bmatrix} = \begin{bmatrix} R/2 & R/2 \\ 0 & 0 \\ R/2L & -R/2L \end{bmatrix} \begin{bmatrix} \dot{\varphi}_R \\ \dot{\varphi}_L \end{bmatrix}, \ \begin{bmatrix} \dot{x}_a^i \\ \dot{y}_a^i \\ \dot{\theta} \end{bmatrix} = \begin{bmatrix} R/2\cos\theta & R/2\cos\theta \\ R/2\sin\theta & R/2\sin\theta \\ R\,/\,2L & -R\,/\,2L \end{bmatrix} \begin{bmatrix} \dot{\varphi}_R \\ \dot{\varphi}_L \end{bmatrix} \tag{9}$$

Dynamics of the Differential Drive Mobile Robot

The nonholonomic mobile robot with n generalized coordinates $q_1, q_2, \dots, q_n$ and subject to m constraints can be described by following Equation (Swadi et al., 2016; Ali et al., 2014; Tawfik et al., 2014; Dhaouadi and Hatab., 2013; Mohareri, 2009; Sidek, 2008):

$$M(q)\ddot{q} + V(q,\dot{q})\dot{q} + F(\dot{q}) + G(q) + \tau_d = B(q)\tau - A^T(q)\lambda \tag{10}$$

In this Equations; $M(q)$ is the symmetric positive definite inertia matrix, $V(q,\dot{q})$ is the centripetal coriolis matrix, $F(\dot{q})$ is the friction matrix, $G(q)$ is the gravitation matrix, τ_d is the unknown disturbance matrix, $B(q)\tau$ is the input matrix, $A^T(q)$ is the kinematic constraints matrix, λ is the Lagrange multipliers matrix.

The equation of the motion can be derived with using the kinetic and potential energies of the given system by Lagrange Method (Dhaouadi and Hatab., 2013; Mohareri, 2009; Sidek, 2008). The Lagrange equation is expressed into the following form:

$$L = T - U \tag{11}$$

$$d/dt\,(\partial L/(\partial \dot{q}_i)) - \partial L/\partial q_i = F - A^T(q)\lambda \tag{12}$$

In the Lagrangian function expressions; T is the kinetic energy, U is the potential energy, F are generalized forces, A is the constraints matrix and q are generalized coordinates. For the differentially drive mobile robot, generalized coordinates can be defined as $q = [x_a,\ y_a,\ \theta,\ \varphi_R,\ \varphi_L]^T$. Using kinematic Equations (9), transformation matrix can be redefined according to the point D (Solea et al., 2015);

$$\eta = \begin{bmatrix}\dot{\varphi}_R \\ \dot{\varphi}_L\end{bmatrix},\ S_d(q)\eta = S(q)\eta = \begin{bmatrix}\dot{x}_d \\ \dot{y}_d \\ \dot{\theta} \\ \dot{\varphi}_R \\ \dot{\varphi}_L\end{bmatrix} = \begin{bmatrix} R(L\cos\theta - d\sin\theta)/_{2L} & R\,(L\cos\theta + d\sin\theta)/_{2L} \\ R(L\sin\theta + d\cos\theta)/_{2L} & R\,(L\sin\theta - d\cos\theta)/_{2L} \\ R/_{2L} & R/_{2L} \\ 1 & 0 \\ 0 & 1 \end{bmatrix}\begin{bmatrix}\dot{\varphi}_R \\ \dot{\varphi}_L\end{bmatrix} \tag{13}$$

Robot's kinetic energy expressions can be defined as following Equations:

$$m = m_d + 2m_w\ ,\ I = I_d + m_d d^2 + 2m_w L^2 + 2I_m \tag{14}$$

$$T = \tfrac{1}{2}m(\dot{x}_a^2 + \dot{y}_a^2) + m_d d\dot{\theta}(\dot{y}_a\cos\theta - \dot{x}_a\sin\theta) + \tfrac{1}{2}I_w(\dot{\varphi}_R^2 + \dot{\varphi}_L^2) + \tfrac{1}{2}I\dot{\theta}^2 \tag{15}$$

In these Equations (14), (15); m_d is the mass without driving wheels and actuators, m_w is the mass of each driving wheel, I_d is the moment of the inertia of the robot without driving wheels and actuators, I_w is the moment of the inertia of each driving wheel and actuators, I_m is the moment of the inertia of each driving wheel and actuators about wheel axis. Using Lagrange method with the energy expression above (15), following matrices of equations can be obtained for this study:

$$M(q)\ddot{q} + V(q,\dot{q})\dot{q} = B(q)\tau - A^T(q)\lambda \tag{16}$$

$$M(q) = \begin{bmatrix} m & 0 & -m_a d \cos\theta & 0 & 0 \\ 0 & m & m_a d \sin\theta & 0 & 0 \\ -m_a d \sin\theta & m_a d \cos\theta & I & 0 & 0 \\ 0 & 0 & 0 & I_w & 0 \\ 0 & 0 & 0 & 0 & I_w \end{bmatrix} \tag{17}$$

$$V(q, \dot{q}) = \begin{bmatrix} 0 & 0 & -m_a d\dot{\theta} \cos\theta & 0 & 0 \\ 0 & 0 & -m_a d\dot{\theta} \sin\theta & 0 & 0 \\ 0 & 0 & 0 & 0 & 0 \\ 0 & 0 & 0 & 0 & 0 \\ 0 & 0 & 0 & 0 & 0 \end{bmatrix}, \tag{18}$$

$$B(q) = \begin{bmatrix} 0 & 0 \\ 0 & 0 \\ 0 & 0 \\ 1 & 0 \\ 0 & 1 \end{bmatrix}, \tag{19}$$

$$A^T(q)\lambda = \begin{bmatrix} -\sin\theta & \cos\theta & \cos\theta \\ \cos\theta & \sin\theta & \sin\theta \\ -d & L & -L \\ 0 & -R & 0 \\ 0 & 0 & -R \end{bmatrix} \begin{bmatrix} \lambda_1 \\ \lambda_2 \\ \lambda_3 \\ \lambda_4 \\ \lambda_5 \end{bmatrix} \tag{20}$$

Next, the system is transformed into the alternative form to eliminate Lagrange multipliers. The first derivative of the transformation matrix Equation (13) with respect to time is;

$$\dot{q} = S(q)\eta, \;\; \ddot{q} = \dot{S}(q)\eta + S(q)\dot{\eta} \tag{21}$$

The transformation matrix (13) is the null space of the constraints matrix (4) and this expression can be written as below;

$$S^T(q)A^T(q) = 0 \tag{22}$$

By replacing these Equations (20), (21) with equivalent terms in dynamic Equations of the robot, the new dynamic equation can be derived that can be used in simulations;

$$M(q)\left[\dot{S}(q)\eta + S(q)\dot{\eta}\right] + V(q, \dot{q})[S(q)\eta] = B(q)\tau - A^T(q)\lambda \tag{23}$$

$$S^T(q)M(q)S(q)\dot{\eta} + S^T(q)\left[M(q)\dot{S}(q) + V(q, \dot{q})S(q)\right]\eta = S^T(q)B(q)\tau - S^T(q)A^T(q)\lambda \tag{24}$$

The dynamic equations reduced to the form as below:

$$\bar{M}(q)\dot{\eta} + \bar{V}(q, \dot{q})\eta = \bar{B}(q)\tau \tag{25}$$

Actuator Modelling

Permanent magnet DC motors were used to drive the mobile robot. DC motors can be controlled with voltage, so the following equations are used for simulations (Solea et al., 2015)

$$v(t) = R_a i(t) + L_a d(i(t))/dt + e_a \tag{26}$$

$$e_a = K_b \omega(t) \tag{27}$$

$$\tau_m = K_t i(t) \tag{28}$$

$$\tau = N\tau_m \tag{29}$$

In these Equations (26), (27), (28), (29), $v(t)$ is the input voltage, R_a is the resistance of the armature, L_a is the inductance of the armature, $\omega(t)$ is the angular speed of the motor, $i(t)$ is the current input electromotive voltage, e_a is the counter electromotive voltage, K_b is the back electromotive force constants , K_t is the torque constant , N is the transmission ratio, τ is the output torque, τ_m is the motor torque.

CONTROLLER DESIGN

In the proposed control system, two postures will be used: the reference posture $q_r = [x_r \quad y_r \quad \theta_r]^T$ and the current posture $q = [\mathrm{x} \quad \mathrm{y} \quad \theta]^T$.

An error posture e_p will be defined as follows (Kanayama et al., 1990; Mohareri, 2009; Yuan, 2001):

$$e_p = \begin{bmatrix} e_x \\ e_y \\ e_\theta \end{bmatrix} = \begin{bmatrix} cos\theta & sin\theta & 0 \\ -sin\theta & cos\theta & 0 \\ 0 & 0 & 1 \end{bmatrix} \begin{bmatrix} x_r - x \\ y_r - y \\ \theta_r - \theta \end{bmatrix} \tag{30}$$

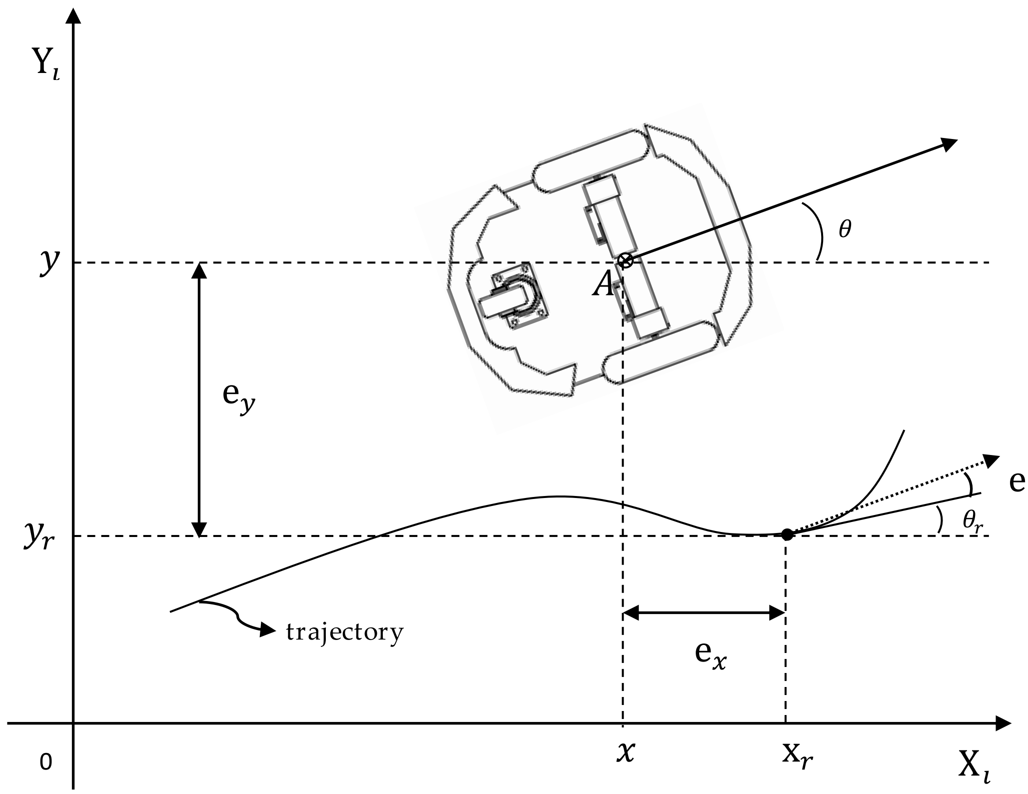

Figure 2. Trajectory tracking errors

The control problem will be to determine a control rule for the nonholonomic mobile robot, which can estimate the velocities (v linear velocity, ω angular velocity) that make the system asymptotically stable. The proposed kinematic based control rule is (Kanayama et al., 1990):

$$\begin{bmatrix} v \\ w \end{bmatrix} = \begin{bmatrix} v_r cose_\theta + K_x e_x \\ \omega_r + K_y v_r e_y + K_\theta v_r sine_\theta \end{bmatrix} \tag{31}$$

where K_x, K_y and K_θ are positive constants. These constants are gains of the kinematic based backstepping controller. Lyapunov stability method will be used to prove the stability of the control rule in the next section.

Lyapunov stability analysis

The Lyapunov stability analysis of the control rule in equation is described as follows (Kanayama et al., 1990; España Cabrera, 2014; Hwang, et al., 2013; Mohareri, 2009):

Lemma 1:

From Equation (30):

$$\begin{bmatrix} \dot{e}_x \\ \dot{e}_y \\ \dot{e}_\theta \end{bmatrix} = \dot{e}_p = f(t, e_p) = \begin{bmatrix} \omega e_y - v + v_r cos e_\theta \\ -\omega e_x + v_r sine_\theta \\ \omega_r - \omega \end{bmatrix} \tag{32}$$

This result can be proved by using Equation (10) and Equation (30):

$$\begin{bmatrix} e_x \\ e_y \\ e_\theta \end{bmatrix} = \begin{bmatrix} cos\theta & sin\theta & 0 \\ -sin\theta & cos\theta & 0 \\ 0 & 0 & 1 \end{bmatrix} \begin{bmatrix} x_r - x \\ y_r - y \\ \theta_r - \theta \end{bmatrix} = \begin{bmatrix} (x_r - x)\cos\theta + (y_r - y)\sin\theta \\ -(x_r - x)\sin\theta + (y_r - y)\cos\theta \\ \theta_r - \theta \end{bmatrix} \tag{33}$$

$$\begin{aligned} \dot{e}_x &= (\dot{x}_r - \dot{x})cos\theta + (\dot{y}_r - \dot{y})sin\theta - (x_r - x)\dot{\theta}sin\theta + (y_r - y)\dot{\theta}cos\theta \\ &= e_y\omega - v + \dot{x}_r \cos(\theta_r - \theta) + \dot{y}_r \sin(\theta_r - \theta) = e_y\omega - v + v_r cose_\theta \end{aligned} \tag{34}$$

$$\begin{aligned} \dot{e}_y &= -(\dot{x}_r - \dot{x})sin\theta + (\dot{y}_r - \dot{y})cos\theta - (x_r - x)\dot{\theta}cos\theta - (y_r - y)\dot{\theta}sin\theta \\ &= -e_x\omega - \dot{x}_r \sin(\theta_r - \theta) + \dot{y}_r \cos(\theta_r - \theta) = -e_x\omega + v_r sine_\theta \end{aligned} \tag{35}$$

$$\dot{e}_\theta = \dot{\theta}_r - \dot{\theta} = \omega_r - \omega \tag{36}$$

Substituting v and ω by $v(e_p, q_r)$ and $\omega(e_p, q_r)$ Lemma 1 was obtained.

Lemma 2:

$$\begin{bmatrix} \dot{e}_x \\ \dot{e}_y \\ \dot{e}_\theta \end{bmatrix} = \dot{e}_p = f(t, e_p) = \begin{bmatrix} (\omega_r - v_r(K_y e_y + K_\theta \sin e_\theta))e_y + K_x e_x \\ -(\omega_r - v_r(K_y e_y + K_\theta \sin e_\theta))e_x + v_r \sin e_\theta \\ -v_r(K_y e_y + K_\theta \sin e_\theta) \end{bmatrix} \tag{37}$$

Proposition 1:

By using the in Equation (31), it can be said that when the reference velocity $v_r > 0$, $e_p = 0$ is a stable equilibrium.

When a scalar function V is proposed as a Lyapunov function candidate for the system:

$$V = \frac{1}{2}\left(e_x{}^2 + e_y{}^2\right) + {(1 - \cos e_\theta)}/{K_y} \tag{38}$$

Clearly, $V \geq 0. e_p = 0 \Rightarrow V = 0$ and $if\ e_p \neq 0 \Longrightarrow V > 0$, thus the Equation (38) above is a positive definite function. By Lemma 2:

$$\begin{aligned}\dot{V} = \dot{e}_x e_x + \dot{e}_y e_y + \frac{\dot{e}_\theta \sin(e_\theta)}{K_y} \\ = \left[\left(\omega_r + v_r\left(K_y e_y + K_\theta sin(e_\theta)\right)\right) e_y - K_x e_x\right] e_x \\ + \left[-\left(\omega_r + v_r\left(K_y e_y + K_\theta sin(e_\theta)\right)\right) e_x + v_r \sin(e_\theta)\right] e_y \\ + \frac{[-v_r\left(K_y e_y + K_\theta sin(e_\theta)\right)]\sin(e_\theta)}{K_y} = -K_x {e_x}^2 - \frac{v_r K_\theta sin^2 e_\theta}{K_y} \leq 0\end{aligned} \quad (39)$$

Consequently the Lyapunov function V's derivative is a negative definite function. That means uniformly asymptotically stability around $e_p = 0$ under the conditions that are v_r, ω_r, K_x, K_y, K_θ are bounded and v_r, ω_r are continuous. The above Lyapunov stability analysis and controller are used in reference (Kanayama et al., 1990).

SYSTEM SIMULATION

In Figure 3, general description of systems and controllers were shown below:

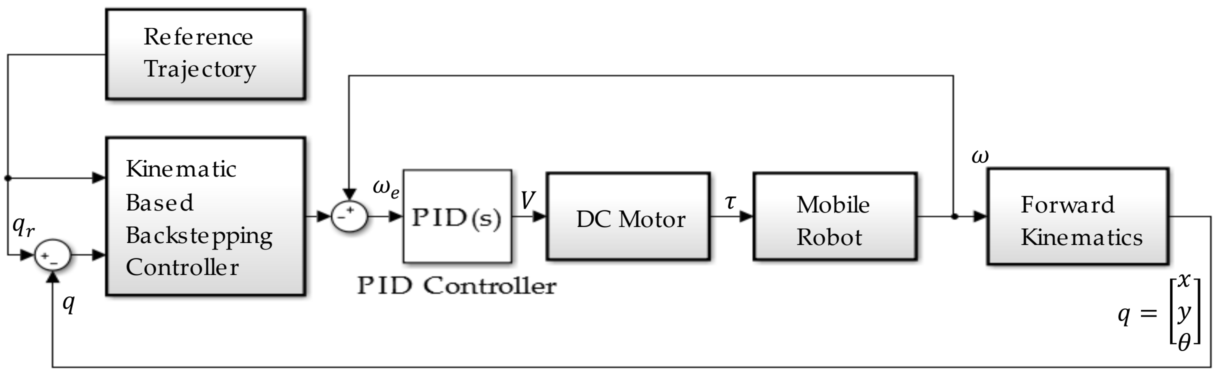

Figure 3. Control block diagram

The PID controller that is shown in the Figure 4 is used to control volt inputs for the DC motors. The simulation block diagram that is based on the general diagram was shown below:

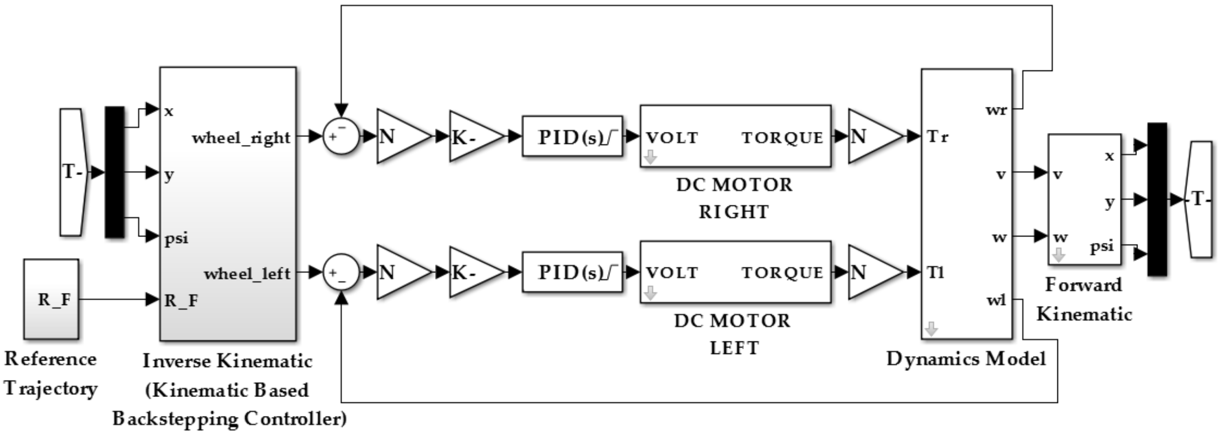

Figure 4. Simulation block diagram

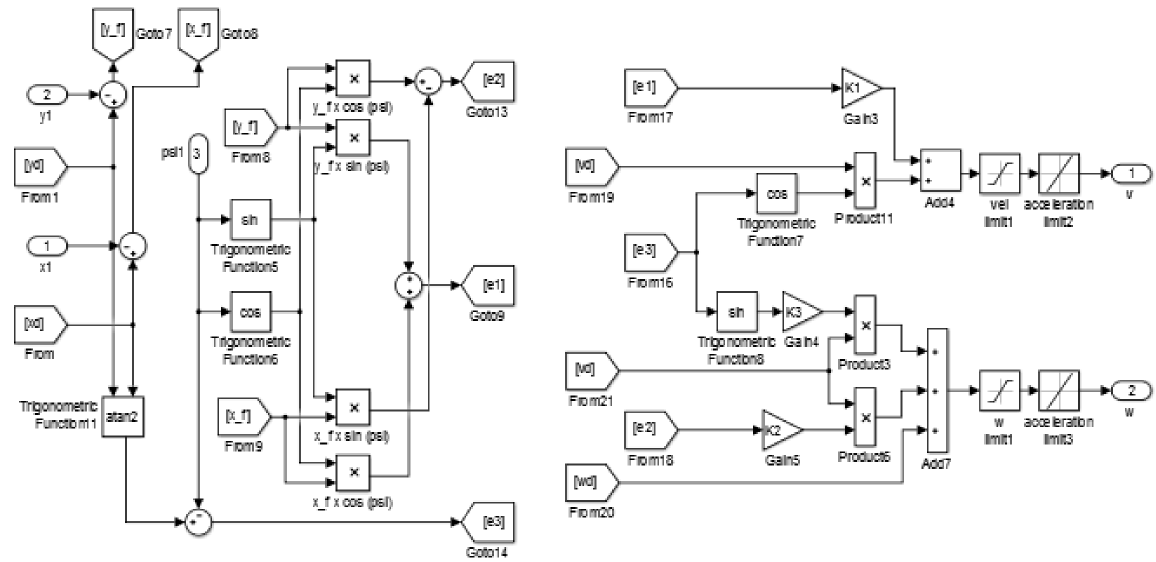

Figure 5. KBBC block diagram

Table 1. Parameters For Robot and DC-Motors

Robot			DC-Motor		
Term	**Unit**	**Value**	**Term**	**Unit**	**Value**
m_d	kg	27	$v(t)$	V	12
m_w	kg	0.5	$i(t)$	A	2.85
I_d	$kg * m^2$	0.732	R_a	Ω	1.01
I_w	$kg * m^2$	0.0025	L_a	$H = V * s/A$	$0.088 * 10^{-3}$
I_m	$kg * m^2$	0.0012	K_b	$V * s$	$12{,}939 * 10^{-3}$
d	m	0.05	K_t	$N * m/A$	$12{,}939 * 10^{-3}$
R	m	0.0975	τ	$N * m$	0.1537
L	m	0.164	$i(t)$	A	11.8
N	-	53	$\omega(t)$	rpm	6640

Numerical values of imposed constraints are;

the linear velocity $v_{max} = \pm 1.2\, m/s$, the angular velocity $\omega_{max} = \pm 1.65\, rad/s$, the linear acceleration $a_{max} = \pm 1.2\, m/s$ and *the* angular acceleration $\alpha_{max} = \pm 1.5\, m/s$.

In the following simulations; initial values for linear and angular velocities are selected as 0. The simulation time t = 65 seconds, the angular speed for the trajectory w = 0.1 rad/s, the scale factor k = 1.5 meter. The square trajectory general equation defined as below for (x, y, θ) is (0, 0, 0);

$$k * abs(sin(w * t)).* sin(w * t) + k * abs(cos(w * t)).* cos(w * t) \tag{40}$$

RESULT AND DISCUSSION

Trajectory following results for $K_x = 0.3685, K_y = 49, K_\theta = 0.3685$ without the PID controller and with the PID controller are considered below. The PID controller parameters are tuned as $K_p = 10, K_i = 1, K_d = 1$. For graphically presented initial pose [x, y, θ] for the first condition is [0, 0, 0], for the second condition is [0, 0, pi/2], for the third condition is [0, 0, pi/2].

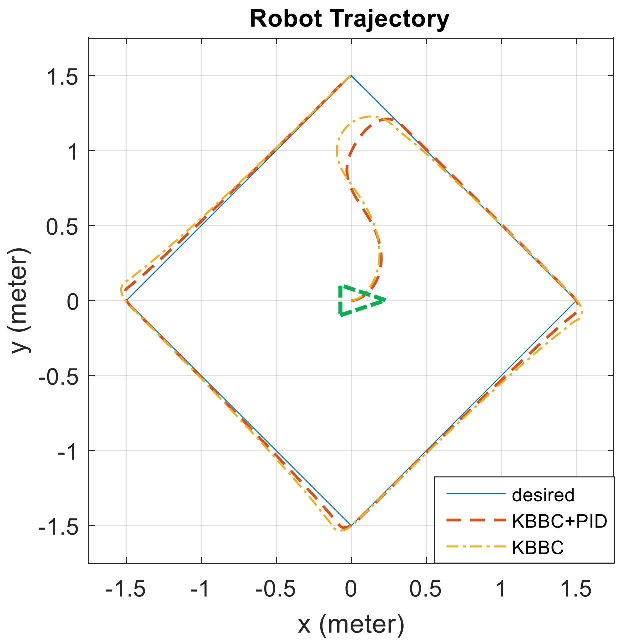

Figure 6. Controllers with starting position [0, 0, 0].

In the Figure 6, the results show that after applying the PID controller to the kinematic based backstepping controller; settling time decrease. Also, decereasing of error were observed at small rate.

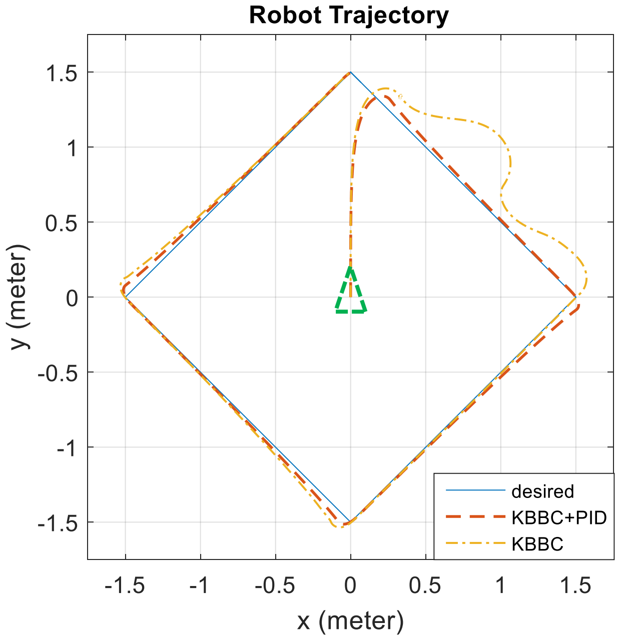

Figure 7. Controllers with starting position [0, 0, pi/2].

In the Figure 7, the results show that after applying the PID controller to the kinematic based backstepping controller; the settling time and overshot decrease significantly. Also, decreasing of the error were observed at the small rate.

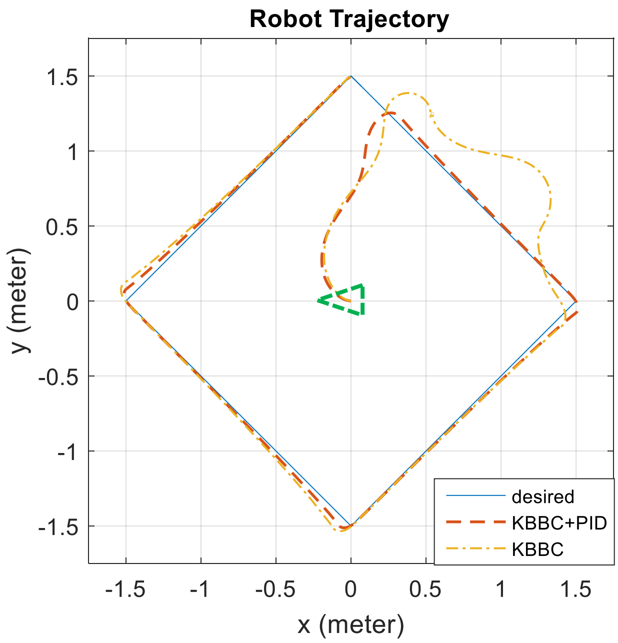

Figure 8. Controllers with starting position [0, 0, pi].

In the Figure 8, the results show that after applying the PID controller to the kinematic based backstepping controller; the settling time and overshot decrease significantly. Also, decreasing of the error were observed at the small rate.

For detailed examination, the KBBC Controller's chosen parameters are $K_x = 0.3685, K_y = 49, K_\theta = 0.3685$ without the PID controller and with the PID controller. Controller parameters are tuned as $K_p = 10, K_i = 1, K_d = 1$ for PID controller. Initial pose is [0, 1.5, -pi/4].

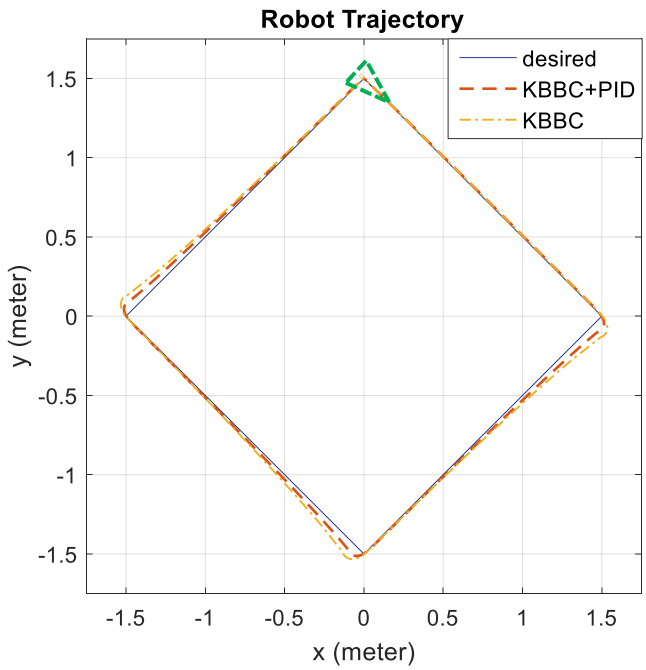

Figure 9. Conrtrollers with starting position [0, 1.5, -pi/4].

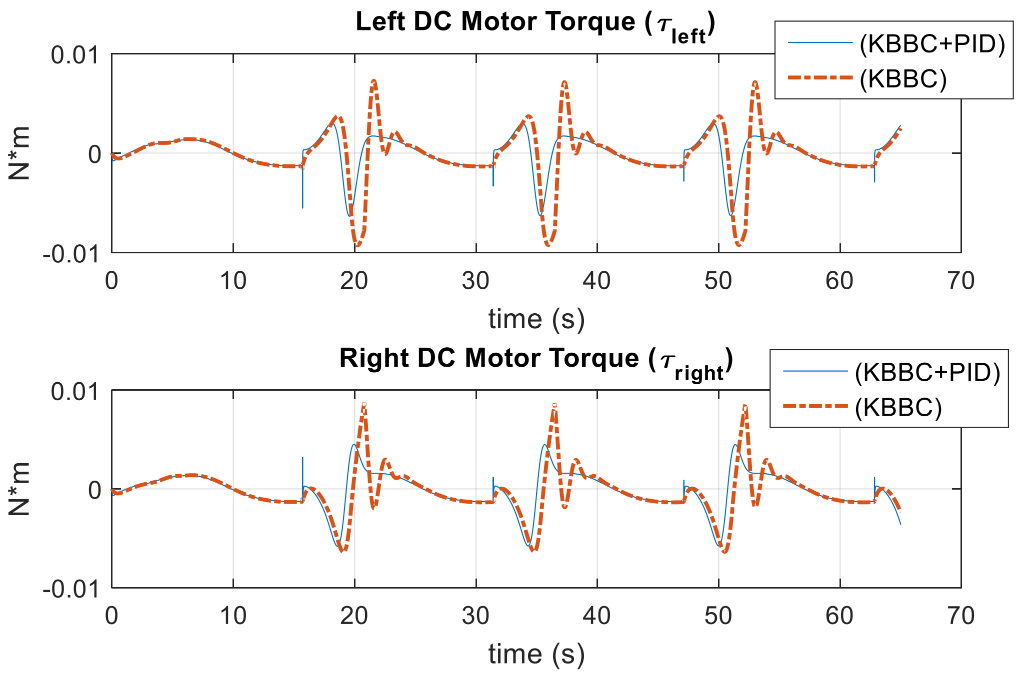

Figure 10. Torque outputs

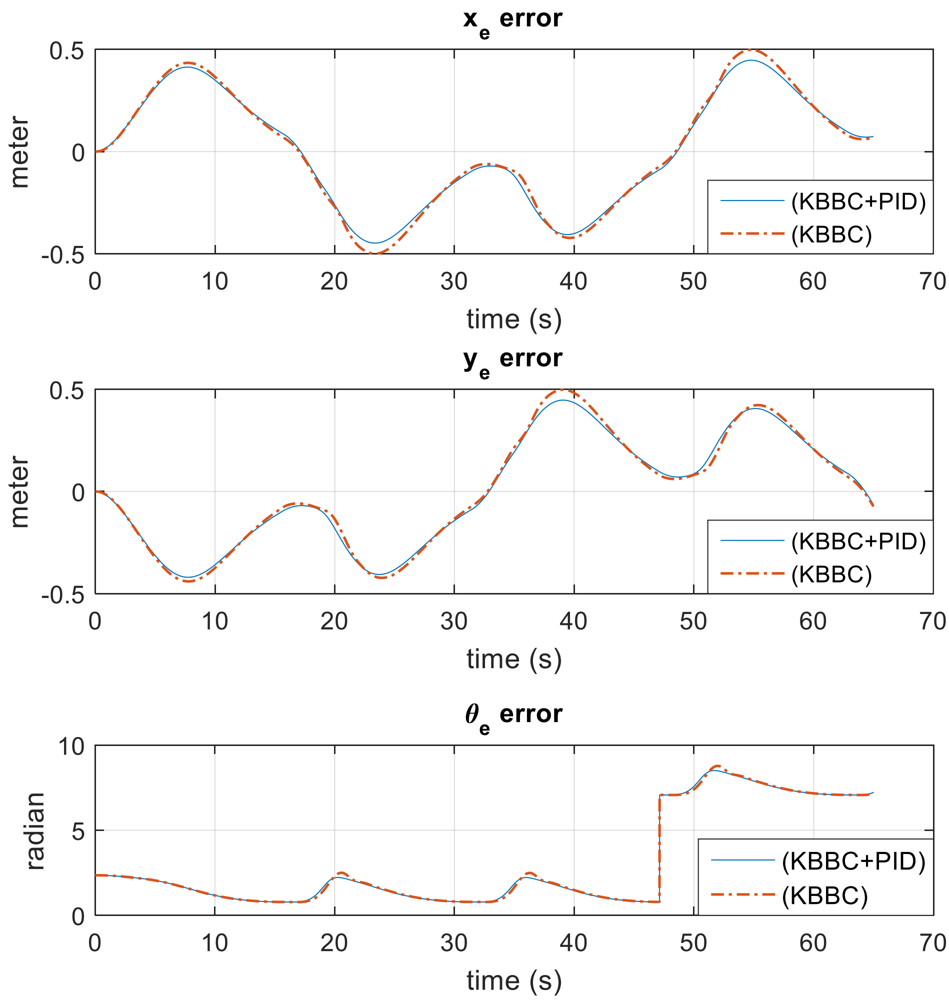

Figure 11. x_y_theta Errors

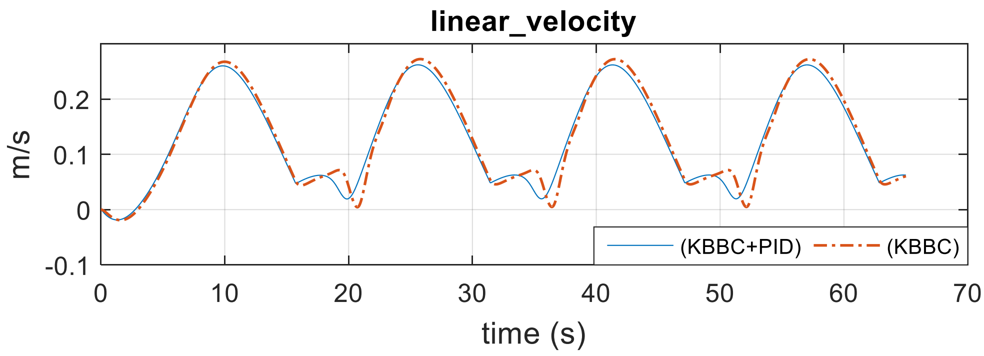

Figure 12. Linear velocities

In the Figure 9, for the comparison between the KBBC+PID and KBBC minimum errors were chosen. In the Figure 11, differences between controllers' errors were at the small rate. In the Figure 10, for the KBBC, it can be said that it needs more torque than the KBBC+PID. At the 15.71, 31.42 , 47.13, 62.84 seconds for both DC motors instantaneous change at the torque rate for the KBBC+PID. As estimated, in the Figure 12, a sudden change in the linear velocity can be seen at the same times for the KBBC+PID.

CONCLUSION

In this present study, a differential drive mobile robot dynamic equations were derived by Lagrange method. The stable control method, capable of dealing with the tracking square trajectory of the differential drive mobile robot, had been derived using the kinematic based backstepping controller and had been combined with the PID controller for the DC motors. The square shaped trajectory was selected. Simulations were performed by with the proposed control law using Matlab/Simulink. The validity of the proposed controller was proved by Lyapunon function. The proposed controller (KBBC+PID) showed a good tracking performance and stability for the different initial positon. Obtained results showed that the proposed controller can be developed effectively by the tuning parameters.

ACKNOWLEDGE

This article was derived and supported from Faik DEMİRBAŞ's master thesis "Trajectory Tracking Control of an Obstacle Avoiding Mobile Robot".

REFERENCES

Ali, R. S., Aldair, A. A., Almousawi, A. K., 2014, ''Design an Optimal PID Controller using Artificial Bee Colony and Genetic Algorithm for Autonomous Mobile Robot'', *International Journal of Computer Applications (0975 – 8887),* Vol. 100 (1), pp. 8-16.

Dhaouadi, R., Hatab, A. A., 2013, "Dynamic Modelling of Differential-Drive Mobile Robots using Lagrange and Newton-Euler Methodologies: A Unified Framework", *Research Article, Advances in Robotics & AutomationTechnology*, Vol. 2 (2), pp. 1-7.

España Cabrera, A., 2014, *Rapid Prototyping of Mobile Robot Control Algorithms*, Degree of Master of Science in Faculty of Electrical Engineering, Department of Control Engineering, Czech Technical University In Prague.

Fierro, R., Lewis, F. L., "Control of A Nonholonomic Mobile Robot: Backstepping Kinematics Into Dynamics," *in Proceedings of 34th IEEE Conference on Decision and Control,* New Orleans, Louisiana, USA, pp. 3805-3810, 13-15 December 1995.

Hwang, E. J., Kang, H. S., Hyun C. H., Park, M., 2013, ''Robust Backstepping Control Based on a Lyapunov Redesign for Skid-Steered Wheeled Mobile Robots'', *International Journal of Advanced Robotic Systems,* Vol.10, 26.

Kanayama, Y., Kimura, Y., Miyazaki, F., Noguchi, T., "A Stable Tracking Control Method for An Autonomous Mobile Robot," *in Proc. IEEE International Conference on Robotics and Automation*, Cincinnati, Ohio, pp. 384–389, 13-18 May 1990.

Mac, T. T., Copot, C., De Keyser, R., Tran T. D., Vu, T., 2016, ''MIMO Fuzzy Control for Autonomous Mobile Robot'', *Journal of Automation and Control Engineering,* Vol. 4 (1), pp. 65-70.

Mohareri, O., 2009, *Mobile Robot Trajectory Tracking Using Neural Networks*, Degree of Master of Science in Mechatronics Engineering, American University of Sharjah, United Arab Emirates.

Oubbati, M., Schanz, M., Levi, P., "Kinematic and Dynamic Adaptive Control of A Nonholonomic Mobile Robot Using A RNN", *in Proceedings of IEEE International Symposium on Computational Intelligence in Robotics and Automation (CIRA '05),* Espoo, Finland, pp. 27–33, 27-30 Jun 2005.

Sidek, S. N., 2008, *Dynamic Modeling and Control of Nonholonomic Wheeled Mobile Robot Subjected to Wheel Slip*, Degree of Doctor OF Philosophy in Faculty of the Graduate School, Department of Electrical Engineering, Vanderbilt University.

Solea, R., Filipescu, A., Filipescu Jr., A., Minca, E., Filipescu, S., ''Wheelchair Control and Navigation Based on Kinematic Model and Iris Movement Robots'', *2015 IEEE 7th International Conference on Cybernetics and Intelligent Systems (CIS) and IEEE Conference on Robotics, Automation and Mechatronics (RAM),* Angkor Wat, Cambodia, pp. 78-83,15-17 July 2015.

Swadi, S. M., Tawfik, M. A., Abdulwahab E. N., Kadhim, H. A., ''Fuzzy-Backstepping Controller Based on Optimization Method for Trajectory Tracking of Wheeled Mobile Robot'', *2016 UKSim-AMSS 18th International Conference on Computer Modelling and Simulation*, Cambridge, United Kingdom, pp. 147-152, 6-8 April 2016.

Tawfik, M. A., Abdulwahb E. N., Swadi, S. M., 2014, ''Trajectory Tracking Control for a Wheeled Mobile Robot Using Fractional Order PID Controller'', *Al-Khwarizmi Engineering Journal,* Vol. 10 (3), pp. 39- 52.

Yuan, G., 2001, *Tracking Control of A Mobile Robot Using Neural Dynamics Based Approaches,* Degree of Master of Science in School of Engineering, University of Guelph, Canada.

SUJEST, c.5, s.1, 2017
SUJEST, v.5, n.1, 2017
ISSN: 2147-9364 (Electronic)

COMPARISON OF ASTER AND SRTM DIGITAL ELEVATION MODELS AT ONE-ARC-SECOND RESOLUTION OVER TURKEY

[1]İbrahim Öztuğ BİLDİRİCİ, [2]Ramazan Alpay ABBAK

[1,2]Selcuk University, Department of Geomatics Engineering, Campus, Selcuklu, Konya, TURKEY

[1] bildirici@selcuk.edu.tr, [2]aabbak@selcuk.edu.tr

(Geliş/Received: 08.08.2016; Kabul/Accepted in Revised Form: 11.11.2016)

ABSTRACT: In February 2000, the "Shuttle Radar Topography Mission (SRTM)" satellite captured elevation data by scanning the Earth landmasses between the 60° North and South latitudes. After the mission of 11 days, the collected data were processed, and a Digital Elevation Model (DEM) within one arc-second resolution for United States and three arc-second resolutions for the other parts of the globe was created and published on the NASA servers. Recently, a global SRTM DEM with one-arc-second resolution has been released. Additionally, ASTER (Advanced Spaceborne Thermal Emission and Reflection Radiometer) is a sensor boarded on the Terra satellite in 1999. The sensor has been collecting satellite imagery since 2000. The ASTER GDEM at one-second resolution was released to the public, which is the most complete DEM of the earth ever made. In this study, SRTM and ASTER DEMs with one arc-second resolution over Turkish territory was evaluated by means of a local DEM produced from 1:25K national topographic maps. Results show that the accuracy of the SRTM DEM is better than the ASTER GDEM with respect to the local DEM.

Key Words: *ASTER GDEM, Evaluation, Digital elevation model, SRTM, 1:25K topographic maps.*

1 Saniye Çözünürlüklü ASTER ve SRTM Sayısal Yükseklik Modellerinin Türkiye'de Karşılaştırması

ÖZ: 2000 yılında SRTM (Shuttle Radar Topography Mission) uydusu yeryüzünü 60° kuzey ve güney enlemleri arasını tarayarak yükseklik bilgisi elde etmiştir. 11 günlük görevinden sonra toplanan veriler işlenmiş ve ABD için 1 saniye diğer ülkeler için 3 saniye çözünürlükte olmak üzere bir Sayısal Yükseklik Bilgisi üretilmiş ve NASA sunucularında yayınlanmıştır. Son zamanlarda 1 saniye çözünürlüklü global SRTM SYM yayınlanmaya başlamıştır. Ayrıca, ASTER (Advanced Spaceborne Thermal Emission and Reflection Radiometer) Terra uydusuna 1999 yılında montelenmiş bir algılayıcıdır. Bu algılayıcı 2000 yılından beri uydu görüntüsü toplamaktadır. 1 saniye çözünürlüklü ASTER SYM dünyanın en geniş kapsamlı SYM'si olup kullanıma açılmıştır. Bu çalışmada 1 saniye çözünürlüklü ASTER ve SRTM SYM'ler Türkiye'de 1:25 000 ölçekli topografik haritalarda türetilen yerel SYM ile değerlendirilmiştir. Sonuçlar, SRTM SYM'nin ASTER SYM'ye göre daha iyi olduğunu göstermektedir.

Anahtar Kelimeler: *ASTER SYM, Değerlendirme, Sayısal yükseklik modeli, 1:25000 ölçekli topografik harita.*

INTRODUCTION

Digital Elevation Model (DEM) is a computer representation of physical surface of the Earth. DEM is utilized by a wide range of geospatial applications such as gravity interpolation in geodesy, risk assessments in Geographic Information Systems, run-off simulations in Hydrology, morphologic analyses in Geology etc.

DOI: 10.15317/Scitech.2017.66

Like other models, DEMs are subject to errors (e.g. systematic or random). Thus, end users of DEMs should be aware of the accuracy of the DEM in a project area. Hence DEM should be evaluated by means of the ground truth data such as local DEM or leveling points.

Recently, SRTM (Shuttle Radar Topography Mission) and ASTER (Advanced Space-borne Thermal Emission and Reflection Radiometer) DEMs at one arc-second resolution are released to the public on the Internet. Accuracies of these DEMs are subject to investigation for end users over the world (Jing *et al*, 2014; Hirt *et al* 2010; Rexer and Hirt 2014). Moreover, Bildirici et al (2016) compares ASTER DEM and an enhanced version of SRTM3 (3 arc-second resolution) in the same study area. In this study, accuracies of the both DEMs within one-arc resolution (SRTM1) were assessed with help of local DEM obtained from 1:25K scaled topographic maps of Turkish territory. It is concluded that SRTM DEM is superior to ASTER DEM over Turkey from the point of the accuracy of height data.

The present paper starts with brief review of SRTM and ASTER missions. Then comparison methodology is discussed shortly. Subsequently, numerical applications for the comparison of both DEMs are performed in Turkey. Finally concluding remarks were outlined for further studies.

MATERIALS AND METHOD

Study area

Our study area lies on Turkish territory which covers 780 000 square km. The study area is delimitated by 36°—42° northern latitudes and by 26°—45° western longitudes. Maximum and minimum heights in the area are 5197 m at the summit of Agri (Ancient ararat) mountain and 0 m at the sea side, respectively. The average height is approximately 1000 m for the area. This area was selected for our study because it is one of the most complicated regions over the world from the point of the view of topographic variation. Figure 1 and 2 show the topography of the study area together with test data.

SRTM DEM

The SRTM project was jointly realized by NASA, the National Imagery and Mapping Agency (NIMA), the German Space Agency (DLR) and Italian Space Agency (ASI). The mission collected three-dimensional image of the Earth's land surface by exploiting the radar interferometry, which matches two radar images in order to derive the elevation information. Then, the images were transformed to a global DEM, which is spanning from 60°N to 56°S over the world.

The SRTM DEM does not include any bathymetric data which means that water bodies (i.e. ocean and sea) are attributed with "0" m. The vertical accuracy of the DEM is globally estimated to be 16 m at the 90% confidence level. The detailed documentation and technical specification of the SRTM DEM can be found at NASA servers (SRTM, 2016a).

SRTM Data Products is distributed freely to the public via Internet data portals such as Earth Explorer (USGS, 2016), and NASA Jet Propulsion Laboratory (JPL) Data Distribution Center (http://dds.cr.usgs.-gov/srtm/version2_1). The level of processing and the resolution of the data will vary. Currently following data products are available at Earth Explorer (SRTM, 2016b):

- SRTM Non-Void Filled elevation data were processed from raw C-band radar signals spaced at intervals of 1 arc-second at NASA's Jet Propulsion Laboratory (JPL). This version was then enhanced by the National Geospatial-Intelligence Agency (NGA). Data for regions outside the United States were sampled at 3 arc-seconds (approximately 90 meters) using a cubic convolution resampling technique for public distribution.
- SRTM Void Filled elevation data are the result of additional processing to address areas of missing data or voids in the SRTM Non-Void Filled collection. The voids occur in areas where the initial processing did not satisfy quality specifications. Since SRTM data are one of the most

widely used elevation data sources, the NGA filled the voids by using interpolation techniques. The resolution for SRTM Void Filled data is the same as the SRTM Non-Void Filled Data.

- SRTM 1 Arc-Second Global elevation data is the worldwide coverage of void filled data at a resolution of 1 arc-second (30 meters), and presented to the public. Some tiles may still contain voids. It should be noted that tiles above 50° north and below 50° south latitude are sampled at a resolution of 2 arc-second by 1 arc-second.

Due to the worldwide coverage and high resolution, SRTM 1 dataset is used in current study data.

SRTM data with a regularly spaced grid of elevation points can be downloaded from Earth Explorer in three file formats:

- Digital Terrain Elevation Data (DTED) is a standard mapping format designed by the NGA. Each file or cell contains a matrix of vertical elevation values spaced at regular horizontal intervals measured in geographic coordinates
- Band interleaved by line (BIL) is a binary raster format with an accompanying header file which describes the layout and formatting of the file.
- Georeferenced Tagged Image File Format (GeoTIFF) is a TIFF file with embedded geographic information.

SRTM data specifications are given in Table 1 in comparison to ASTER GDEM.

Table 1. Specifications of SRTM and ASTER DEMs

Features	**SRTM**	**ASTER**
Projection	Geographic	Geographic
Horizontal Datum	WGS84	WGS84
Vertical Datum	EGM96	EGM96
Vertical Units	Meters	Meters
Spatial Resolution	1 arc-second for globe 3 arc-seconds for globe	1 arc-second
Data Size	1 degree tiles	1 degree tiles
File Format	HGT, DTED, BIL, GeoTIFF	GeoTIFF

ASTER GDEM

ASTER, which is an observing sensor, was placed on the satellite "Terra" in December 1999. This sensor is an achievement of an international joint project between NASA and Japanese Ministry of Economy, Trade and Industry (METI).

The DEM was generated from a stereo image pair acquired with nadir and backward angles over the same area, and then it was released in 2009. This strategy provided a global DEM with enhanced accuracy due to multiple images. As a result of the project, ASTER GDEM covers all land area ranging from 83°N to 83°S even in steep mountainous areas.

ASTER GDEM is available in geo-tiff format by 1°×1° tiles at 1 arc-second resolution. Vertical and horizontal datum of the DEM are EGM96 and WGS84, respectively. Zero for water surfaces (i.e. sea and ocean) and −9999 for voids are assigned in the data files. Vertical accuracy of the DEM is estimated to be 7–14 m over the United States. The detailed documentation and technical specification of ASTER GDEM can be found at Japanese Space System server (ASTER 2016).

ASTER data specifications are given in Table 1 in comparison to SRTM.

Local Height Data

For local heights digitized contour lines of 25K topographic maps are used. In order to create a local DEM, General Command of Mapping (GCM) in Turkey vectorized the contour lines of 25K maps. The data was distributed in CAD (Computer Aided Design) files, each sheet being an individual file. The authors obtained a collection of these files within a previous project (Bildirici et al 2009), and utilized this data set in this study. Today, GCM distributes DTED (Digital Terrain Elevation Data) files in one arc-second resolution, which is generated from the digitized contour lines mentioned above. Accuracy of the DEM is estimated to be ~2 m in the vertical direction by Ozturk and Kocak (2007). The DEM from GCM is not free of charge.

The point density on contour lines is very high due to automatic vectorization. A point thinning process is necessary to use this data set properly. The coordinate system of the DEM is UTM on European Datum 1950, and its vertical datum is mean sea level at Antalya tide gauge. In order to perform a comparison, point density on contour lines is to be reduced, and horizontal and vertical datum conversions are performed.

Comparison Methodology

For the statistical evaluation local DEM is assumed ground truths. Before the height comparison, two preprocessing steps are performed. After point thinning mentioned in the previous section local height data is undergone to horizontal datum transformation. Thereafter local points are transformed to WGS84 ellipsoid with geographical coordinates. Each point is in local height data is interpolated with IDW method by using global DEMs. Doing so, for each point, local height, height from SRTM, and height from ASTER are prepared.

In geodetic literature, two types of height data are not comparable directly due to systematic errors (e.g. datum shifts). Thus a corrector surface is used to remove systematic errors between data before detailed discussion. Corrector surfaces which area from a simple linear model to more sophisticated similarity transformation model can be found in literature (Kotsakis and Sideris, 1999; Abbak, 2014).
Such a comparison is based on a traditional method as follows,

$$H_{LOCAL} - H_{GLOBAL} = Ax - \varepsilon \tag{1}$$

where **A** is a design matrix, **x** is a vector of unknown parameters, ε is the random noise term. The parametric model is assumed to absorb all systematic errors.
In this study, four parameters model was used because it gives more reasonable results. Four parameters model,

$$a = \begin{bmatrix} \cos f \cos l \\ \cos f \sin l \\ \sin f \\ 1 \end{bmatrix} \tag{2}$$

where φ and λ are geographical coordinates of a check point. The vector a is extended for each checkpoint, then the design matrix **A** is obtained. Subsequently, unknown parameters are solved by Least Squares (LS) approach. Finally, the Root Mean Square Errors (RMSE) is calculated that are supposed to be the accuracy of global DEM. However, the RMSE value still contains errors of the local DEM.

For all steps in comparison in-house programs developed in C programming language are used.

APPLICATION

In this section, validation of ASTER and SRTM DEMs were performed by means of the local DEM. For this purpose, local DEM that covers 37 of 25K map sheets were selected to represent various topographic features throughout the country. After thinning process mentioned above, the total number of points for all sheets are about 3 770 421, being 101 903 points for each sheet in average.

The evaluation steps are as follows:

- ASTER GDEM tiles were downloaded in Geo-TIFF format. By using GDAL programming package (http://www.gdal.org), data files are converted into binary grid files, in which heights are recorded as 2 bytes integer sequentially.
- SRTM 1 tiles were downloaded from Earth Explorer in binary grid files (BIL format).
- The points on digitized contour lines are thinned with 30 m distance criterion. Thereafter projection and datum conversion were undertaken.
- For each point within ground truth data neighboring 4 points in grid file (ASTER or SRTM) are found. By using IDW (Inverse Distance Weighting) interpolation method the height of the point is determined (Gruver, 2016). For each 25K file, a file with geographical coordinates, local heights and interpolated heights are formed. By using this file a vertical datum conversion is performed and heights are compared. For this step another program was developed in C language programming language.
- Finally Global DEMs were matched against to Local DEM in terms of accuracy. In order to avoid systematic errors (e.g. datum shifts), two types of heights (Local DEM and ASTER/SRTM DEMs) were compared with four parameters corrector surface model.

Table 2 shows results that are obtained from four parameters corrector surface model. According to the table, SRTM is better than ASTER, but in some rough topography, ASTER is superior to SRTM in regarding to the accuracy of height data. In the table the RMS values where ASTER is better than SRTM is indicated with bold text. In seven of 37 sheets ASTER is better. The distribution of the test sheets over Turkey is depicted in Figure 1 and 2.

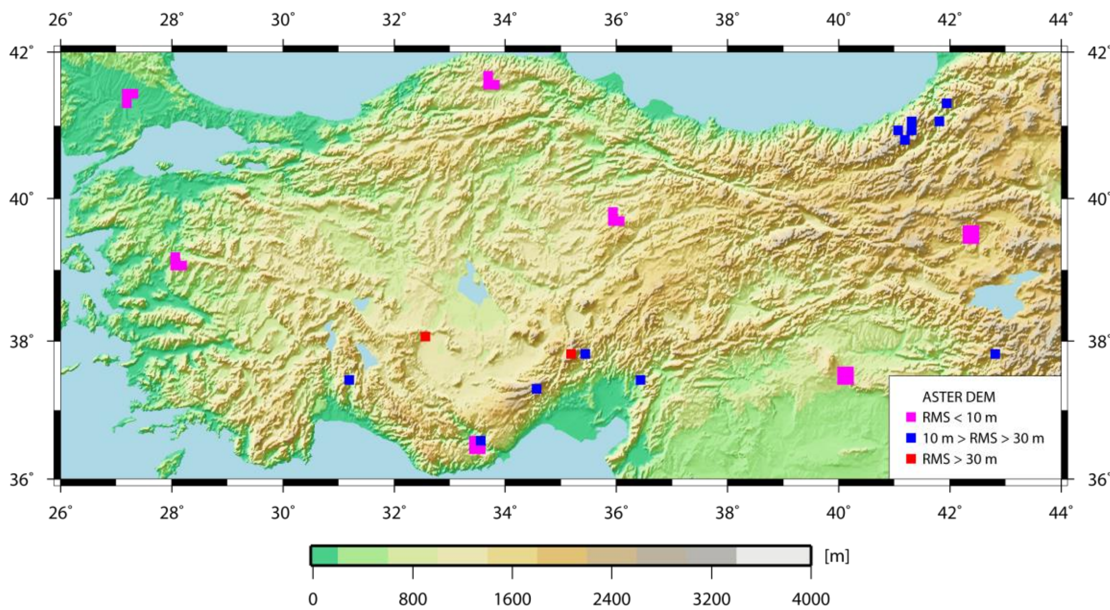

Figure 1. ASTER GDEM validation over Turkey

In order to identify what extent affects four parameters corrector surface model on the accuracy, we directly compared the SRTM and local DEMs. It was concluded that improvements in accuracy change from 2 cm to 6 m, in average of 1 m. Hence corrector surface models gave us more optimistic results.

In Figure 1 and 2 the distribution of the test data over Turkey and obtained results are visualized over Turkish territory.

Table 2. Validation of SRTM and ASTER DEMs with help of the local DEM (unit: meter)

Sheet	**ASTER**				**SRTM**			
	Min	Max	Mean	RMS	Min	Max	Mean	RMS
e31c4	-36.02	53.97	-0.01	8.14	-31.17	35.95	0.00	5.60
e31d2	-36.97	45.65	-0.02	7.81	-30.83	30.30	-0.01	5.62
e31d3	-38.28	60.03	-0.01	7.51	-24.03	25.47	0.02	4.72
f18a2	-23.26	20.89	0.03	4.00	-12.93	16.10	0.00	2.75
f18a3	-25.58	19.76	-0.00	3.72	-12.48	12.57	0.00	2.46
f18b1	-19.28	26.89	-0.00	3.80	-17.11	15.92	0.00	2.82
f46c4	-148.85	109.28	0.02	**15.97**	-181.15	164.41	0.01	23.87
f47b3	-146.73	137.06	-0.01	**15.35**	-186.88	137.79	0.00	16.52
f47c4	-215.63	217.23	0.01	**18.71**	-192.31	161.87	0.00	19.02
g46a1	-198.62	103.82	-0.00	**17.26**	-211.88	109.76	0.01	17.45
g46a3	-215.48	124.22	-0.00	18.84	-108.75	135.27	0.02	12.42
g46b1	-168.99	109.54	-0.01	23.47	-117.31	89.36	-0.02	17.67
i35b3	-41.33	38.81	-0.00	7.58	-33.13	26.45	0.02	5.53
i35c2	-43.85	54.24	0.00	8.28	-29.71	28.81	-0.01	5.91
i36d1	-43.07	74.40	-0.00	9.03	-23.43	32.81	0.02	6.25
i48c3	-42.27	34.74	-0.00	6.82	-39.80	31.51	0.00	5.09
i48c4	-29.95	43.86	-0.00	6.62	-23.62	21.32	0.00	4.69
j20d1	-42.42	55.70	0.02	8.00	-35.55	32.39	0.00	7.00
j20d3	-42.41	78.33	-0.00	6.71	-27.66	33.99	0.00	5.80
j20d4	-78.92	121.50	0.01	9.32	-50.87	68.57	0.00	7.02
j48b1	-35.67	41.28	-0.01	7.08	-26.86	28.83	0.00	5.46
j48b2	-33.21	43.94	-0.00	6.35	-26.32	24.74	0.00	4.92
l29d4	-135.24	228.32	0.01	41.62	-129.73	207.90	0.03	40.90
m34a3	-496.22	409.43	-0.02	**64.91**	-511.40	410.66	0.00	**77.94**
m34b3	-204.69	217.68	-0.01	**23.36**	-190.41	317.72	-0.06	31.30
m44d3	-58.35	27.14	0.01	4.70	-21.14	21.75	0.00	3.99
m44d4	-16.10	20.14	-0.01	3.59	-13.59	14.52	0.00	2.84
m49b4	-175.29	226.22	0.02	17.66	-181.50	404.43	-0.01	15.53
n26a2	-230.14	211.00	-0.00	15.64	-185.47	225.89	-0.03	12.53
n33a4	-225.38	180.66	-0.00	**27.78**	-239.78	215.03	0.01	31.10
n36b2	-257.09	175.50	-0.00	19.87	-233.74	146.93	0.00	19.30
n44a1	-93.93	29.56	-0.00	5.64	-96.04	19.61	-0.01	4.61
n44a2	-35.10	62.95	0.00	7.77	-23.57	27.96	0.00	5.48
o30c3	-53.39	46.89	-0.01	9.27	-56.68	34.39	0.00	6.72
o31d4	-61.84	69.27	-0.00	10.83	-50.87	63.87	-0.01	8.20
p30b2	-57.39	64.37	-0.00	10.93	-48.22	53.53	-0.01	7.05
p31a1	-53.37	62.14	-0.01	8.29	-53.69	40.17	0.00	6.57

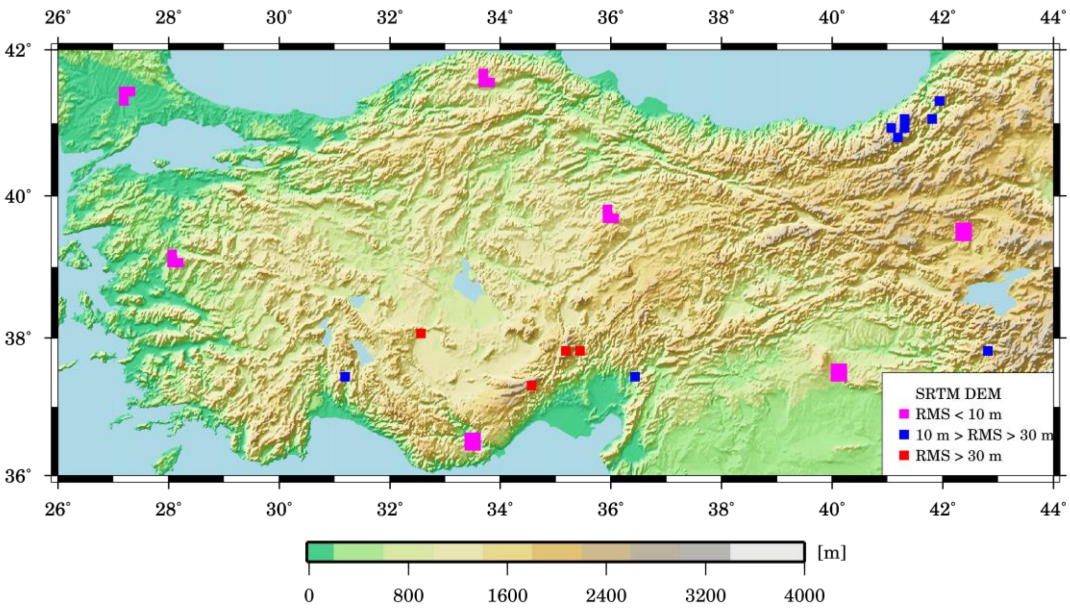

Figure 2. SRTM1 validation over Turkey

Among the 37 test sheets M34A3 is the one with highest RMS values after ASTER and SRTM validation. For this reason the topography of this region and differences between local and ASTER, and local and SRTM are depicted in Figures 3 to 5.

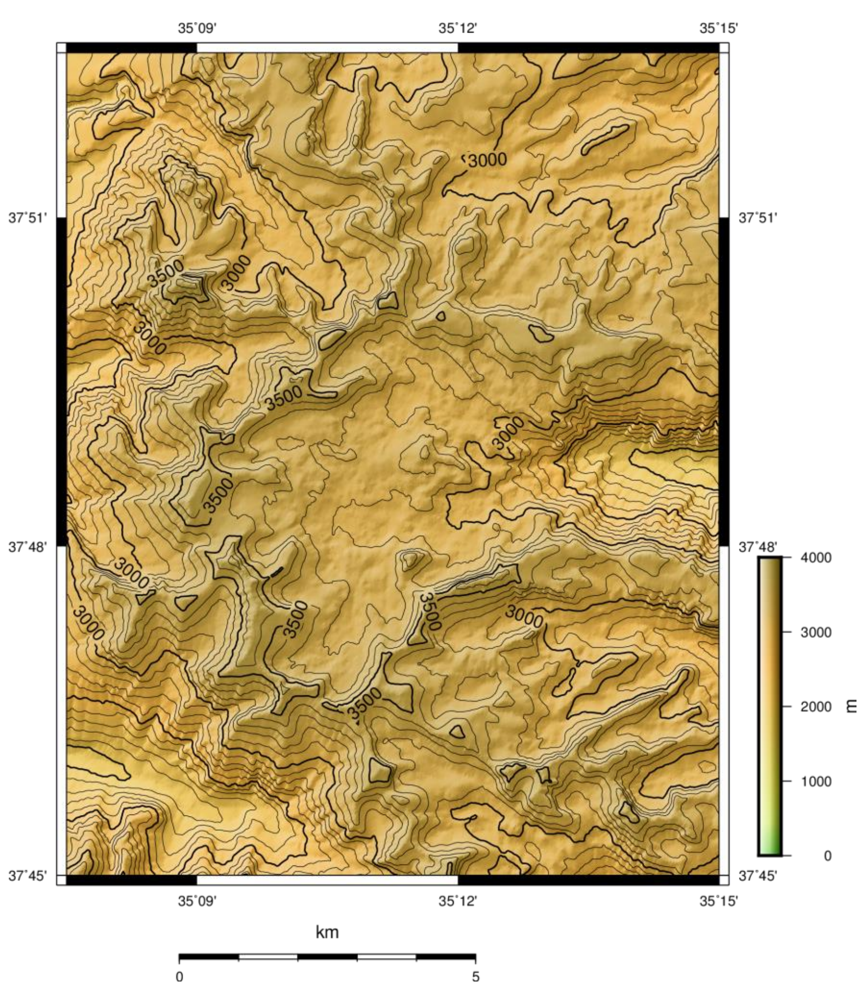

Figure 3. Topography of the M34A3 based on local data

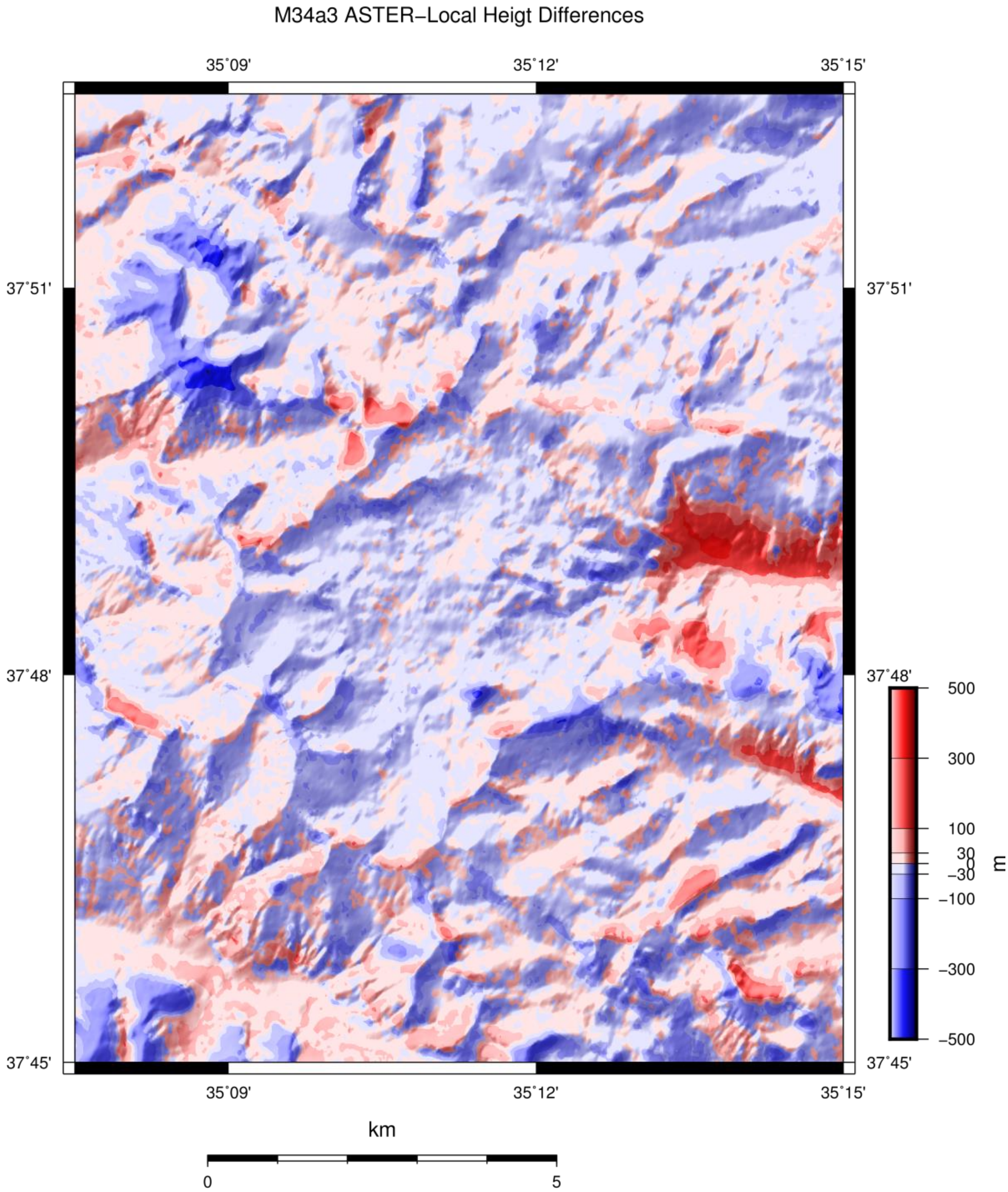

Figure 4. Differences between Local and ASTER GDEM heights

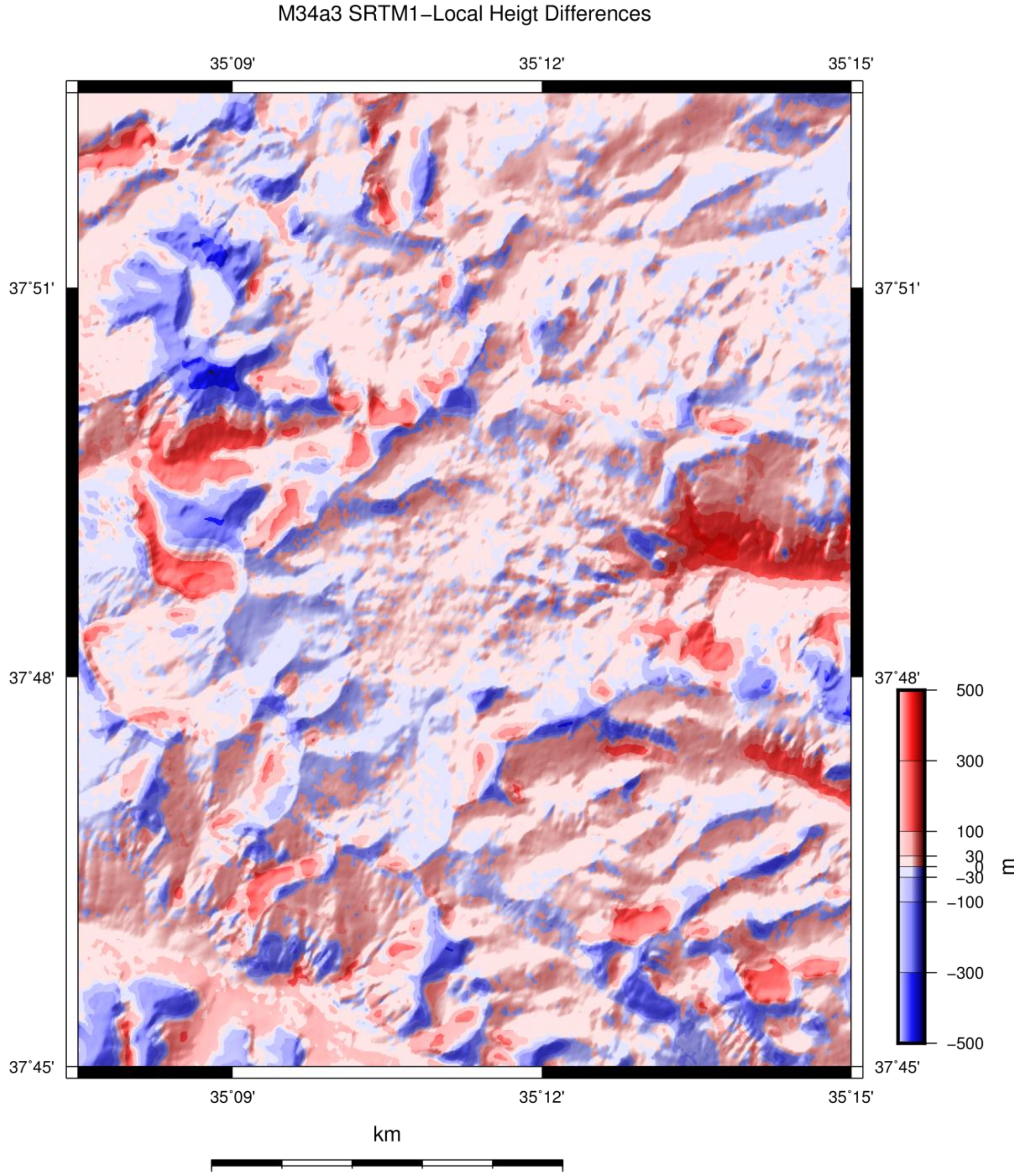

Figure 5. Differences between Local and SRTM heights

CONCLUSIONS

In this study, SRTM and ASTER DEMs at one arc second resolution were compared in terms of a local DEM which is produced from 1:25K topographic map sheets over the Turkish territory. For this purpose, 37 map sheets, which are covers different characteristic topography, were selected.

According to our numerical results, ASTER GDEM is better than SRTM DEM in some rough areas (in 7 map sheets) whereas SRTM gives more reasonable results in other parts of test area. Considering overall statistics, SRTM DEM is superior to ASTER GDEM from the point of view of accuracy. In a very rough topography (m34b3 map sheet), maximum RMSs for ASTER and SRTM DEMs are about 65 m and 78 m, respectively. At the end, we can say that the both DEMs are beneficial for geospatial applications such as GIS, cartography, remote sensing etc., if the accuracies that are found in this study are acceptable.

REFERENCES

Abbak, R. A., 2014, "Effect of ASTER DEM on The Prediction of Mean Gravity Anomalies: A Case Study Over The Auvergne Test Region", *Acta Geodaetica et Geophysica*, Vol. 49(4), pp. 491-502.

ASTER, 2016, The Advanced Spaceborne Thermal Emission and Reflection Radiometer. http://gdem.ersdac.jspacesystems.or.jp accessed: August 2016.

Bildirici, I. O., Abbak, A. R., Ulugtekin, N., 2016, "ASTER GDEM AND SRTM DEM in Turkish Territory: An Evaluation in Terms of Height Accuracy and 3D Visualization", *Proceedings of 6th International Conference on Cartography and GIS,* Albena, Bulgaria, ISSN: 1314-0604, Eds: Bandrova T., Konecny M., pp. 266-272, 13-17 June 2016.

Bildirici, I.O., Ustun, A., Selvi, H.Z., Abbak, R. A., Bugdayci I., 2009, "Assessment of SRTM Based on Topographic Maps in the Territory of Turkey", *Cartography and Geographic Information Science*, Vol. 36 (1), pp. 95-104.

Gruver, A., 2016, Cartography and Visualization, online course pages, https://www.e-education.psu.edu/geog486/node/1877, accessed: August 2016.

Hirt, C., Filmer, M. S., Featherstone, W. E., 2010, "Comparison and Validation of The Recent Freely Available ASTER-GDEM Ver1, SRTM Ver4.1 And GEODATA DEM-9S Ver3 Digital Elevation Models Over Australia", *Australian Journal of Earth Sciences*, Vol. 57(3), pp. 337-347.

Jing, C., Shortridge, A., Lin, S., Wu, J., 2014, "Comparison And Validation of SRTM and ASTER GDEM for A Subtropical Landscape in Southeastern China", *International Journal of Digital Earth*, Vol. 7(12), pp. 969-992.

Kotsakis C, Sideris M. G., 1999, "On The Adjustment of Combined GPS/Levelling/Geoid Networks". *Journal of Geodesy*, Vol. 73(8), pp. 412– 421.

Ozturk, E., Kocak, E., 2007, "Farklı Kaynaklardan Değişik Yöntem ve Ölçeklerde Üretilen Sayısal Yükseklik Modellerinin Doğruluk Araştırması (Accuracy Assessment of Digital Elevation Models Produced in Different Scales Form Different Sources by Using Various Techniques)". *Harita Dergisi*, Vol. 137, pp. 25– 41.

Rexer, M., Hirt, C., 2014, "Comparison of Free High Resolution Digital Elevation Data Sets (ASTER GDEM2, SRTM V2.1/V4.1) and Validation Against Accurate Heights from The Australian National Gravity Database", *Australian Journal of Earth Sciences*, Vol. 61(2), pp. 213-226.

SRTM (2016a), Shuttle Radar Topography Mission, http://www2.jpl.nasa.gov/srtm accessed: August 2016.

SRTM (2016b), Shuttle Radar Topography Mission, USGS Long Term Archive, https://lta.cr.usgs.gov/SRTM accessed: August 2016.

USGS (2016) Earth Explorer, http://earthexplorer.usgs.gov, accessed: August 2016.

SUJEST, c.5, s.1, 2017
SUJEST, v.5, n.1, 2017
ISSN: 2147-9364 (Electronic)

RECOVERY OF FORMIC ACID BY REACTIVE EXTRACTION USING AN ENVIRONMENTALLY-FRIENDLY SOLVENT

[1]Mustafa Esen MARTI

[1] *Selçuk Üniversitesi, Mühendislik Fakültesi, Kimya Mühendisliği Bölümü, KONYA*
marti@selcuk.edu.tr

(Geliş/Received:29.12.2016 ; Kabul/Accepted in Revised Form: 30.01.2017)

ABSTRACT: Today many carboxylic acids are recovered from biological production media and industrial wastewaters. Reactive extraction is favored over other separation methods due to its high recovery efficiency, ease of operation, low energy demand and reduced cost. However, use of toxic organic diluents in the organic phases is the main disadvantage of the method. In this study, the appropriateness of an environmentally-friendly solvent, sunflower oil (SFO) to be used as organic phase diluent during the recovery of formic acid (FA) from aqueous solutions by reactive extraction was evaluated. Alamine-336 was used as the extractant and the results obtained with SFO were compared with those obtained using octanol. The separation process reached an equilibrium in 3 hours and the recovery efficiency increased with the increase in extractant percentages. The initial FA concentration positively influenced the recovery when SFO was used as the diluent. In the ranges of the parameters studied, the highest recovery values were 98.6% and 82.6% with octanol and SFO, respectively. This study shows that low molecular weight carboxylic acids, e.g. FA can be recovered from aqueous solutions by reactive extraction using environmentally-friendly solvents such as SFO.

Key Words: *Formic acid, Reactive extraction, Sunflower oil, Alamine-336, Equilibrium*

Formik Asidin Çevre Dostu Bir Çözücü Kullanılarak Tepkimeli Özütleme Yöntemi ile Geri Kazanımı

ÖZ: Günümüzde pek çok karboksilik asit biyolojik üretim ortamlarından ve endüstriyel atık sulardan geri kazanılmaktadır. Tepkimeli özütleme, yüksek geri kazanım verimi, işlem basitliği, düşük enerji gereksinimi ve maliyeti nedeniyle diğer ayırma yöntemlerine tercih edilmiştir. Fakat organik fazlarda zehirli organik seyrelticilerin kullanımı yöntemin en önemli dezavantajıdır. Bu çalışmada çevre dostu bir çözücünün, ayçiçek yağının formik asidin sulu çözeltilerinden tepkimeli özütleme yöntemi ile geri kazanımı sırasında organik faz seyrelticisi olarak zehirli organik kimyasallar yerine kullanımı değerlendirilmiştir. Özütleyici olarak Alamine-336 kullanılmış ve ayçiçek yağı ile elde edilen sonuçlar oktanol ile elde edilen sonuçlarla karşılaştırılmıştır. Ayırma süreci 3 saatte dengeye ulaşmış ve geri kazanım verimi özütleyici yüzdesi ile birlikte artmıştır. Ayçiçek yağı seyreltici olarak kullanıldığında başlangıç asit derişimi geri kazanımı pozitif yönde etkilemiştir. Çalışılan değişken aralıklarında oktanol ve ayçiçek yağı ile en yüksek geri kazanım verimleri sırasıyla %98,6 ve %82,6'dır. Bu çalışma formik asit gibi düşük molekül ağırlıklı karboksilik asitlerin tepkimeli özütleme ile ayçiçek yağı gibi çevre dostu çözücüler kullanılarak sulu çözeltilerden geri kazanılabileceğini göstermiştir.

Anahtar Kelimeler: *Formik asit, Tepkimeli özütleme, Ayçiçek yağı, Alamine-336, Denge*

DOI: 10.15317/Scitech.2017.67

INTRODUCTION

Today, many biochemicals are produced by biological techniques instead of chemical synthesis methods (Straathof, 2014). Likewise, carboxylic acids can be produced as a target- or by-product by fermentation or they can also be found in industrial wastewaters (Yang et al., 2007; Rasrendra et al., 2011; Martı and Gürkan, 2015). However, the recovery of carboxylic acids from dilute aqueous solutions with high efficiency is still a challenging separation problem (Wasewar et al., 2004; Lopez-Garzon and Straathof, 2014; Uslu et al., 2015; Datta et al., 2016). Moreover, most of the industrial separation operations are carried out using toxic chemicals (Harington and Hossain, 2008; Keshav et al., 2009) and the cost of these processes are generally ≥40% of the total cost (Chen and Juang, 2008; Straathof, 2014). Therefore, several researchers from all over the world have been studying the recovery of carboxylic acids from production media and wastewaters, or aqueous solutions having similar characteristics (concentration, pH and etc.) to the former materials to identify promising isolation methods or procedures (Kertes and King, 1986; Wasewar et al., 2004; Uslu et al., 2015).

Despite these studies, carboxylic acids, e.g. formic acid, are still recovered by traditional methods that produce dangerous and toxic waste materials in industry. Due to the energy and environmental problems caused by this waste, the technique should be replaced by efficient, novel and environmentally-friendly alternatives. Several separation techniques such as solvent extraction, distillation, membrane filtration, electrodialysis, ion exchange and adsorption have been tested for the purpose (Martı 2010). Reactive extraction, which is the advanced form of traditional solvent extraction method, has been favored over other techniques due to its high efficiency, ease of operation, low energy demand and cost (Kertes and King, 1986; Martı et al., 2011). Another advantage of the technique is thermal stability of the target molecule during the process (Martı and Gürkan, 2015). Different from its origin, reactive extraction can recover carboxylic acids by chemical extraction besides physical extraction. This is achieved by the extractants that are dissolved in the organic phase diluent or solvent and have the ability to react with the target material. With the help of this, the recovery efficiencies notably increase and the separations carried out in multiple steps can be achieved in a single stage (Martı, 2016).

Long chain aliphatic amines and organophosphoric compounds are known to the most efficient extractants for the recovery of carboxylic acids from aqueous solutions. In particular, tertiary amines and their mixtures have been successfully used for the recovery of several types of carboxylic acids (Tamada et al., 1990; Martı et al., 2011; Lopez-Garzon and Straathof, 2014; Uslu et al., 2015). The tertiary amines form acid-amine complexes with the undissociated form of the target acid in the organic phase during the reactive extraction process. Another advantage of the use of tertiary amines is their ease of regeneration and re-uses in the consecutive recovery operations (Gorden et al., 2016; Reyhanitash et al. 2016).

In general, water-immiscible organic solvents that can dissolve the extractants are used as the diluents during the organic phase preparations. For an industrial application, the organic phase should have operational properties such as viscosity and concentration that are mostly influenced by the diluent. The diluent also promotes the reaction between the acid and amine during the transfer. Thus, it directly influences the stability and solubility of the complex structures that also affect the recovery efficiency. Mostly alcohols, alkanes and ketones are used as the organic phase diluents in the reactive extraction of carboxylic acids (King and Kertes, 1986; Tamada et al., 1990; Martı, 2010; Uslu et al., 2015; Datta et al., 2016).

However, high toxicity and the cost of the solvents (diluent) used during the preparation of the organic phase are the most important disadvantages of the reactive extraction technique. Solving this problem will make the process be environmentally-friendly and economic. Attempts to eliminate this problem have been cited in the literature (Harington and Hossain 2008; Keshav et al. 2009; Wasewar et al., 2011; Waghmare et al., 2011; Keshav et al., 2012; Waghmare et al., 2013; Uslu et al., 2014).

Harington and Hossain (2008) selectively recovered lactic acid with an initial concentration of 0.2-0.3 M from biological production media by reactive extraction. The authors used tributylphosphate (TBP) and sunflower oil (SFO) as the diluents, and trioctylamine (TOA) and Aliquat 336 (trioctylmethylammoniumchloride, TOMAC) as the extractants. The researchers investigated the effects of aqueous phase pH, organic phase constituents and temperature on the recovery. Highest extraction efficiency was achieved with the organic phase containing 15% TOA + 15% Aliquat 336 + 35% TBP + 35% SFO. This extracted 70% of the lactic acid, which was recoverable from the organic phase to a second aqueous phase containing of sodium carbonate (Harington and Hossain, 2008).

Keshav and co-workers (2009) studied the recovery of propionic acid from aqueous solutions using TBP / Aliquat 336 / TOA as extractants dissolved in SFO. In addition, they modified the organic phase using active organic solvents and modifiers. Decanol was reported to be the most efficient modifier among those tested. They achieved the highest recovery with 20% Aliquat 336 (Keshav et al. 2009). In another study, the same researchers extracted citric acid by using TOA as an extractant, which they dissolved in non-toxic diluents: soy, sesame, sunflower and rice bran oil. They obtained more than 90% extraction efficiency with all organic phases studied. Rice-bran oil was the most efficient among those evaluated. The researchers calculated the equilibrium constant and loading ratio for each organic phase system (Keshav et al., 2012).

Wasewar et al. (2011) used TBP or Aliquat 336 dissolved in SFO to recover itaconic acid from aqueous solutions by reactive extraction. The researchers compared the results obtained with two different extractants and determined the equilibrium constants for the acid-amine complexes formed in the organic phases (Wasewar et al., 2011).

In another study, Waghmare and co-workers (2011) compared SFO and castor oil for extracting picolinic acid, using TBP as the extractant. Castor oil provided higher recovery efficiencies compared to SFO (Waghmare et al. 2011). The same researchers used TBP and soy oil in a follow-up study to extract picolinic- and nicotinic acids from aqueous solutions. Their results indicated higher recoveries for picolinic acid as the highest extraction percentage with picolinic acid was 27.22%, while that with nicotinic acid was 6.99% (Waghmare et al., 2013).

Uslu and co-workers (2014) extracted fumaric acid by using tridodecylamine (TDDA) and tributylamine (TBA) as the extractants, with canola, sesame and almond oil as the organic phase diluents. They compared the extraction efficiencies and loading ratios for each system and tried to identify the best organic phase members for the process to maximize recoveries. The results obtained with the two amine extractants were similar to each other; canola oil was superior to the other oils studied (Uslu et al. 2014).

These studies show that there is no exact trend for the reactive extraction systems using vegetable oils as the organic phase diluents. None of the extractants and vegetable oils tested were shown to be superior to the others for all conditions, acids and extractants. Thus, considerable testing is still required. For example, there is no study on the recovery of formic acid using environmentally-friendly solvents, e.g. vegetable oils, nor are there studies in the literature comparing the results obtained with vegetable oils and an organic solvent, e.g. octanol.

In this study, formic acid (FA) was recovered by using the non-toxic diluent, sunflower oil (SFO), instead of organic solvents, previously described in the literature (Şenol, 2000; Qin et al., 2003; İnce et al., 2007; Uslu, 2009; Martı and Oflaz, 2013). This is the first report of the successful use of this extraction strategy on FA. Formic acid is the simplest carboxylic acid and used as preservative and anti-bacterial agent in food and pharmaceutical applications (Cai et al., 2001). Moreover, it is widely used in tanning, coloring and cleaning steps of leather and textile industries (Martı and Oflaz, 2013). It is reported that FA is present in several types of industrial wastewaters (Rasrendra et al., 2011) and has the potential to cause environmental problems. Therefore, its removal or recovery from aqueous streams is needed.

The experimental results obtained with SFO were compared with those obtained with octanol. Alamine-336 (ALA-336), a mixture of long chain aliphatic amines, was chosen as the extractant in the study. This extractant was previously used with several reactive extraction systems (San Martin et al., 1992; İnci et al., 2000; Wasewar et al., 2002). Besides the evaluation of the SFO for FA recovery, the effects of contact time, initial concentrations of acid and extractant on the recovery were also investigated.

MATERIAL AND METHODS

Formic acid and octanol were obtained from Merck Co., while ALA-336 (containing >95% TOA) was from Cognis Co. Sunflower oil (Zade) was obtained from local markets. All chemicals and SFO were used without any pretreatment. Deionized water (UHP) obtained from a Millipore Milli-Q system was used in the experiments. The aqueous phases were prepared by dissolving FA in UHP water at predetermined concentrations. Initial acid concentrations were varied between 0.2- and 1.0 M to reflect their concentrations in biological production media and wastewaters.

Prior to the reactive extraction studies, physical extraction experiments were carried out. These organic phases did not contain any extractant. This enabled the determination of the extractability of FA by the diluent, which was used during the calculation of the amount of acid reacted with the extractant (Tamada et al., 1990; Wasewar et al., 2002; Martı et al., 2011). The organic phases used in reactive extraction experiments were prepared by dissolving ALA-336 (10-50% v/v) in octanol or SFO (Hossain and Harington, 2008; Keshav et al., 2009; Waghmare et al., 2013).

Equal volumes (5 mL) of organic and aqueous phases were equilibrated by shaking for 4 h at 25°C using a constant temperature shaker bath (Jeiotech). Preliminary studies showed that this time is sufficient for reaching equilibrium. Following that, the mixture was centrifuged for 10 minutes at 6000 rpm and settled for 15 minutes. A clear phase separation was obtained and a sample of the aqueous phase was carefully removed with a pipet for analysis of solute concentration. The amount of FA in the aqueous phase before and after the extraction was determined by acid-base titration. Sodium hydroxide and phenolphthalein were used as the titrant and indicator, respectively, during the analyses. Since FA is a monocarboxylic acid, Equation 1 (E-1) was used to calculate the amount of acid in the aqueous phase.

$$M_{Acid} \times V_{Acid} = M_{NaOH} \times V_{NaOH} \quad (1)$$

The amount of FA extracted into the organic phase was determined by a mass balance around the aqueous phase. The experimental results were used to evaluate the efficiency of the extraction process using the equilibrium data and the equations below. The extraction efficiency ($E\%$) and distribution coefficient (K_D) were calculated using E-2 and E-3, respectively. To estimate the stoichiometry of the acid-amine complex in the organic phase, the loading ratio (z) was calculated (E-4).

$$E\% = C_{FA,org.}/C_{FA,total} \times 100 \quad (2)$$

$$K_D = C_{FA,org.}/C_{FA,aq.} \quad (3)$$

$$z = C_{FA,org.}/C_{ALA\text{-}336,total} \quad (4)$$

All experiments and analyses were replicated twice and average values were used to calculate the extraction parameters. Experimental error was found to be ≤1% in the studies.

RESULTS AND DISCUSSION

Effect of Contact Time

It is important to determine the equilibration time for a process that will be integrated into industrial productions, as it can directly affect several parameters including energy and efficiency (Martı et al., 2011). Therefore, prior to the equilibrium experiments, kinetic studies were carried out to estimate the equilibration period. An aqueous solution of 0.63 M FA was used in these experiments. As can be seen in

Figure 1, all systems reached equilibrium in 3 hours. Thus, all equilibrium experiments were carried out at 298 K and constant agitation speed (150 rpm) for four hours to insure consistent results.

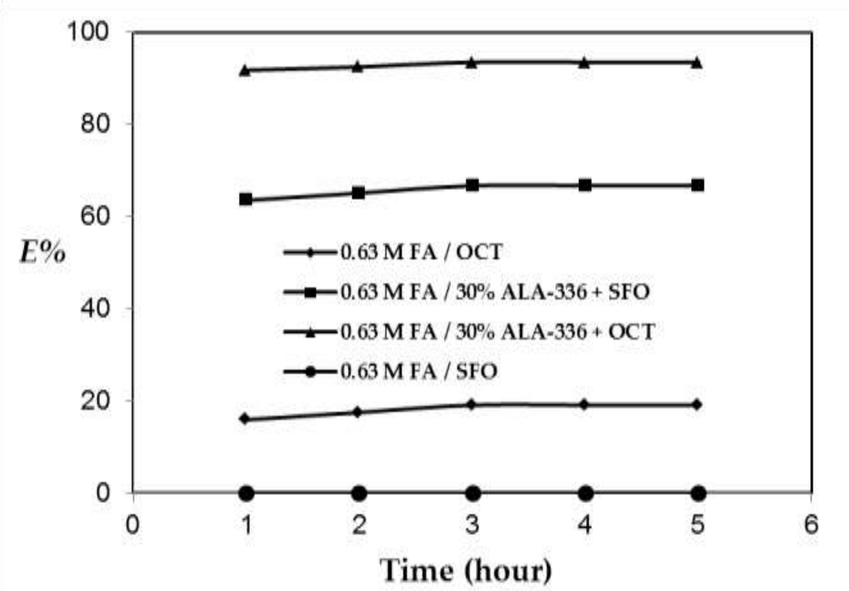

Figure 1. Effect of contact time on the physical- and reactive extraction of formic acid (Kinetic data).

Physical Extraction

Recovery values obtained with organic phases containing only solvents (without extractants) are shown in Figure 1. According to the data, extraction efficiency obtained with the reference organic solvent, octanol was about 19% (K_D=0.23). On the other hand, almost no FA could be extracted from the aqueous phase with SFO. The most important reason for this result is the relatively high polarity of alcohols with intermediate molecular weights. In general, water immiscible organic compounds have low polarity values and this makes them inappropriate for the recovery of polar materials, e.g. carboxylic acids. However, intermediate molecular weight alcohols such as octanol are relatively polar organic chemicals, giving them a significant advantage for the recovery of carboxylic acids.

As shown in Figure 1, the extraction efficiency obtained with octanol was only 19%. This is consistent with the results reported in the literature for different systems (Martı et al., 2011; Martı, 2016, Martı et al., 2016). Due to the weak interactions, the recovery with physical extraction is not efficient and necessitates repetitive extraction processes or the use of extraction columns including several steps (Tamada et al., 1990). For example, to recover 90% of the FA, either the extraction process should be repeated 11 times or an extraction column with 11 stages is needed, thus making the process inefficient and costly. Therefore, the process should be improved using an external parameter to increase the efficiency of the extraction. The addition of chemical extraction is an advantageous alternative to facilitate the process.

Effect of Extractant Concentration

As previously stated, reactive extraction is the advanced form of traditional liquid-liquid extraction processes. The literature shows that the use of chemical extraction or the presence of an extractant in the organic phase significantly increases the efficiency of the recovery (Kertes and King, 1986; Wasewar et al., 2004; Uslu et al., 2015). However, the high toxicity of these organic solvents is a major disadvantage of the reactive extraction technique. Therefore, environmentally-friendly solvents or diluents should be explored. Vegetable oils are important alternatives with their chemistry (composition and structure) and water immiscibility. Even if they cannot extract the acids from the aqueous phase by themselves (by physical means); their availability for the reactive extraction operations should be tested by equilibrium studies.

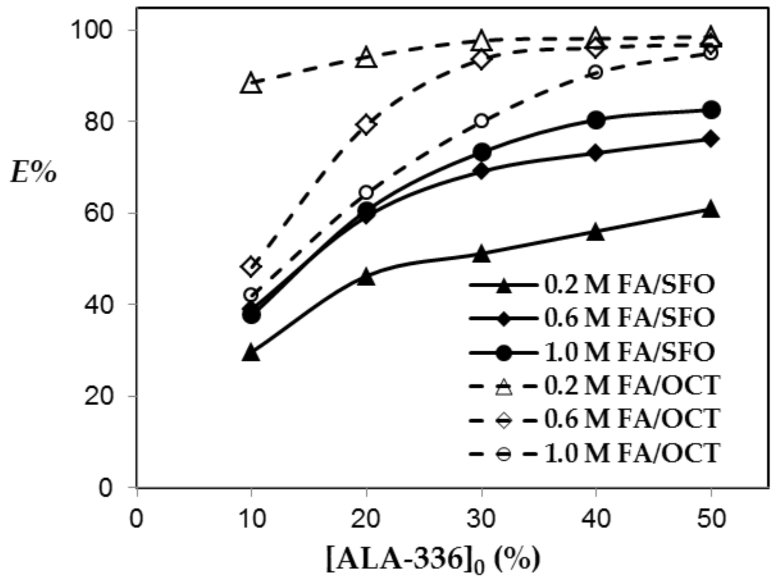

Figure 2. Effect of initial extractant percentage on extraction efficiency of formic acid by reactive extraction.

Figure 2 shows the influence of ALA-336 and its initial amount (% v/v) on the recovery of FA. As shown (Fig. 1), the recovery efficiency was 19% (K_D=0.23) when octanol was the sole component in the organic phase, and the initial FA concentration was about 0.6 M. Adding 10% (v/v) ALA-336 to the octanol increased the extraction efficiency to 48.25% (K_D=0.93). The impact of ALA-336 was higher at lower initial acid concentrations. On the other hand, at the same ALA-336 level and FA concentration, the recovery efficiency was 39% (K_D=0.64) with SFO. Thus, the use of chemical extraction significantly increased the efficiency from ~0% to 39% and facilitated the FA transfer. This result also shows that SFO provides an appropriate media for the acid-amine reaction and that it is a proper diluent for the reactive extraction of FA.

Figure 2 also shows that the extraction efficiency increased with the increase in extractant percentage in the organic phase, which is consistent with the literature (Martı et al. 2011, Datta et al. 2016). When the acid- and ALA-336 concentrations were 0.6 M and 30%, respectively, the recovery efficiencies obtained with octanol and SFO were 93.65% (K_D=14.75) and 69.15% (K_D=2.24), respectively. The positive effect increased with the increase in extractant concentration. At the same acid concentration, 50% (v/v) ALA-336 provided 96.9% (K_D=31.3) and 76.25% (K_D=3.21) recovery with octanol and SFO, respectively. The highest extraction efficiency obtained with SFO was 82.6% (K_D=4.78) at 1.0 M FA, while that with octanol was 98.6% (K_D=70.7) at 0.2 M FA. The results exhibit that SFO has the potential to provide higher efficiency values at higher extractant percentages.

It is seen that the effect of extractant concentration was influenced from initial acid amount and the trends were different for both diluents (Figure 2). For example at 10% ALA-336, the recovery with 0.2 M FA was much higher than that with the other FA concentration levels in octanol. With the increase in extractant concentration, even the results with 0.2 M FA were superior to the others; the difference became small and almost disappeared at 50% ALA-336 level in octanol. Regardless of the initial FA concentration, more than 95% ($K_D \geq 19$) recovery was achieved with 50% (v/v) ALA-336 in octanol. On the other hand, a different trend was observed with SFO. The recoveries for varied FA concentrations are close to each other at 10% (v/v) ALA-336 in SFO. With the increase in initial percentage of the extractant in the organic phase, the difference between the results became greater. The influence could be observed at 30% extractant level. The results with 0.6 and 1.0 M FA were relatively close to each other, but much higher than that with 0.2 at 30-50% (v/v) ALA-336 levels.

As can be seen, the results obtained with SFO are acceptably high and close to those obtained with octanol. In addition, the results also showed that higher or desired recovery efficiencies could also be obtained with SFO with the right selection of extractant type and concentration. This will enable the replacement of toxic organic chemicals with environmentally-friendly diluents for extractive separations.

Effect of Acid Concentration

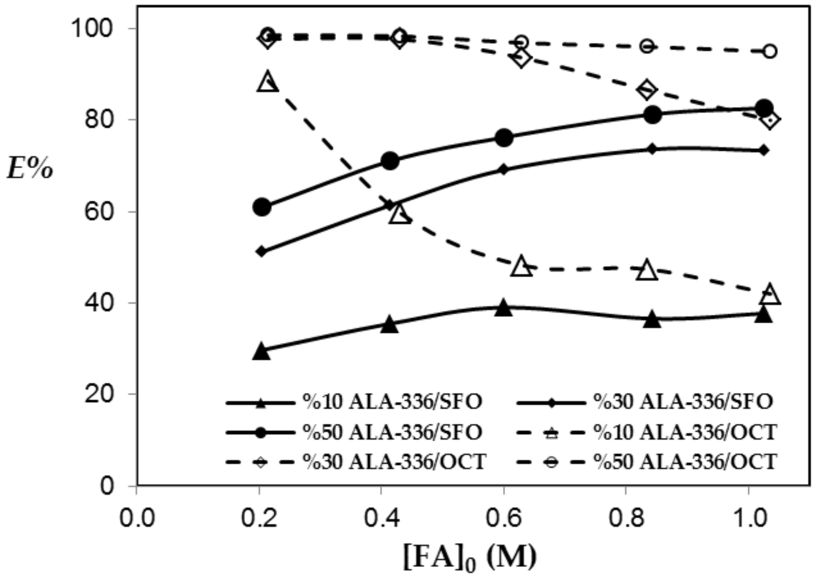

Figure 3. Variation of extraction efficiency with the initial acid concentration for the reactive extraction of formic acid.

Another important parameter affecting the success of a reactive extraction system is the initial amount of acid present in the aqueous phase. It was shown that the recovery with reactive extraction was significantly influenced by the concentration and type of the acid (Gu et al., 1998; Martı et al., 2011; Martı and Gürkan, 2015).

Figure 3 shows that the recovery efficiencies were influenced in different ways by initial FA concentrations when octanol or SFO was selected as the organic phase diluent. With octanol, the extraction efficiency decreased as acid concentration increased. The trend was obvious with 10% v/v ALA-336. At this level, the recovery efficiency was 88.6% (K_D=7.78) for 0.2 M FA; at 1.0 M initial FA, recovery was only 42% (K_D=0.73).

This trend was observed to disappear at higher ALA-336 percentages. At FA molarities of 0.2- and 0.4, recovery efficiencies with 30%- and 50% ALA-336 were identical or nearly same (~98%, K_D~50), and the efficiency losses were insignificant at these ALA-336 percentages. Under these conditions, the initial ALA-336 concentrations were higher than those of FA and the results indicated that almost all acids were extracted by the organic phase or the organic phase diluent was at- or very near saturation for the FA:ALA-336 complexes. At higher FA concentrations (>0.6 M), the efficiency varied inversely with ALA-336 percentages. When initial FA concentration was 1.0 M, the extraction efficiency was 95% (K_D=19) with 50% ALA-336 but only 80% (K_D~4) with 30% ALA-336.

On the other hand, an opposite trend was observed when SFO was used as the diluent. In the ranges of the parameters, the recovery efficiencies obviously increased with the increase in FA concentration, which continued until a FA concentration of 0.8 M level. The success of the extraction obtained with 1.0 M was close to that with 0.8 M FA. The recovery values obtained with 30% ALA-336 were closer to those obtained with 50% ALA-336 compared to 10% ALA-336. This was valid for almost all FA concentrations. The results obtained for the investigation of the acid concentration effect were consistent with the literature (Tamada et al., 1990; Gu et al., 1998; Keshav et al., 2009; Martı et al., 2011; Uslu et al., 2014; Martı et al., 2016).

Stoichiometry

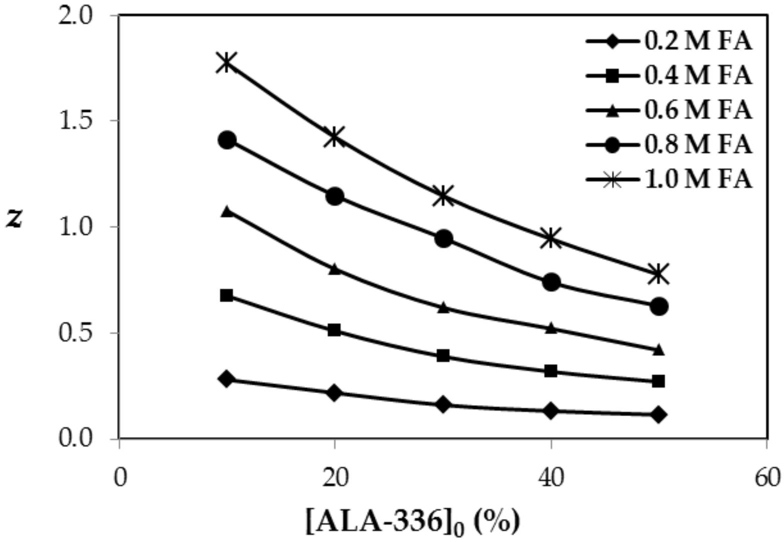

Figure 4. Loading ratios for the reactive extraction of formic acid using sunflower oil as organic phase diluent.

The stoichiometry of the acid-amine complex in the organic phase was estimated using loading ratio (z) values. Data from the literature show that the loading ratio is notably influenced by solvent type (Tamada et al., 1990; Wasewar et al., 2004). Firstly, a 1:1 acid-amine complex forms in the organic phase during the reactive extraction process. Depending on the media, conditions and the solutes present, different types of complex structures may form. Previously, the loading ratios for FA/tertiary amines/organic solvents were calculated (Şenol, 2000; Qin et al., 2003; İnce et al., 2007; Uslu, 2009)

Figure 4 shows the z values for reactive extraction of FA using SFO as the diluent in the organic phase. During the calculations, molar concentration values were used (E-4). Initial or total ALA-336 concentrations were varied between 0.22 M (10% v/v) and 1.09 M (50% v/v). Equilibrium concentration of FA in the organic phase changed between 0.061- and 0.847 M.

The results showed that z values were markedly influenced by acid and extractant concentrations. When the initial amount of ALA-336 was 40-50% (v/v), the z values were lower than unity regardless of the initial amount of acid. At lower ALA-336 percentages and acid concentrations equal and lower than 0.6 M, again the z values were almost equal or lower than 1. This indicates that under these conditions, only a 1:1 type acid-amine complex formed in the organic phase. However, at the same extractant levels and higher FA concentrations, the z values varied between 1 and 2, indicative of the simultaneous presence of 2:1 and 1:1 type acid-amine complexes. The results are consistent with those reported in the literature for tertiary amines and carboxylic acids (Tamada et al., 1990; Wasewar et al., 2002; Qin et al., 2003; Uslu, 2009; Martı et al., 2011)

CONCLUSION

Solvent or diluent type used during reactive extraction is so important for the recovery of carboxylic acids (Kertes and King, 1986). However, the most effective solvents are generally toxic chemicals and this is the most critical disadvantage of the technique that prevents its widespread use in industries. Hence, environmentally-friendly alternatives that can be used in reactive extraction processes should be explored. Evaluating these diluents should be done by the comparison with the most commonly used organic diluents. This will facilitate widespread use of the method and prevent/reduce the release of toxic chemicals from extractive separations.

In this study, sunflower oil was evaluated for use in recovering formic acid by reactive extraction to replace traditional organic solvents such as octanol. Recoveries obtained with SFO were compared with those observed with octanol, which is known to be one of the most effective diluents for the recovery of carboxylic acids. The kinetic data showed that at least 3 hours was required to reach the equilibrium for both physical- and reactive extraction. The physical extraction efficiency was about 19% (K_D=0.23) with octanol while no FA was extracted with SFO alone.

The addition of the extractant positively influenced the recovery for both octanol and SFO. The recovery increased with the increase in initial ALA-336 percentage, and was observed for both diluents. The increase in initial concentration of FA negatively influenced the recovery with octanol while extraction efficiency increased with this parameter when SFO was used as the diluent in the organic phase. The results are consistent with the literature (Keshav et al., 2009; Waghmare et al., 2011; Uslu et al., 2014). The highest recovery values were obtained as 98.6% (K_D=70.7) and 82.6% (K_D=4.78) for octanol and SFO, respectively, at the highest ALA-336 level (50% v/v) studied. The results showed that the recovery efficiencies could be further increased by increasing the initial ALA-336 concentration. With the help of the loading ratios, the stoichiometry of the acid-amine complexes in the diluents was estimated to be 1:1 and 2:1.

The results showed that the recovery efficiencies with SFO were acceptably high and close to those obtained with octanol. The results also showed that with the right selection of extractant type and concentration, the desired recovery efficiencies could be achieved with SFO diluent. This will enable the replacement of toxic organic toxic chemicals with environmentally-friendly solvents for the extractive separations of carboxylic acids.

ACKNOWLEDGEMENT

The author wishes to acknowledge Selçuk University for the funding through the Scientific Research Projects (BAP) Coordination Unit under the Grant Number 16201042.

LIST OF ABBREVIATIONS

ALA-336	Alamine-336
$C_{ALA\text{-}336}$	Concentration of Alamine-336
C_{FA}	Concentration of formic acid
E%	Extraction (Recovery) efficiency (percentage)
FA	Formic acid
K_D	Distribution coefficient
M_{Acid}	Molarity of acid
M_{NaOH}	Molarity of NaOH (base)
OCT	Octanol
SFO	Sunflower oil

V_{Acid}	Volume of acid
V_{NaOH}	Volume of NaOH (base)
TOA	Trioctylamine
z	Loading ratio
org.	Organic phase
aq.	Aqueous phase
total	Total concentration of formic acid or Alamine-336 in the system

REFERENCES

Cai, W., Zhu, S., Piao, X., 2001, "Extraction Equilibria of Formic And Acetic Acids from Aqueous Solution by Phosphate Containing Extractants", *Journal of Chemical and Engineering Data*, Vol. 46, pp. 1472-1475.

Chen, H. L., Juang, R. S., 2008, "Recovery and Separation of Surfactin from Pretreated Fermentation Broths by Physical and Chemical Extraction", *Biochemical Engineering Journal*, Vol. 38 (1), pp. 39–46.

Datta, D., Martı, M. E., Uslu, H., Kumar, S., 2016, "Extraction of Levulinic Acid Using Tri-n-butyl Phosphate and Tri-n-octylamine in 1-octanol: Column Design", *Journal of the Taiwan Institute of Chemical Engineers*, Vol. 66, pp. 407-413.

Gorden, J., Zeiner, T., Sadowski, G., Brandenbusch, C., 2016, "Recovery of Cis, Cis-muconic Acid from Organic Phase After Reactive Extraction", *Separation and Purification Technology*, Vol. 169, pp. 1-8.

Gu, Z., Glatz, B. A., Glatz, C. E., 1998, "Propionic Acid Production by Extractive Fermentation. I. Solvent Considerations", *Biotechnology and Bioengineering*, Vol. 57 (4), pp. 454-461.

Harington, T., Hossain, Md. M., 2008, "Extraction of Lactic Acid into Sunflower Oil and Its Recovery into An Aqueous Solution", *Desalination*, Vol. 218, pp. 287-296.

İnce, E., Kırbaşlar, Ş. İ., Şahin, S., 2007, "Liquid-liquid Equilibria for Ternary Systems of water+formic acid+dibasic Esters", *Journal of Chemical and Engineering Data*, Vol. 52 (5), pp. 1889-1893.

İnci, İ., Hasdemir, M., Bilgin, M., Aydın, A., 2000, "Laktik Asitin Alamin-336 ile Çeşitli Seyreltici Çözücüler Kullanılarak Ekstraksiyonunun İncelenmesi", *Turkish Journal of Engineering and Environmental Sciences,* Vol. 24, pp. 45-51.

Kertes, A. S., King, C. J., 1986, "Extraction Chemistry of Fermentation Product Carboxylic Acids", *Biotechnology and Bioengineering*, Vol. 28 (2), pp. 269-282.

Keshav, A., Wasewar, K. L., Chand, S., 2009, "Reactive Extraction of Propionic Acid using Tri-n-Octylamine, Tri-n-butyl Phosphate and Aliquat 336 in Sunflower Oil as Diluent", *Journal of Chemical Technology and Biotechnology*, Vol. 84 (4), pp. 484-489.

Keshav, A., Norge, P., Wasewar, K. L., 2012, "Reactive Extraction of Citric Acid Using Tri-n-octylamine in Nontoxic Natural Diluents: Part 1—Equilibrium Studies from Aqueous Solutions", *Applied Biochemistry and Biotechnology*, Vol. 167 (2), pp. 197–213.

Lopez-Garzon, C. S., Straathof, A. J., 2014, "Recovery of Carboxylic Acids Produced by Fermentation", *Biotechnology Advances*, Vol. 32 (5), pp. 873-904.

Martı, M. E., 2010, *Reactive Extraction of Pyruvic Acid From Aqueous Single and Mixed Acid Solutions*, PhD Thesis, Middle East Technical University, Graduate School of Natural and Applied Sciences, Ankara.

Martı, M. E., Gürkan, T., Doraiswamy, L. K., 2011, "Equilibrium and Kinetic Studies for Reactive Extraction of Pyruvic Acid with Trioctylamine in 1-octanol", *Industrial and Engineering Chemistry Research*, Vol. 50 (23), pp. 13518-13525

Martı, M. E., Oflaz, K., 2013, "Formik Asidin Alamıne-336 Ve Çeşitli Çözücülerle Tepkimeli Özütlenmesi", *Selçuk Üniversitesi Mühendislik, Bilim ve Teknoloji Dergisi*, Vol. 1 (3), pp. 1-8.

Martı, M. E., Gürkan, T., 2015, "Selective Recovery of Pyruvic Acid From Two and Three Acid Aqueous Solutions by Reactive Extraction", *Separation and Purification Technology*, Vol. 156 (2), pp. 148-157.

Martı, M. E., Zeidan, H., Uslu, H., 2016, "Reactive Extraction of Pimelic (heptanedioic) Acid from Dilute Aqueous Solutions Using Trioctylamine in decan-1-ol", *Fluid Phase Equilibria*, Vol. 417, pp. 197-202.

Martı, M. E., 2016, "Solvent Modification Effect on The Physical And Chemical Extraction of Acetic Acid", *Separation Science and Technology*, Vol. 51 (11), pp. 1806-1816.

Qin, W., Li, Z., Dai, Y., 2003, "Extraction of Monocarboxylic Acids With Trioctylamine: Equilibria and Correlation of Apparent Reactive Equilibrium Constant", *Industrial and Engineering Chemistry Research*, Vol. 42 (24), pp. 6196-6204.

Rasrendra, C. B., Girisuta, B., Van de Bovenkamp, H. H., Winkelman, J. G. M., Leijenhorst, E. J., Venderbosch, R. H., Windt, M., Heeres, H. J., 2011, "Recovery of Acetic Acid from an Aqueous Pyrolysis Oil Phase by Reactive Extraction Using Tri-n-octylamine", *Chemical Engineering Journal*, Vol. 176-177, pp. 244-252.

Reyhanitash, E., Zaalberg, B., Kersten, S. R. A., Schuur, B., 2016, "Extraction of Volatile Fatty Acids from Fermented Wastewater", *Separation and Purification Technology*, Vol. 161, pp. 61-68.

San-Martin, M., Pazos, C., Coca, J., 1992, "Reactive Extraction of Lactic Acid with Alamine-336 in The Presence of Salts and Lactose", *Journal of Chemical Technology and Biotechnology*, Vol. 54 (1), pp. 1-6.

Straathof, A. J. J., 2014, "Transformation of Biomass into Commodity Chemicals Using Enzymes or Cells" *Chemical Reviews*, Vol. 114 (3), pp. 1871–1908.

Şenol, A., 2000, "Extraction Equilibria of Formic and Levulinic Acids Using Alamine 308/Diluent and Conventional Solvent Systems", *Separation and Purification Technology*, Vol. 21 (1-2), pp. 165–179.

Tamada, J. A., Kertes, A. S., King, C. J., 1990, "Extraction of Carboxylic Acids with Amine Extractants. 1. Equilibria and Law of Mass Action Modeling", *Industrial and Engineering Chemistry Research*, Vol. 29 (7), pp. 1319-1326.

Uslu, H., 2009, "Reactive Extraction of Formic Acid by Using Tri octyl amine (TOA)", *Separation Science and Technology*, Vol. 44 (8), pp. 1784–1798.

Uslu, H., Gemici, A., Gök, A., Kırbaşlar, İ., 2014, "Reactive Extraction of (E)-butenedioic Acid (fumaric acid) by Nontoxic Diluents", *Journal of Chemical and Engineering Data*, Vol. 59 (11), pp. 3767–3772.

Uslu, H., Yankov, D., Wasewar, K. L., Azizian, S., Ullah, N., Ahmad, W., 2015, "Separation of Organic and Inorganic Compounds for Specific Applications" *Journal of Chemistry*, Vol. 2015, Article ID: 698259, pp. 1-3.

Waghmare, M. D., Wasewar, K. L., Sonawane, S. S., Shende, D. Z., 2011, "Natural Nontoxic Solvents for Recovery of Picolinic Acid by Reactive Extraction", *Industrial and Engineering Chemistry Research*, Vol. 50 (23), pp. 13526–13537.

Waghmare, M. D., Wasewar, K. L., Sonawane, S. S., Shende, D. Z., 2013, "Reactive Extraction of Picolinic and Nicotinic Acid by Natural Non-toxic Solvent", *Separation and Purification Technology*, Vol. 120, pp. 296-303.

Wasewar, K. L., Heesink, B. M., Versteeg, G. F., Pangarkar, V. G., 2002, "Reactive Extraction of Lactic Acid Using Alamine-336 in MIBK: Equilibria and Kinetics", *Journal of Biotechnology*, Vol. 97 (1), pp. 59-68.

Wasewar, K. L., Yawalkar, A. A., Moulijn, J. A., Pangarkar, V. G., 2004, "Fermentation of Glucose to Lactic Acid Coupled With Reactive Extraction: A review", *Industrial and Engineering Chemistry Research*, Vol. 43 (19), pp. 5969-5982.

Wasewar, K. L., Shende, D., Keshav, A., 2011, "Reactive Extraction of Itaconic Acid Using Tri-n-butyl Phosphate and Aliquat 336 in Sunflower Oil as A Non-toxic diluent", *Journal of Chemical Technology and Biotechnology*, Vol. 86 (2), pp. 319-323.

Yang, S. T., Huang, H., Tay, A., Qin, W., De Guzman, L., San Nicolas, C., 2007, *Extractive Fermentation for The Production of Carboxylic Acids*, S. T. Yang (Ed.), Bioprocessing for value-added products from renewable resources: New technologies and applications, 1. Edition, Elsevier, New York, pp. 421.

SUJEST, c.5, s.1, 2017
SUJEST, v.5, n.1, 2017
ISSN: 2147-9364 (Electronic)

UÇUCU KÜL İÇEREN YÜKSEK PERFORMANSLI GÜÇLENDİRME HARCINDA NANO SİLİKATIN ETKİSİ

[1]Kenan TOKLU, [2]Seyedrahim BAHARAVAR, [3]Osman ŞİMŞEK

[1,2,3]Gazi Üniversitesi, Teknoloji Fakültesi, İnşaat Mühendisliği, Ankara
[1]kenan0106toklu@gmail.com, [2] seyedbah80@gmail.com, [3] *simsek@gazi.edu.tr*

(Geliş/Received: 13.05.2016; Kabul/Accepted in Revised Form: 28.06.2016)

ÖZ: Bu çalışmada 8 farklı karışım yapılmıştır. Bu karışımlarda, Nano Silikat %0 'dan %2' ye kadar % 0.25 arttırılarak çimento yerine ikame edilmiştir. Hazırlanan numunelerde su oranı düşük tutulup yüksek hacimde kullanılan Uçucu Külün etkisi altında ikame edilen Nano Silikatlı karışımların basınç ve eğilme altındaki davranışları araştırılmıştır. Numunelerde basınç dayanımı testi için 5×5×5 cm küp prizma betonlar hazırlanmış ve 1., 3. ve 7. günlerde deneylere tabi tutulmuştur. Bu çalışmanın amacı Nano Silikatlı numunelerin 1. günden itibaren Uçucu Külün erken yaş dayanımdaki negatif etkisini önlemek ve yüksek performanslı beton elde etmektir.

Anahtar Kelimeler: Nano silikat, Puzolan, Uçucu kül, Yüksek performanslı beton

The effects of Nano Silicate Mixtures with High Volume Fly Ash on High Performance Strengthening Mortar

ABSTRACT: In this study, 8 different mixtures were made. In these mixtures, silica nanoparticles were substituted for cement by 0% to 2% by 0.25%. The compressive and flexural strength of Nano Silicate Mixtures under the influence of high volume fly ash with low water content were investigated. 5×5×5 cm concrete cubic prisms were produced and subjected to compressive strength test on the 1st, 3rd and 7th days. These prepared concrete specimens were subjected to experiments on 1, 3 and 7 days. The aim of this study is to prevent the negative effect of high volume fly ash on the early age strength of concrete from the first day and to obtain high performance concrete.

Key Words: Nano silica, Pozzolan, Fly ash, High performance concrete

GİRİŞ (Introduction)

İnşaat sektöründe Portland Çimentolu (PÇ) ürünler ve betonun en çok kullanılan malzemelerden biri olarak kabul görmesinde en önemli etkenlerden biri; beton teknolojisindeki hızlı gelişmeler ile beton kalitesinin çok yüksek mertebelere ulaşmasıdır. Beton kalitesindeki bu yükseliş büyük oranda, betonu oluşturan temel malzemeler olan çimento, agrega, su ve mineral katkıların yanında katılan kimyasal katkı maddeleri ile sağlanmıştır. Katkı tanımı, "Betonun veya harcın ana bileşenlerini oluşturan su, agrega, hidrolik çimento ve fiber takviye malzemeleri haricinde betonun üretim aşamasında veya öncesinde katılan malzemeler" (ACRA, 2006) olarak yapılmaktadır. Kimyasal katkılar esas olarak betonun veya harcın taze ve

DOI: 10.15317/Scitech.2017.68

sertleşmiş durumdaki özelliklerini iyileştiren, suda çözünebilen maddelerdir. Farklı özelliklerdeki kimyasal katkıların beton özellikleri üzerinde sağladığı iyileştirmelere örnek olarak, basınç ve eğilme dayanımları üzerinde artış, geçirimsizlik özellikleri ve buna bağlı olarak durabilite özellikleri üzerindeki iyileştirmeler, korozyon önleme, rötre azaltma, ayrışmadan yüksek kıvam artırma gibi işlenebilirlik özellikleri üzerindeki iyileştirmeler sayılabilir. Ayrıca, priz süresinin ayarlanması, yüksek pompalanabilirlik, amaca yönelik düzenlenebilir reolojik özellikler, çimento etkinliğinin artırılması ve alkali silika reaksiyon riskinin azaltılması gibi performans artırıcı etkiler de sayılabilir (Cilason, 1992).

Nanoteknoloji maddeyi oluşturan atomları kontrol ederek maddenin fiziksel ve kimyasal özelliklerinin değiştirilmesine ve yeni ürünlerin geliştirilebilmesine olanak sağlayan bir teknolojidir. Nanoteknoloji hemen hemen tüm alanlarda geniş bir uygulama alanına sahip en aktif araştırma alanlarından biridir. Beton inşaat sektöründe en çok kullanılan malzeme olduğundan Nanoteknoloji ile kalitesi arttırılmaya çalışılmış ve geleneksel betonlardan çok daha üstün özellikler elde edilmiş (Alexander ve Stanish, 2005).

DENEYSEL ÇALIŞMALAR (Experimental Study)

Malzemeler (Materials)

Bu çalışmada, Çizelge 1'de sunulan betonlar üretildikten sonra 1, 3 ve 7 günlük deneylere tabi tutulmuştur.

Çizelge 1. Nano silikat ve kullanılan malzemelerin karışım oranları

Table 1. *Mixing ratios of nano-silicate and used materials*

Malzeme	KB	UK55 nSi 25	UK55 nSi 50	UK55 nSi75	UK55 nSi 100	UK55 nSi 125	UK55 nSi 150	UK55 nSi 175	UK55 nSi 200
(nAl) /B	0.000	0.0025	0.0050	0.0075	0.0100	0.0125	0.0150	0.0175	0.0200
B/Kum	2,50	2,50	2,50	2,50	2,50	2,50	2,50	2,50	2,50
S/B	0,27	0,27	0,27	0,27	0,27	0,27	0,27	0,27	0,27
S/Ç	0,61	0,61	0,62	0,62	0,62	0,62	0,62	0,62	0,63
UK/Ç	1,22	1,22	1,22	1,22	1,22	1,22	1,22	1,22	1,22
CF / B	0,02	0,02	0,02	0,02	0,02	0,02	0,02	0,02	0,02
PVA/B	0.0124	0.0124	0.0124	0.0124	0.0124	0.0124	0.0124	0.0124	0.0124

Kısaltmalar	Açıklama
KB	Kontrol Betonu (%55 UK +% 45 Çimento+KK+CF+PVA+ n Si 0.00)
(UK55nSi 25)	Yüksek performans amaçlı karışım
UK	Uçucu Kül
55	Uçucu külün bağlayıcı grubu içindeki yüzdesi
n	Nano
Si	Nano silikat
25	Nano malzemenin % si
B	Bağlayıcı= (Çimento+UK+Nano malzeme+Kalsiyum Format)
CF	Calcium Formia(Kalsiyum Format)
PVA	*Poly(vinyl alcohol)* lif
S	Karışım suyu
Ç	Çimento

Çizelge 1'de görüldüğü gibi beton karışımlarında Portland Çimento yerine yüksek oranda uçucu kül kullanımının çevresel ve ekonomik açıdan birçok pozitif etkisi bulunmaktadır. Ayrıca, bu malzemeler yüksek performanslı çimento bağlayıcılı kompozitlerin performanslarını önemli ölçüde iyileştirmeleri sebebiyle son zamanlarda yüksek performanslı lif donatılı çimento bağlayıcılı kompozitlerin özel bir türü olan YPLDÇK karışım tasarımları için vazgeçilmez bileşenler olmuşlardır. Bilindiği üzere YPLDÇK üretiminde kullanılan mikro-mekanik tabanlı tasarım yaklaşımı kısıtları nedeni ile matris karışımında kullanılan S/B oranının belli bir seviyenin üzerine geçmemesi gerekmektedir. Performansı iyi olan düşük kalsiyum oksit oranına sahip Çatalağızı Termik Santrali UK'lerin çalışmamızda kullanılması kararlaştırılmıştır. Ayrıca, karışımlarda çimento türü olarak CEM I 52,5 R PÇ'nin kullanılması planlanmıştır.

Geleneksel betona kıyasla, matrise lif dağılımının kolaylığı için gerekli reolojik özelliklerin elde edilmesi ve mikro-mekanik tabanlı tasarım yaklaşımı gereksinimlerinden biri olan düşük matris tokluk değeri elde edebilmek için YPLDÇK üretiminde Manisa ilinden temin edilen 400μm'lik silis kumu kullanılmıştır. Şekil 1 ve 2 'de kullanılan malzemelerin çekilen resimleri verilmektedir.

Şekil 1. Çalışmalarda kullanılan uçucu kül, çimento ve silis kumu
Figure 1. *Fly ash, cement and silica sand used in the study*

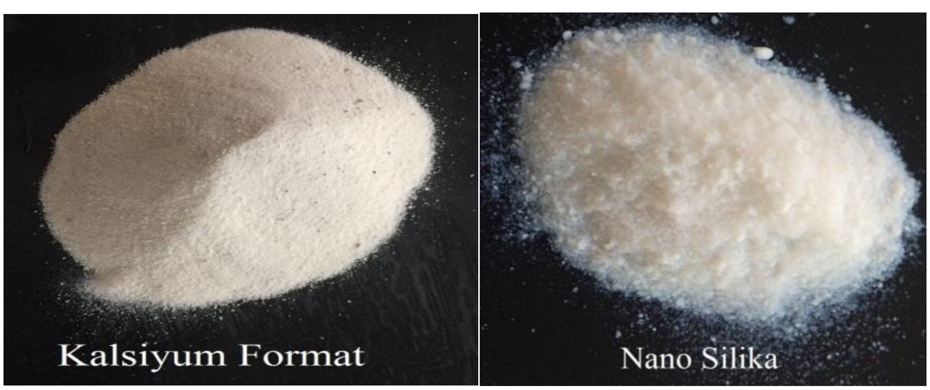

Şekil 2. Çalışmada kullanılan nano silica ve kalsiyum format
Figure 2. *Nano silica and calcium format used in the study*

Mikro-mekanik modellerle kompozitin mikroyapısı, istenen mekanik özelliklerin elde edilmesi için en uygun hale getirilmektedir (Kanda ve Li, 1999). Bu şekilde, lif, matris ve lif-matris arayüz etkileşiminin kontrolü ile yüksek performanslı kompozitler elde edilmektedir. Mikro-mekanik tabanlı tasarım aşamasında lifin mekanik ve fiziksel özellikleri gibi parametreler kullanılmaktadır. Bu çalışmada, YPLDÇK üretiminde başarılı bir şekilde kullanılan, mikro-mekanik tabanlı tasarım sonucu geliştirilmiş PVA lifleri (Shahmaran ve diğ., 2007), 20 mm ve 6 mm boyutlarında kullanılarak numuneler üretilmiştir. Sadece 20 mm lik PVA lifle yapılan deneyde karıştırma sorunu ile karşı karşıya kalınmıştır. Bu sorun 6 mm lik PVA lif kullanılarak çözülmüştür. Yeterli eğilme dayanımı her iki lif çeşidinden eşit olarak kullanılarak elde edilmiştir.

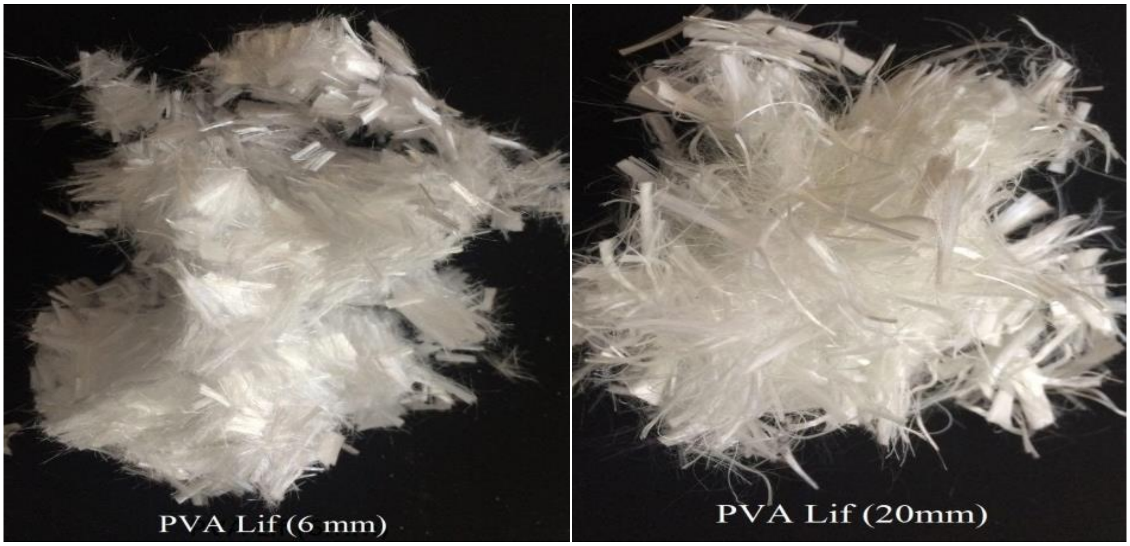

Şekil 3. Çalışmalarda kullanılan PVA lifleri
Figure 3. *PVA fibers used in the study*

Araştırmada kullanılan çimento, uçucu kül ve silis kumun fiziksel ve kimyasal özellikleri Çizelge 2 ‘de verilmektedir.

Çizelge 2. Malzemelerin fiziksel ve kimyasal özellikleri
Table 2. *Physical and chemical properties of materials*

Kimyasal Özellikler	PÇ52,5 Beyaz	UK	Silis Kumu 400 (SK)
CaO	65.70	2.18	0.05
SiO_2	21.60	55.44	99.31
Al_2O_3	4.05	24.93	0.29
Fe_2O_3	0,26	6.33	0.05
MgO	1.30	2.38	-
SO_3	3.30	0.14	-
K_2O	0,35	3.87	0.02
Na_2O	0,32	0.49	-
Kızdırma Kaybı	3.20		0.09
$SiO_2+Al_2O_3+Fe_2O_3$	25.91	86.70	99.65
Yoğunluğu (g/cm^3)	3.06	2.13	2.65
Blaine İnceliği (cm^2/g)	4600	2698	-
Hacim genleşmesi(mm)	1.00	-	-
90 µm elek üstü (%)	5. 18	17,58	63.22
45 µm elek üstü (%)	22,22	33,42	94,68

Çizelge 3′ de kullanılan Nano Silikanın fiziksel ve kimyasal analizinin özetini ayrıntılı bir şekilde gösterilmektedir.

Çizelge 3. Araştırmada kullanılan Nano Al_2O_3 ve Nano SiO_2 malzemelerin fiziksel ve kimyasal özellikleri
Table 3. *Physical and chemical properties of Nano Al_2O_3 and Nano SiO_2*

Özelikler	**Nano Al_2O_3**	**Nano SiO_2**	
APS	20 nm	15-20nm	
SSA:	~150 m^2/g	~300m^2/g	
Yapısı	Hemen hemen küresel	Gözenekli	
Renk	Beyaz	Beyaz	
Yogunluk:	3890 kg/m^3	Gerçek Yogunluk	2.4 g/cm^3
		Birim Hacim Ağırlıgı	<0.05 g/cm^3
Ultraviole Reflektivite	-	>85%	
Hidroksil İçeriği	-	>45%	
Analiz - ppm			
Ca	<25	<20	
Al	-	<20	
Fe	<80	<10	
Cr	<4	-	
Mg	-	<10	
Na	<70	-	
Mn	<3	-	
Co	<2	-	
Cl	-	<10	

Çalışmada kullanılan silis kum, uçucu kül ve çimentonun elek analizleri Çizelge 4′ te verilmiş ve bu analize ait diyagram Şekil 4′te görünmektedir.

Çizelge 4. Karışımda kullanılan malzemelerin tane büyüklüğü dağılımı
Table 4. *Particle size distribution of materials used in the mixture*

Elek Çap (μm)	**Silis Kum (% Geçen)**	**Uçucu Kül (% Geçen)**	**Çimento 52,5 (% Geçen)**
500	100	100	100
355	99,32	100	100
250	86,96	100	100
200	75,04	92,14	100
180	65,04	89,62	100
125	50,04	83,1	97,32
90	30,78	82,42	94,82
63	14,36	73,68	87,82
45	5,32	60,58	77,78
38	2,00	41,5	53,16
0	0	0	0

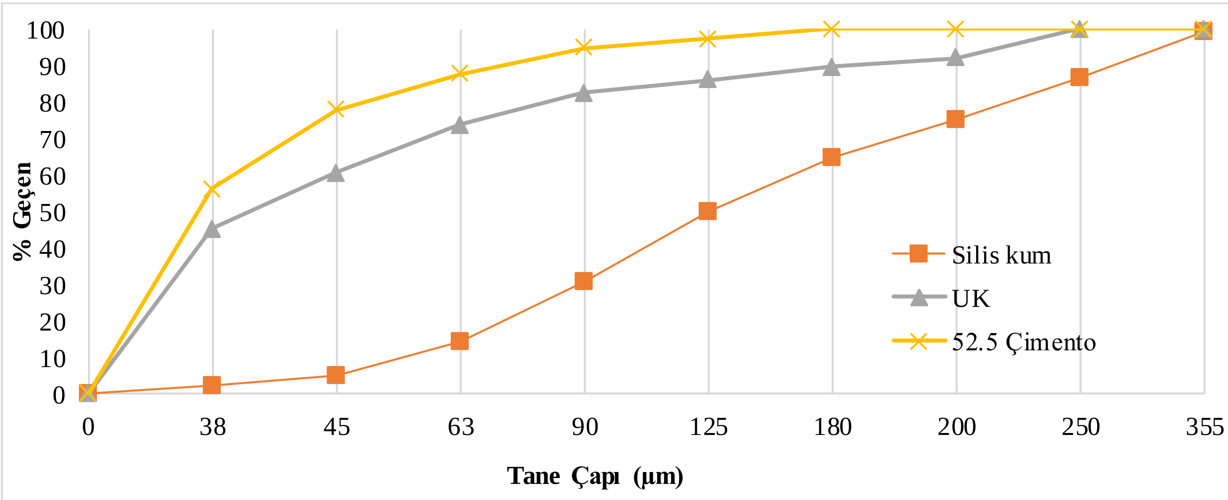

Şekil 4. Karışımda kullanılan çimento, uk ve silis kumunun elek analizi eğrisi
Figure 4. *Graphs of sieve analysis of the cement, fly ash and silica sand used in the mixture*

METOT (Method)

Çizelge 5'te Nano Silikat içeren numunelerin karışım miktarları 1m3 için verilmiştir. Hazırlanan karışımların her birinden 1, 3 ve 7 günlük basınç dayanımı için her yaşta 3 adet numune kullanılmak üzere 50×50 mm boyutlarında toplamda 9 adet küp numunesi hazırlanmıştır. Numuneler ortalama sıcaklığı 23 ± 2 °C ve nemi %95 ± 5 olan özel kür tankında deney tarihine kadar muhafaza edilmiştir. Basınç dayanımı testi ASTM C39 (ASTM C39/C39M, 2016) standardına uygun olarak 100 ton kapasiteli test cihazı kullanılarak 5 cm boyutlu küp numuneler üzerinde yapılmıştır.

Numunelerin üretilmesi için ilk aşamada %50 su miktarı ile nano malzeme 20 dakika karıştırılmış ve Şekil 5 'te görünen mikserde karıştırılmış olan malzemeye eklenmiştir. Karışım makinesinin içindeki malzemeler 5 dakika normal hızda ve nano malzeme eklendikten sonra 5 dakika hızlı şekilde karıştırılmıştır.

Çizelge 5. 1 m^3 için Nano Silikat karışım miktarları
Table 5. *Nano-Silica mixture quantities for 1* m^3

Malzeme	KB	UK55 nSi 25	UK55 nSi 50	UK55 nSi 75	UK55 nSi 100	UK55 nSi 125	UK55 nSi 150	UK55 nSi 175	UK55 nSi 200
Silis Kum(kg)	485,53	483,20	480,80	478,50	476,20	473,90	471,65	469,40	467,15
Çimento (kg)	535,30	531,37	527,38	523,51	519,65	515,81	512,04	508,27	504,52
Su (lt)	327,73	326,16	324,54	322,99	321,44	319,88	318,36	316,85	315,33
PVA Lif (kg)	15,00	15,00	15,00	15,00	15,00	15,00	15,00	15,00	15,00
UK (kg)	654,25	649,45	644,57	639,84	635,13	630,44	625,82	621,22	616,64
nSi (kg)	0,00	3,02	6,01	8,97	11,91	14,81	17,69	20,54	23,36
KK (kg)	18,20	18,20	18,20	18,20	18,20	18,20	18,20	18,20	18,20
CF (kg)	24,28	24,16	24,04	23,93	23,81	23,70	23,58	23,47	23,36

Şekil 5. Deneyde kullanılan mikser
***Figure 5.** Mixer used in the experiment*

Tüm numuneler döküldükten sonra yapılan kürde bekletilmiş ve kendi yaşlarında Şekil 6'da görünen basınç makinesinde basınca tabi tutularak kırılmış ve sonuçlar kaydedilmiştir.

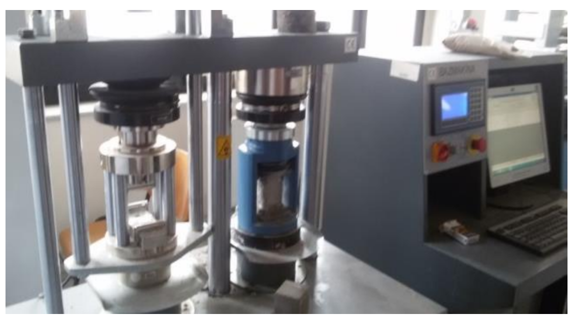

Şekil 6. Basınç makinesinin görüntüsü
***Figure 6.** The view of compression machine*

Betonlar 1, 3 ve 7 gün sonunda kırılarak betonların erken yaşta gelişmesi ve mukavemet kazanılması gözlenmiştir. Yapılan basınç deneylerin sonuçları Şekil 7'de verilmektedir.

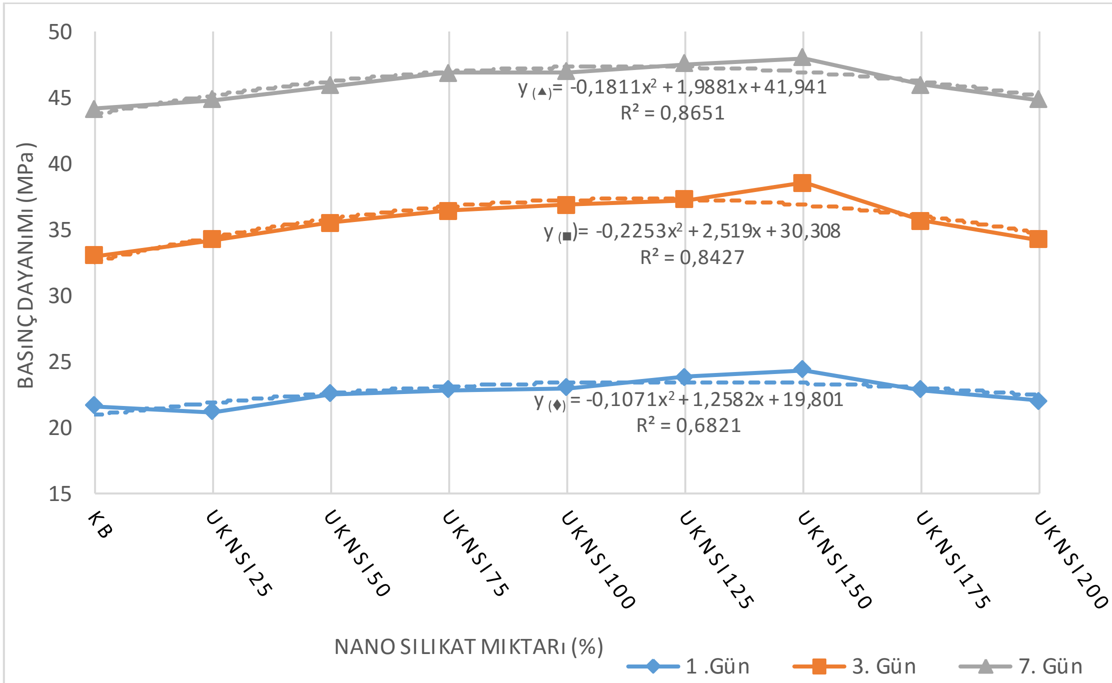

Şekil 7. Nano Silikatlı numunelerde basınç dayanımı-Nano Silikat oranı ilişkisi
Figure 7. *The relationship between Nano Silicate ratio and compressive strength in Nano Silicate mixtures*

ARAŞTIRMA SONUÇLARI (RESEARCH RESULTS)

Şekil 7 incelendiğinde Nano Silikatın değişik oranlarda ikame edilmiş numunelerde 1, 3 ve 7. günlerde etkisi görünmektedir. En iyi sonucu tüm yaşlarda %1.5 ikame edilmiş Nano Silikat vermiştir. Nano silikat %1.5 tan fazla olduğu zaman karışım üzerinde olumsuz etki etmiştir. Şekil 7'yi dikkate aldığımızda Nano Silikatın bu çalışmada doygunluk derecesi %1.5 olarak belirlenmiştir.

TEŞEKKÜR (ACKNOWLEDGEMENT)

Bu makale, TÜBİTAK tarafından desteklenen TÜBİTAK 1001 projesinin 214 M 041 numaralı araştırma projesi kapsamında üretilmiştir. Destekleri için TÜBİTAK'a teşekkür ederim.

KAYNAKLAR (REFERENCES)

ACRA and CSIRO Australian Standards, 2006, *"Guide to Concrete Repair and Protection"*, Australian Concrete Repair Association, Sydney, Australia.

Alexander, M.G., Stanish K., "Durability Design and Specification of Reinforced Concrete Structures Using a Multi-Factored Approach", *Mindess Symposium, Third International Conference on Construction Materials*, Vancouver, 22 - 24 August 2005.

ASTM C39/C39M, 2016, *"Standard Test Method for Compressive Strength of Cylindrical Concrete Specimens"*, American Society for Testing and Materials, Philadelphia, USA.

Cilason, N., "Quality Assurance and Quality Control for Concrete in Hot Climates", *9th International RILEM Conference on Concrete in Hot Climates*, Torquay, England, No. 3, pp. 167-171, 21-25 September 1992.

Kanda, T., Li, V.C., 1999, "A New Micromechanics Design Theory for Pseudo Strain-Hardening Cementitious Composite", *ASCE Journal of Engineering Mechanics*, Vol. 125 (4), pp. 373-381.

Sahmaran M., Li M., Li V.C., 2007, "Transport Properties of Engineered Cementitious Composites under Chloride Exposure", *ACI Materials Journal*, Vol. 104, No. 6, pp. 604-611.

SUJEST, c.5, s.1, 2017
SUJEST, v.5, n.1, 2017
ISSN: 2147-9364 (Electronic)

A GIS BASED NEW NAVIGATION APPROACH FOR REDUCING EMERGENCY VEHICLE'S RESPONSE TIME

[1]Fatih SARI

[1]*Selçuk University Çumra Vocational School Konya, TURKEY*
[1]fatihsari@selcuk.edu.tr

(Geliş/Received: 07.09.2016; Kabul/Accepted in Revised Form: 04.01.2016)

ABSTRACT: Recently, for ensuring human life and safety, routing and intervening emergency vehicles as soon as possible an important subject. Ambulance, firefighter, police and other emergency vehicles are the main object of the intervention. Reaching the emergency area as soon as possible is important for saving human life and preventing economic loss. Directing and routing emergency vehicles from the moment they receive an emergency call to the event location must be considered carefully. In this study, ensuring the shortest response time for the emergency vehicles, obstacles like speed bumps, traffic lights, parking status of the streets, railroad crossings and crossroads which reduce the speed of emergency vehicles and increasing the intervention time are detected. In order to determine the effect of obstacles, a new Segment Effect Value (SEV) formula is developed. Values are assigned to the street segments according to obstacles in particular streets. SEV formula makes possible to determine the routes that provides the shortest intervention time. Results are compared with the shortest route and the shortest time route.

Key Words: *Emergency response time, Network analyst, Geographical information systems, Navigation systems*

Acil Müdahale Araçlarının Müdahale Zamanını Azaltmak İçin Cbs Tabanlı Bir Navıgasyon Yaklaşım

ÖZ: İnsan yaşamını ve güvenliğini sağlamak için acil durum araçlarının olabildiğince hızlı müdahalesi önemli bir konu haline gelmiştir. Ambulans, itfaiye, polis ve diğer araçları acil durum müdahale araçlarının başında gelmektedir. Yaşam kayıplarının ve ekonomik kayıpların önüne geçmek için hızlı müdahale büyük önem taşımaktadır. İhbar alınmasından itibaren olay yerine gidene kadarki yönlendirme dikkatle yapılmalıdır. Müdahale zamanını kısaltmak için hız bariyerleri, trafik ışıkları, park etmiş araçlar, demiryolu geçitleri ve kavşaklar gibi hız kesici engellerin bilinmesi gerekmektedir. Bu engellerin etkisini ortaya koymak için Segment Etki Değeri (SED) isimli bir formül geliştirilmiştir ve bu formül ile her bir cadde segmentine değer atanmıştır. Böylece araçların bu engellerle karşılaşmayacakları en hızlı güzergah üzerinden gitmelerinin sağlanması amaçlanmıştır. En kısa yol ve en hızlı yol arasındaki farklar paylaşılmıştır.

Anahtar Kelimeler: *Acil müdahale zamanı, Ağ analizi, Coğrafi bilgi sistemleri, Navigasyon sistemleri*

INTRODUCTION

The importance of intervention methods are increasing in health, crime, fire and natural disasters (Paraskevi et al., 2010; Konstantinos et al., 2000, Zhang et al., 2016; Lam et al., 2015). Responding to emergency call needs to be managed effectively using decision support systems to save human life and

DOI: 10.15317/Scitech.2017.69

provide public security (Bandyopadhyay and Singh, 2016). Generating decision support systems provide the right decisions in emergency situations and manage the reasons and solutions of the emergency status (Yoon et al., 2008; Mincardi et al., 2007; Aktas and Swalehe, 2016).

Technological developments have led to new techniques in vehicle routing processes. Emergency vehicles use navigation devices to find the shortest routes. These devices lead vehicles to a marked destination point and determine the shortest route. One the other hand, when the working principle is considered, it can be observed that the navigation considers only directions, highways, primary and local roads. This method principle provides only the shortest route information to the emergency vehicles. In addition to this, emergency stations direct vehicles using vehicle tracking systems, but neither drivers nor emergency station workers know the situation on the street itself. Besides, sometimes driver experiences maybe more reliable then the navigation. Additionally, there are various obstacles which reduce vehicle speed. Speed bumps, traffic lights, parking status, railroad crossings and crossroads are the main obstacles for emergency vehicles. When emergency vehicles encounter one of these obstacles, vehicles are forced to slow down or even recalculate or change their route.

In the literature, there are some predicted values about response time of the vehicles. Mohd et al, (2008), provide response times for some countries as shown in Table 1.

Table 1. Ambulance response times 1

Country	ART(Minutes)
United Kingdom	7-14
Australia	7-11
Ankara, Turkey	**9**
Singapore	15
ED of HUSM	15.20
City of New York	11.40
City of Chicago	11.30

Ateş et al, (2011), in their work for determining most appropriate locations for ambulance stations, give also other response times as can be seen in the Table 2.

Table 2. Ambulance response times 2

Country	ART(Minutes)
Mecklenburg, USA (Blackwell and Kaufman, 2001)	6.97
Ankara, Turkey (Altıntaş and Bilir, 2001)	**8.81**
New York, USA (Peters and Hall, 1999)	10.00
Ontario, Canada (Kobusingnye, 2010)	10.30
Ontario, Canada (Peters and Hall, 1999)	8.0
California, USA (Narad and Iesbock, 1999)	8.0
Singapore (Ong et al., 2009)	8.0

As is shown, there is quite a short time to decide, travel and intervene. All the parameters and obstacles must then be known by the drivers and emergency staff to provide the shortest response time.

In the literature, there are a lot of investigations concerning decision support, emergency response and vehicle routing problems (VRP), which developed new methods, new algorithms and emergency response simulations. Many of these are interested in the mathematical algorithm of the methods which are used for vehicle routing. Some of them focused on the simulations that represent the emergency response.

Huang et al., (2012), created a framework for the purpose of response to traffic accidents on highways. Haghani et al., (2003), proposed an optimization model for vehicle routing and dispatching in real time. Liu and Hall, (2002), developed a software to analyze accidents and dispatch ambulances to the accident area. Ozbay and Bartın, (2003), developed a simulation for the analysis of traffic accidents in different situations. Campell et al., (2008), studied routes after disasters using two different methods. Stefan and Walter, (2014), proposed a warehouse location routing problem (WLRP) method and a new formula. Kerstin et al., (2011), studied on high speed ambulances for time savings. Ho and Casey, (1998), Ho and Lindquist (2001), studied on the sirens and lights of ambulances and their time savings in urban areas and in rural areas. Brown et al., (2000), investigated the effects of sirens and lighting of ambulances response times.

In order to determine the shortest route, Ahuja et al., (2002), developed a model to find the shortest travel time. Ziliaskopoulos and Mahmassani, (1993), worked on the shortest route for highway vehicles.

In the literature, it is seen that when determining routes, obstacles were not considered. Generally, the shortest way may not correspond to the shortest time because of the speed factor on route. In this work, obstacles are considered to find the shortest time in addition to the shortest way.

MATERIAL AND METHOD

The purpose of this study is to develop a model providing the shortest response time for emergency vehicles involving street structure and the environment. The model is based on six steps. These are namely; determining of obstacles, choosing the study area, digitizing, calculating the effect coefficient of obstacles, generating Segment Effect Value (SEV) formula and finally determining and comparing the routes.

Determination of the Obstacles

In the first step a discussion was made to detect the obstacles faced by 30 drivers of some emergency vehicles, chosen from 6 different emergency stations. The two questions asked to the drivers were the type obstacles reducing the speeds of vehicles and the importance of specified obstacle. As is shown in Table 3 and 4, the drivers declared 5 types of obstacles namely, speed bumps, traffic lights, parking status, level crossings and crossroads. They claimed that especially speed bumps and traffic lights reduce vehicle speeds considerably. Although the emergency vehicles have transition superiority at traffic lights, the other vehicles waiting usually prevent using this superiority. Parking status and level crossings are less effective obstacles since they depend on width of the street and the frequency of closed level crossings. Particularly in narrow streets, parking status strongly affects the vehicle speed.

Table 3. Obstacle distribution to groups

Groups(Drivers)	Speed Bumps	Traffic Lights	Parking Status(One Side)	Parking Status (Two-Side)	Level Crossing	Crossroads
Group1 (8 drivers)	x	x	x	x	x	x
Group2 (6 drivers)	x	x			x	x
Group3 (4 drivers)	x	x	x	x		
Group4 (4 drivers)	x		x	x		x
Group5 (5 drivers)	x	x			x	
Group6 (3 drivers)	x	x	x	x		x

Table 4. Obstacle importance

Groups	Speed Bumps	Traffic Lights	Parking Status	Level Crossing	Crossroads
Group1 (8 drivers)	1	3	4	5	2
Group2 (6 drivers)	2	1	3	5	4
Group3 (4 drivers)	1	4	2	5	3
Group4 (4 drivers)	3	1	2	5	4
Group5 (5 drivers)	1	2	4	5	3
Group6 (3 drivers)	1	4	2	5	3

Deciding the Study Area

Study area was chosen a region in the city of Konya, Turkey, which has a population of 1.250.000 in the city centre. The population of the region is 4250 which is approximately a responsibility area of one ambulance. Its properties reflect the aim of the study and have freeways, main roads and alleys. There are narrow streets with parking on two sides and the surrounding area is covered by three lane freeways. There exist speed bumps, traffic lights and crossroads in the study area. It has totally 498 street segments with intensively occupied residence buildings. The study area is shown in Figure 1.

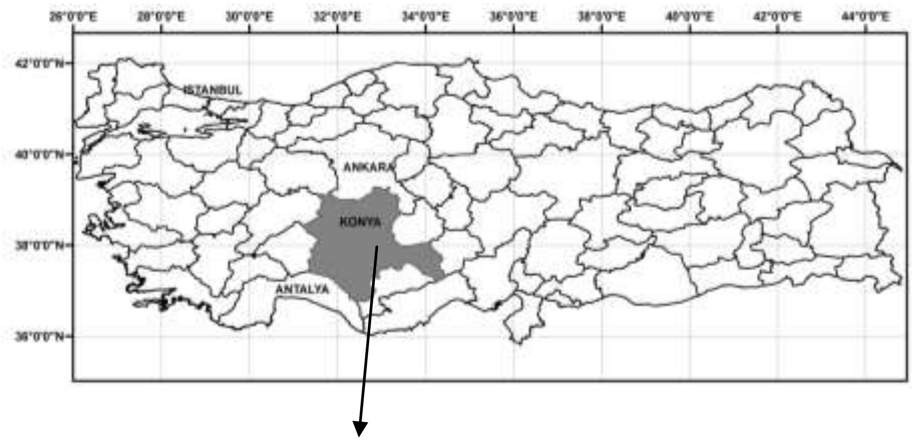

Figure 1. Study area

Digitizing

In this process, all the street segments are digitized by ArcGIS software with using aerial imagery to use the network analyst extension. For the purpose of routing, street names are stored in the database with segment geographic information. After the digitization process, speed bumps, parking status and traffic lights are positioned using Google Earth Street view extension. As can be seen in Figure 2, speed bumps, traffic lights and parking status of segments are defined clearly by using street view. Then the obstacles are integrated with street map by using ArcGIS software and the coordinates are linked with the street segments as attribute data. The parking status of each segment is investigated as one-sided or two sided.

Figure 2. Google Earth street view for obstacle detection

In Figure 3, the attribute table of the segments are given. Name column represents the names of the segments to be able to use street names in route navigation process. Parking status column includes a code list that explain one sided parking (1), two sided parking (2) and no parking (3). Similar to parking status, speed bumps are converted to 1 (segment include speed bumps) and 2 (no speed bump) codes. The width of the street is related to parking status and the maximum limit of the emergency vehichle. The codes then will be used in Segment Effect Value to calculate the delay times for each segment.

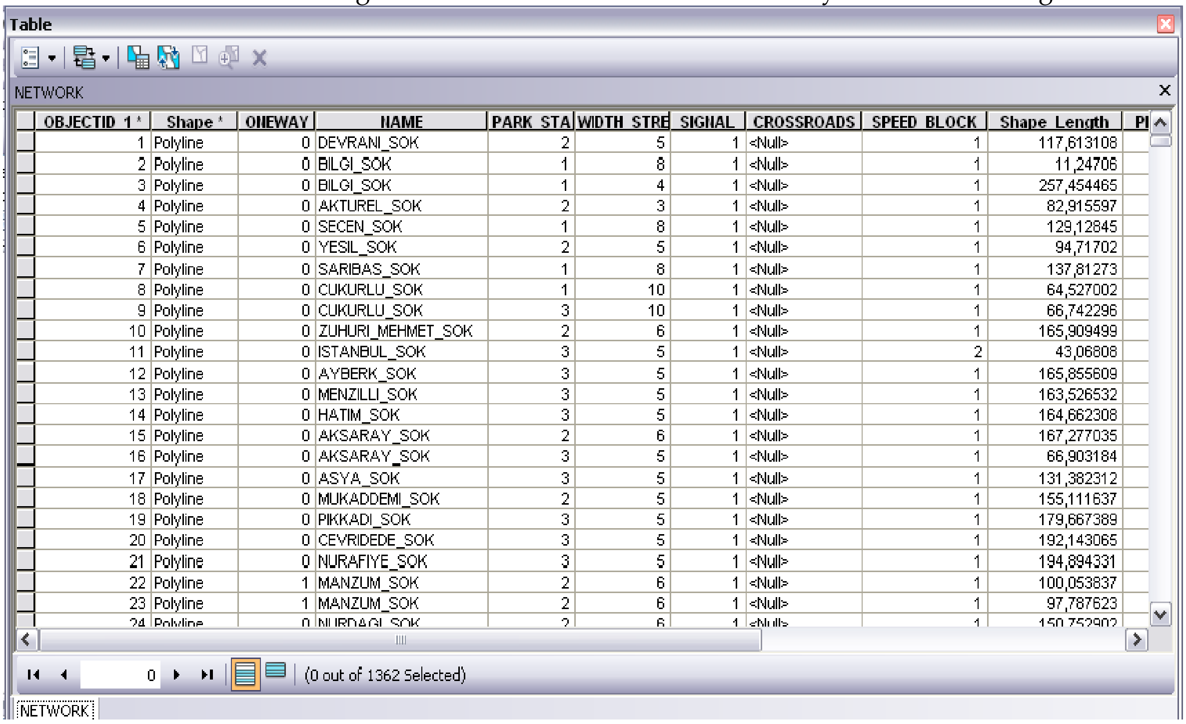

Table

NETWORK

OBJECTID 1 *	Shape *	ONEWAY	NAME	PARK STA	WIDTH STRE	SIGNAL	CROSSROADS	SPEED BLOCK	Shape Length
1	Polyline	0	DEVRANI_SOK	2	5	1	<Null>	1	117,613108
2	Polyline	0	BILGI_SOK	1	8	1	<Null>	1	11,24706
3	Polyline	0	BILGI_SOK	1	4	1	<Null>	1	257,454465
4	Polyline	0	AKTUREL_SOK	2	3	1	<Null>	1	82,915597
5	Polyline	0	SECEN_SOK	1	8	1	<Null>	1	129,12845
6	Polyline	0	YESIL_SOK	2	5	1	<Null>	1	94,71702
7	Polyline	0	SARIBAS_SOK	1	8	1	<Null>	1	137,81273
8	Polyline	0	CUKURLU_SOK	1	10	1	<Null>	1	64,527002
9	Polyline	0	CUKURLU_SOK	3	10	1	<Null>	1	66,742296
10	Polyline	0	ZUHURI_MEHMET_SOK	2	6	1	<Null>	1	165,909499
11	Polyline	0	ISTANBUL_SOK	3	5	1	<Null>	2	43,06808
12	Polyline	0	AYBERK_SOK	3	5	1	<Null>	1	165,855609
13	Polyline	0	MENZILLI_SOK	3	5	1	<Null>	1	163,526532
14	Polyline	0	HATIM_SOK	3	5	1	<Null>	1	164,662308
15	Polyline	0	AKSARAY_SOK	2	6	1	<Null>	1	167,277035
16	Polyline	0	AKSARAY_SOK	3	5	1	<Null>	1	66,903184
17	Polyline	0	ASYA_SOK	3	5	1	<Null>	1	131,382312
18	Polyline	0	MUKADDEMI_SOK	2	5	1	<Null>	1	155,111637
19	Polyline	0	PIKKADI_SOK	3	5	1	<Null>	1	179,667389
20	Polyline	0	CEVRIDEDE_SOK	3	5	1	<Null>	1	192,143065
21	Polyline	0	NURAFIYE_SOK	3	5	1	<Null>	1	194,894331
22	Polyline	1	MANZUM_SOK	2	6	1	<Null>	1	100,053837
23	Polyline	1	MANZUM_SOK	2	6	1	<Null>	1	97,787623
24	Polyline	0	NURDAGI_SOK	2	6	1	<Null>	1	150,752902

0 (0 out of 1362 Selected)

NETWORK

Figure 3. Digitized study area with obstacles and parking status

Calculating the Effect Coefficient of the Obstacles

Obstacles affect vehicle speeds for different time periods. In order to determine the time delay on vehicles, information on 54 routes of 10 emergency vehicles were obtained from the vehicle tracking systems. The route information includes the speed of the vehicle at any time, acceleration-deceleration information and total response. The streets in the 54 routes were examined considering the obstacles and motions of the vehicles in order to find the delay time of the 10 different vehicles.

The calculated effects and delay times are shown in Table 5 for speed bumps, parking status (one-side), parking status (two-side), traffic lights, level crossings and crossroads. For each obstacle two time values have determined to find the delay time. The first values are the travel times with 50 km/h fixed speed without any obstacles. The second values are the travel times of the vehicles with obstacles. The difference between these two values gives the delay time. Finally, the average delay time of 10 different vehicles assigned as the delay time of the stated obstacles. Delay times of the obstacles are shown in the Table 5.

Table 5. Delay times

Obstacles	Delay time(Sec)
Speed Bumps	7.83
Parking Status(One-Sided)	2.05
Parking Status (Two-Sided)	6.22
Traffic Lights	18.02
Level Crossing	3.24
Crossroads	11.41

In Figure 4, acceleration graphics of the vehicles are shown for each obstacle. The graphics are drawn by using the average of the values obtained from 10 different vehicles values.

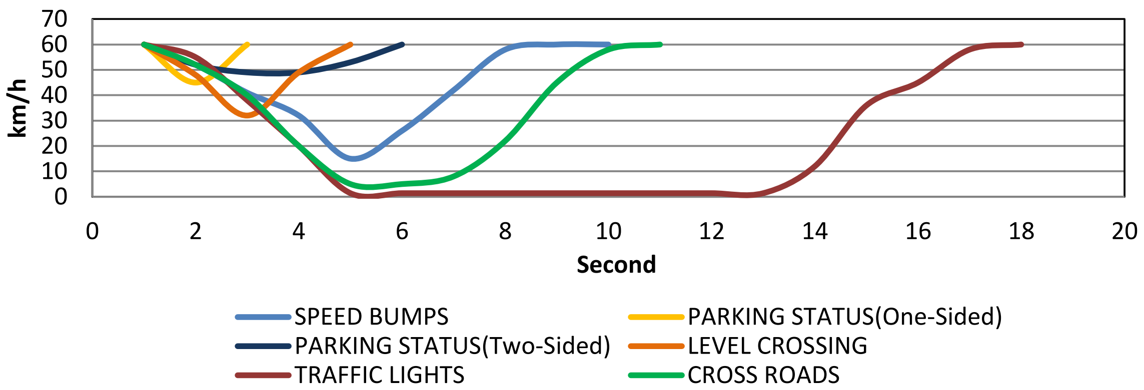

Figure 4. Acceleration graphics

Generating Segment Effect Value (SEV) Formula

Each road segment may contain one or more obstacles. For example speed bumps, two side parking and at the end of the street traffic lights may exist. Each segment should be examined with the obstacles it has. For finding the total effect of the obstacles on vehicle speeds, total delay time value should be calculated. To do this, Segment Effect Value formula is developed to calculate a delay time for each segment. Finally, these values will be used in determining the shortest response time routes.

The Segment Effect Value Formula is,

$$\bar{x} = (n\,S_i + ((SL_{i(m)}\,PO_i)/100_{(m)}) + ((SL_{i(m)}\,PT_i)/100_{(m)}) + n\,T_i + n\,L_i) \qquad (1)$$

Where n is the count of objects, Si, POi ,PTi ,Ti, Li are the delay times in second and SLi is the road segment length in meter. The coefficients are representing;

Si: Speed Bumps (sec);
Poi: One-Side parked streets (sec),
Pti: Two-Side parked street (sec),
Ti: Traffic Lights (sec),

Li: Level Crossing (sec)

In SEV formula, parking status coefficients are multiplied with the segment length and divided by 100 meter. The reason for this is parking status affects the vehicle continuously until the end of the segment. For example, if one vehicle is drawn at 50 km/h speed, in a road with one sided parking status the actual vehicle speed is 47 km/h. This status therefore, is affecting the vehicle speed depending on the segment length. The other obstacles are also affecting the vehicle speed at the point of obstacles the vehicles pass through the obstacles. Then the coefficients should be multiplied by the number of concerned obstacles. Multiplying the obstacle number by the coefficient gives the total effect. For example, in one segment if there is no speed bump, "n" value will be equal to zero and there will be no speed bump effect.

Delay times are determined by using the SEV formula for each 498 segments. Some of these values are shown in Table 6. SEV determining includes total delay time considering the obstacles that segments have as a sum of every obstacle delay time which are given in Table 5. Si, Poi, PTi, Ti and Li values represent the delay times for each obstacle and nSi, nPOi, nPTi, nTi, and nLi values represent the count of obstacle in each segment. As shown, segments number 17, 56 and 223 provide the shortest response times for vehicles with minimum delay times. These segments are seen to be freeways without traffic lights.

Table 6. SEV determining

Segment Number	Segment Length	nSi	Si	nPOi	POi	nPTi	PTi	nTi	Ti	nLi	Li	Delay Time(sec)
1	375.85	0	7.83	1	2.05	0	6.22	0	18.02	0	3.24	7.83
19	519.96	1	7.83	0	2.05	1	6.22	0	18.02	0	3.24	18.49
56	331.73	0	7.83	0	2.05	0	6.22	0	18.02	0	3.24	0.00
…	…	…	…	…	…	…	…	…	…	…	…	…
182	107.25	1	7.83	1	2.05	0	6.22	0	18.02	0	3.24	10.02
223	359.93	1	7.83	0	2.05	0	6.22	0	18.02	0	3.24	7.83
257	113.06	1	7.83	1	2.05	0	6.22	0	18.02	0	3.24	10.14
311	30.47	1	7.83	0	2.05	1	6.22	0	18.02	0	3.24	8.45
424	356.24	0	7.83	0	2.05	1	6.22	1	18.02	0	3.24	29.46

Another example is the segments 19 and 311. Although these segments have the same obstacles, their effect delay times are different since their lengths are different. In 311, the vehicle will return or pass to another segment after a speed bump under its normal speed. But in segment 19, after passing a speed bump for 520 meters the vehicle reaches its normal speed. So, the SEV formula is considers the segment length and calculates the delay times.

Determining and Comparing the Routes

As a result, routes in status are calculated by ArcGIS Network Analyst Tool, the shortest path and the shortest response time. There are two network datasets for each situation and some properties are the same for both network datasets. These are lengths and travel time properties. Travel times are the time which vehicles need to pass through the segment and total route. Travel times calculated for 40, 50 and 60km/h speeds. This value changes with which segment route is followed. With these different calculations, the travel time will be estimated more accurately.

For calculating the shortest response time routes, a new facility is added to the network dataset. This is a hierarchy property which will decide the shortest response time route. The hierarchy property is shown in network dataset properties window in Figure 5.

Figure 5. Network dataset properties

.

In this network dataset, the entire segment's effect values are stored in segment attribute table and by using hierarchy; a decision making process calculates the route comparing the effect values and choose the segments. The routes follow the segments having fewer obstacles. By hierarchy, 3 intervals are specified to make a preference between segments comparing the Segment effect values. These interval groups are given in Table 7. As shown, the first interval (0-5) represents the best segments for the shortest response time. The second interval (5-18) is for the normal segments. These segments will be used if there are no segments for which segment effect value is in the first interval. The third interval (18-50) has the worst segments that most reducing vehicle speeds considerably.

Table 7. Hierarchy interval

Group	Interval(sec)
1	0.00-0.05
2	0.05-0.18
3	0.18-0.36

Finally, to see the results, all calculated values and the routes are compared by using both numerical and graphical methods. In Figure 6, the shortest route and the shortest response time routes are shown for the same origin and for 8 different destination points. The blue routes are the shortest response time routes and the red routes are the shortest distance routes.

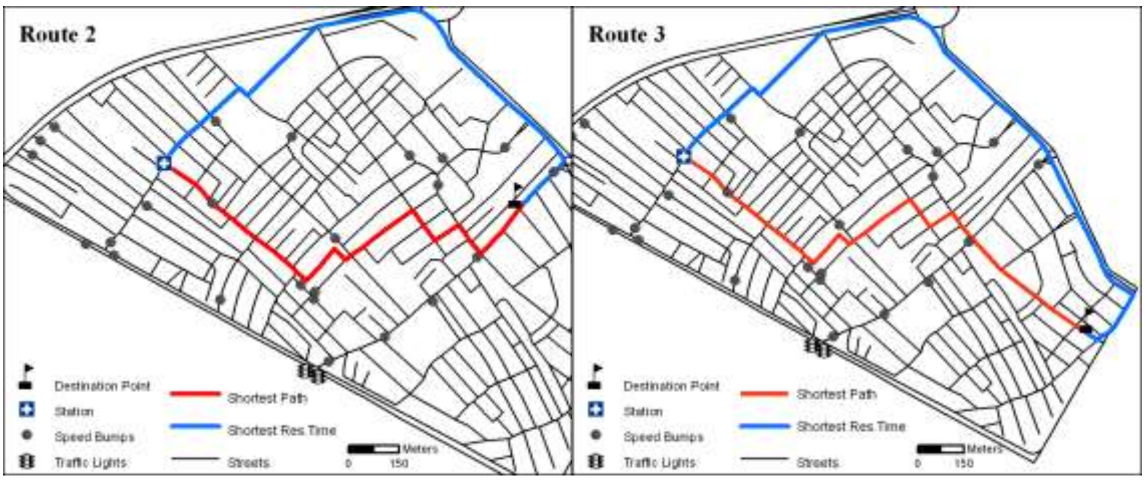

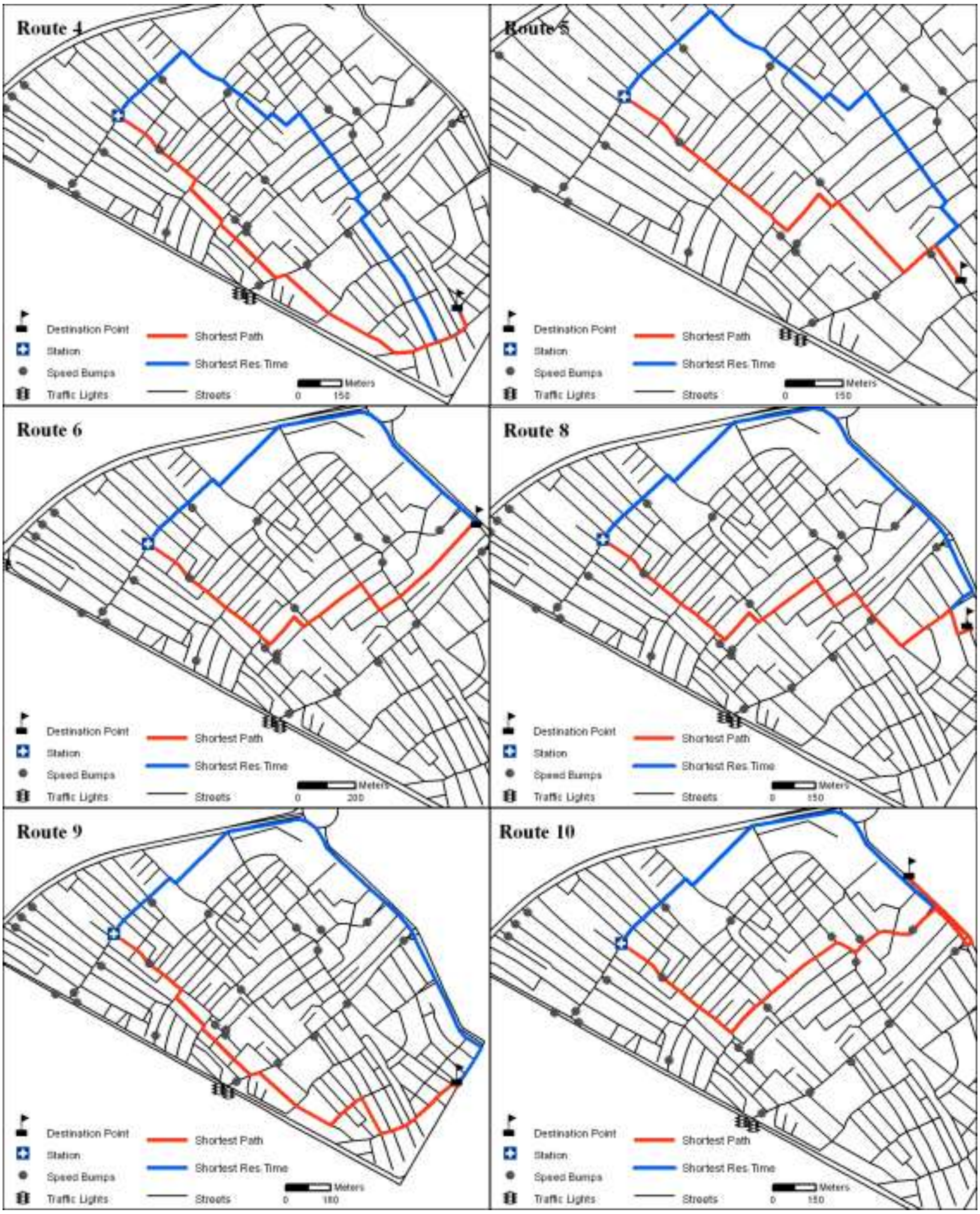

Figure 6. Routes and comparisons

One of the important obstacles which affect the vehicle speeds are crossroads. Crossroads may reduce vehicle speeds to zero and according to the type of vehicle it takes some time to reach to the normal speed. One important point is that, the crossroads can only be calculated after determining the routes, because we actually do not know where the route will go and how many crossroads the vehicle will encounter. Therefore, the crossroad factor is not considered in the SEV formula and it will be added to the total travel time of the shortest route or the shortest response time route. The final results are given in Table 8.

In Table 8, SL represents total length of the shortest way route, SLi total length of the SEV route, T is travel time of shortest way route, Ti travel time of SEV route, C is crossroad number of shortest way route, Ci crossroad number of SEV route, Total T is total travle time of shortest way route, Total Ti total travle time of SEV route and T-Ti is the benefit of travel times in second unit. .

As can be seen from Table 8, the travel time is calculated for each of the 15 routes. When the results are compared, it is shown that vehicles are gaining a minimum of 5.9 and a maximum of 82.18 seconds. In routes that follow freeways, the vehicles can go faster in the shortest response time routes. (Figure 6-a.b.e.g.h). On freeways there are only traffic lights, and therefore vehicles are going faster than in alleys. One advantage of the freeways is having less crossroads, so the vehicles can travel at a fixed speed.

Table 8. Time and length compare of two situation

Route No	SL	SLi	(SL - SLi)	T	Ti	C	Ci	Total T	Total Ti	T-Ti
R1	938.65	947.03	-8.35	103.88	101.53	8	3	195.16	135.76	59.40
R2	1482.92	1763.12	-280.20	149.97	127.26	6	2	218.43	150.08	68.35
R3	1834.73	2258.55	-423.82	189.44	150.65	4	1	235.08	162.06	73.02
R4	1990.01	1677.54	312.47	197.38	170.21	5	2	254.43	193.03	61.40
R5	1848.54	1925.65	-77.11	190.08	147.56	4	2	235.72	170.38	65.34
R6	1775.53	2011.22	-235.69	177.76	149.63	6	3	246.22	183.86	62.36
R7	1284.77	1300.70	-15.93	139.09	133.41	5	2	196.14	156.23	39.91
R8	1543.40	1417.75	125.65	155.41	105.82	2	0	178.23	105.82	72.41
R9	1934.30	2263.16	-328.86	208.53	149.17	3	1	242.76	160.58	82.18
R10	1026.03	1052.83	-26.80	111.74	105.84	1	1	123.15	117.25	5.90
R11	894.79	894.58	0.21	105.08	80.51	6	4	173.54	126.15	47.39
R12	1475.52	1462.69	12.83	172.58	145.71	3	1	206.81	157.12	49.69
R13	996.78	1197.35	-200.57	126.85	117.70	4	2	172.49	140.52	31.97
R14	694.25	694.75	-0.50	54.87	48.10	5	3	111.92	82.33	29.59
R15	1992.78	2161.74	-168.96	178.73	147.76	5	2	235.78	170.58	65.20

The most remarkable result of this study is that usually the shortest response time routes are longer than the shortest way routes. For instance, Route 3 in Table 8, the shortest response time route is 424 meter longer than the shortest route. If have a look to the response times, the shortest response time route results a gain of 73 seconds. This is a serious time to intervene to the emergency calls like fire and heart attack. The SEV formula may provide faster and earlier intervention for emergency calls. SL-SLi, T-Ti, Total T-Total Ti and nC-nCi comparisons are given in Figure 7.

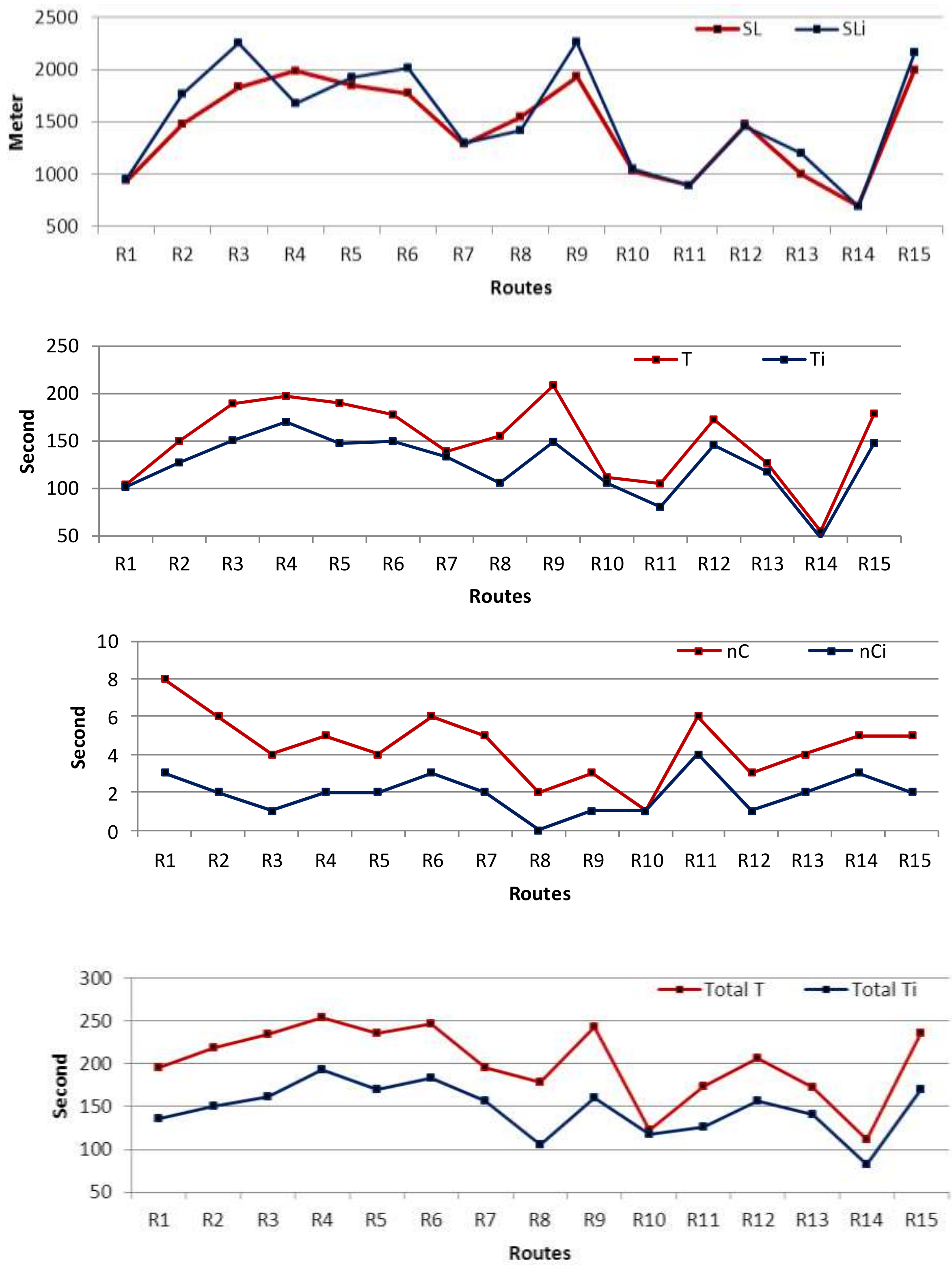

Figure 7. Routes and comparisons

RESULT AND DISCUSSION

Traditional navigation systems determine routes with only limited parameters. These systems do not give actual travel times to the vehicles on shortest routes. In emergency calls, human life especially depends on the travel times of the emergency vehicles. Considering the vehicle, sizes and emergency types, the travel times are being more important. By the Segment Effect Value formula, the shortest response time route can be calculated as well as the shortest route. Therefore, the formula provides the vehicles the most suitable routes allowing vehicles to gain a respectable time for intervention. At this point, data collection and defining routes should be investigated carefully. Especially closed or under construction roads, speed bumps and recent traffic status should be updated periodically. Nowadays, some municipalities have traffic monitoring and automatic vehicle counting systems to determine the traffic status of cities. Addition to this, Google Traffic service provides real time traffic data for main roads of the cities. This study can be integrated with one of these systems to determine real time navigation. Closed or roads that under construction data can be retrieved from the General Directorate of Highways provincial offices to determine real time shortest response time routes.

On the other hand, determining new fire and ambulance station locations can be investigated via SEV infrastructure. Thus, more realistic intervention times and related locations can be determined more accurately. New service areas, location-allocation and vehicle routing problems, which are related to network analysts, should be investigated for all emergency stations with environmental parameters such as population, topography of the streets and regions like industry, living and agriculture.

This study can be modified according to the types of emergency vehicles and for different conditions of the regions and countries. Especially for large vehicles, street width parameter can be added to the SEV Formula. The SEV Formula is designed allowing for adding new parameters.

REFERENCES

Ahuja, R., Orlin, K., James, B., Pallottino, S., Scutella, M. G., 2002, *Dynamic Shortest Paths Minimizing Travel Times and Costs*, MIT Sloan Working Paper; No. 4390-02.

Aktas, S.G., Swalehe, M., 2016, "Dynamic Ambulance Deployment to Reduce Ambulance Response Times using Geographic Information Systems: A Case Study of Odunpazari District of Eskisehir Province, Turkey", *Procedia Environmental Sciences*, Vol. 36, pp. 199 – 206.

Altınbaş, K. H., Bilir, N., 2001, Ambulance Times of Ankara Emergency Aid and Rescue Services Ambulance System", *European Journal of Emergency Medicine,* Vol. 8, pp. 43-50.

Ateş, S., Coşkun, Z. M., Aydınoğlu, A. Ç., "Coğrafi Bilgi Sistemleri ile En Uygun Ambulans Yerlerinin Belirlenmesi", *13. Türkiye Harita Bilimsel ve Teknik Kurultayı*, Ankara, 18-22 Nisan 2011.

Bandyopadhyay, M., Singh, V., 2016, "Development of Agent Based Model For Predicting Emergency Response Time", *Perspectives in Science,* Vol. 8, pp. 138—141.

Blackwell, T. H. Kaufman, J . S., 2001, "Response Time Effectiveness: Comparison of Response Time and Survival in an Urban Emergency Medical Services System", *Academic Emergency Management*, Vol. 9, pp. 288-295.

Brown, L.H., Whitney, C.L., Hunt, R.C., Addario, M., Hogue, T., 2000, "Do Warning Lights and Sirens Reduce Ambulance Response Times?", *Prehospital Emergency Care*, Vol. 4, pp. 70–74.

Campbell A, M., Vandenbussche D., Hermann W., 2008, "Routing for Relief Efforts", *Transportation Science,* Vol. 42, pp. 127–145.

Haghani, A., H. Hu., Q. Tian., "An Optimization Model for Real-Time Emergency Vehicle Dispatching and Routing". In: the 82nd Annual Meeting of the Transportation Research Board, Washington, D.C., 12-16 January 2003.

Ho, J., Casey, B., 1998, "Time Saved with Use of Emergency Warning Lights and Sirens During Response to Requests for Emergency Medical Aid in Urban Environment", *Annals of Emergency Medicine, Vol.* 32 (5), pp. 585–588.

Ho, J., Lindquist, M., 2001, "Time Saved with Use of Emergency Warning Lights and Siren While Responding to Requests for Emergency Medical Aid in A Rural Environment", *Prehospital Emergency Care*, Vol. 5, pp. 159–162.

Huang, D., Chu, X., Mao Z., 2012, "A Simulation Framework for Emergency Response of Highway Traffic Accident", *Procedia Engineering,* Vol. 29, pp. 1075 - 1080.

Kerstin P., Jan, P., Jörgen, J., Gun N., 2011, "Time Saved with High Speed Driving of Ambulances", *Accident Analysis and Prevention*, Vol. 43(3), pp. 818–822.

Kobusingye OC, Hyder AA, Bishai D, Joshipura M, Hicks ER, Mock C., 2010, *Emergency Medical Services,*New York: John Wiley & Sons Ltd; 2010.p.167-. 169. 17.

Konstantinos G. Zografos., George M. Vasilakis., Ioanna M. Giannouli., 2000, "Methodological Framework for Developing Decision Support Systems (DSS) for Hazardous Materials Emergency Response Operations", *Journal of Hazardous Materials*, Vol. 71 (1–3.7), pp. 503–521.

Lam, S.S., Zhang, J., Zhang, Z. C., Oh, H. C., Overton, J., Ng, Y. Y., Ong, M. E., 2015, "Dynamic Ambulance Reallocation for The Reduction of Ambulance Response Times Using System Status Management", *The American Journal of Emergency Medicine,* Vol. 33, pp. 159-166.

Liu, H., Hall, R., 2002, *W. INCISIM: User's Manual. California Path Research Report*; UCB-ITS-PWP-2000-15.

Minciardi, R., Sacile, R., Trasforini, E., 2007, "A Decision Support System for Resource Intervention in Real-Time Emergency Management", *International Journal of Emergency Management,* Vol. 4 (1), pp. 59-71.

Mohd, S., Mohd, I., Syed, M., 2008, "Ambulance Response Time and Emergency Medical Dispatcher Program: A study in Kelantan, MALAYSIA", *Southeast Asian Journal of Tropical Medicine and Public,* Vol 39 (6).

Narad, R. A., Iesbock, K. R., 1999, "Regulation of Ambulance Response Time in California", *Prehospital Emergency Care*, Vol. 3, pp. 131-135.

Ong M, E., Ng FS., Overton J., Yap S., Andresen D., Yong DK., Lim SH., Anantharaman V., 2009, "Geographic Time Distribution of Ambulance Calls in Singapore: Utility of Geographic Information System in Ambulance Deployment", *Annals Academy of Medicine*, Vol. 38, pp.91-94.

Ozbay, K., Bartin, B., 2003, "Incident Management Simulation", *Simulation*, Vol. 79(2), pp. 69-82.

Paraskevi S. Georgiadoua, Ioannis A. Papazoglou, Chris T. Kiranoudisa, Nikolaos C. Markatosa., 2010, "Multi-Objective Evolutionary Emergency Response Optimization for Major Accidents", *Journal of Hazardous Materials*, Vol. 178, pp. 792–803.

Peter S, J., Hall, G. B., 1999, "Assessment of Ambulance Response Performance Using A Geographic Information System", *Social Science & Medicine*, Vol. 49, pp. 1551-1556.

Stefan, R., Walter,.G., 2014, "A Math-Heuristic for The Warehouse Location–Routing Problem in Disaster Relief", *Computers & Operations Research*, Vol. 42, pp. 25 – 39.

Yoon, S,W., Velasquez, J.D., Partridge, B.K., Nof., S,Y., 2008, "Transportation Security Decision Support System for Emergency Response: A Training Prototype", *Decision Support Systems*, Vol. 46, pp. 139–148.

Zhang, Z., He, Q., Gou, J., Li,X., 2016, "Performance Measure for Reliable Travel Time of Emergency Vehicles, *Transportation Research Part C*, Vol. 65, pp. 97–110.

Ziliaskopoulos, A., H. Mahmassani., 1993, "Time Dependent, Shortest-Path Algorithm for Real-Time Intelligent Vehicle Highway System Applications", *Transportation Research Record,* 1480; pp. 94-100

Lin, S.H., Lai, C.L., 2000, "Kinetic Characteristic of Textile Wastewater Ozonation in Fluidized and Fixed Activated Carbon Belts", *Water Research, Vol.* 34, pp. 763-772.

SUJEST, c.5, s.1, 2017
SUJEST, v.5, n.1, 2017
ISSN: 2147-9364 (Electronic)

OBJE YÜZEY EĞİMLERİNİN YERSEL LAZER TARAYICILARIN KONUM DOĞRULUĞUNA ETKİLERİ

[1]Aydan YAMAN, [2]Hacı Murat YILMAZ, [3]Müge AĞCA YILDIRIM

[1,2,3]*Aksaray Üniversitesi, Mühendislik Fakültesi, Harita Mühendisliği Bölümü, AKSARAY*
[1]aydan.ketenci@hotmail.com, [2]hmuraty@gmail.com, [3]mugekaan@gmail.com

(Geliş/Received: 05.10.2016; Kabul/Accepted in Revised Form: 03.12.2016)

ÖZ: Lazer tarama, henüz yeni bir teknoloji olmasına rağmen günümüzde teknolojideki ilerlemelerle birlikte bu teknoloji de gelişmekte olup bununla beraber kullanım alanı da giderek artmaktadır.Lazer tarama teknolojisi ile istenilen objelerin üç boyutlu görüntüleri diğer klasik ölçme yöntemlerine göre çok daha hızlı, pratik, kolay ve yüksek doğrulukla elde edilebilmekte ve ölçümler her türlü hava koşulunda yapılabilmektedir. Ayrıca bu yöntem ile objeler, temas zorunluluğu olmadan uzaktan ölçülebilmektedir. Yapılan çalışmada Topcon Yersel Lazer Tarayıcı ile belirli bir mesafeden çeşitli açılar verdirilen test alanının taratılarak bu açıların yersel lazer tarayıcının konum doğruluğuna etkisi araştırıldı. Bunun için düşey konumda duran 2.10 m x2.80 m boyutlarına sahip bir test alanı 35 m mesafeden dik, 15^0, 30^0, 45^0 ve 60^0 lik açılar ile tarandı. Taramalardan elde edilen Y ve Z koordinatları yer değiştirilerek test alanı yatay hale getirildi. Bu durumda oluşan yarım dikdörtgen prizmanın olması gereken hacmi ile taramalardan elde edilen hacimleri hesaplandı. Hacim farklarına göre yapılan değerlendirmeler sonunda bu tarayıcının 35 m' lik tarama mesafesinde konum doğruluğunun 2.9 mm ile 12.1 mm arasında olduğu görüldü. Ayrıca en uygun taramanın objenin 15^0 lik açıya sahip iken yapılan tarama olduğu gözlendi.

Anahtar Kelimeler: *Lazer tarama teknolojisi, Konum doğruluğu, Tarama açısı, Hacim*

Effects Of Different Object Surface Tilts On Terrestrial Laser Scanner Position Accuracy

ABSTRACT: The terrestrial laser scanning systems are a relatively new measurement technology. Along with technological advances, these systems are gaining popularity and have been increasingly used in many different fields. With terrestrial laser scanning technology, three- dimensional (3D) information and images of objects can be obtained more practical, easy and with high accuracy compared to conventional methods. Additionally, measurement of an object is performed without being in physical contact. In this study, our test area 2.10m×2.80m in vertical position was scanned at 35 m distance from different angles(vertical, 15^0, 30^0, $45^0$and 60^0) with Topcon laser scanner and laser scanner's position accuracy according to this angles were investigated. By switching Y and Z coordinates obtained from laser scanning, test area was changed to horizontal position. In this case, expected a half rectangular prism' volume and volumes obtained from laser scanning were calculated. Based on our volume differences evaluation results, it was found that within scanning distance of 35 meters position accuracy of this laser scanner is between 2.9 mm and 12.1 mm. In addition, the optimal laser scanning was 15^0 angle.

Key Words: *Laser scanning technology, Position accuracy, Scan angle, Volume*

DOI: 10.15317/Scitech.2017.70

GİRİŞ (INTRODUCTION)

Lazer teknolojisi alanındaki araştırmalar 1960 yılından bu yana 40 yılı geçkin bir tarihe sahiptir. Yersel lazer tarama teknolojisinin bir ölçüm aracı olarak gerçekten bir araştırma alanı haline gelmesi sadece son 10 yılda olmuştur. Tek renklilik, iyi kolimasyon, yüksek güç, kısa atımlar veya lazer ışığının ayarlanmasının muhtemelliği gibi lazer radyasyonunun belirli niteliklerinden dolayı ölçümler için kullanılan bu teknolojinin avantajı daha yeni fark edildi. Hızlı ve minimum giderle acilen bütün obje (3 boyutlu model) hakkında eksiksiz 3 boyutlu geometrik ve görsel bilgiye ulaşmak lazer tarama teknolojileri ile olmaktadır (Gümüş ve Erkaya, 2007).

Bu teknoloji ile istenilen obje yüzeyi hızlı bir şekilde taranarak objeye ait çok sayıda üç boyutlu nokta koordinatlarını içeren nokta bulutu verileri kısa sürede ve ekonomik olarak elde edilmektedir.

Lazer tarayıcılarla elde edilen ve nokta bulutu olarak adlandırılan 3 boyutlu nokta verilerinin işlenmesiyle 3 boyutlu modeller elde edilebilmektedir. Elde edilen bu üç boyutlu modeller ile gerekli geometrik ve görsel birçok veriye ulaşmak mümkün hale gelmektedir (Karşıdağ, 2011).

Lazer tarama işlemiyle elde edilen nokta bulutundan; temel ölçme verileri, ortofoto görüntüler, iki veya üç boyutlu çizimler, 3 boyutlu animasyon, katı yüzey modelleri ya da doku giydirilmiş üç boyutlu modeller elde edilebilir. Etkin bir veri toplama tekniği olan lazer tarayıcılar hem ölçmecilere hem de bu ölçüleri kullananlara büyük kolaylık sağlar. Lazer tarama yönteminin avantajları; hızlı ve obje ile temas kurmadan ölçme, aynı ölçme alanı için daha fazla veri toplama, lazer ölçülerinin var olan başka tür ölçülerle kolayca entegrasyonu, daha güvenli veri toplama imkanı, gerçek renkli görüntü üretebilme, ölçme alanının belirli periyotlarla tamamen ölçülebilmesi olarak sıralanabilir. (Altuntaş ve Yıldız, 2008).

Bu teknoloji ile yapılacak çalışmalar da çok hızlı olarak tamamlanmaktadır. Ayrıca elde edilen sonuçlar da yeterli duyarlılıktadır. Yersel lazer tarayıcıların, kısa zamanda ve hızlı bir şekilde üç boyutlu (x, y, z) nokta bilgisi ölçmesi, nokta sıklığının ayarlanabilmesi ve ölçüm sonucu elde edilen verinin farklı formatlarda görüntülenebilme imkanı sağlaması yöntemin diğer önemli avantajlarındandır.

Yersel lazer tarama yönteminin sağlamış olduğu bir başka avantaj ise, özellikle karmaşık geometrideki objelerin ve yüzeylerin diğer ölçme yöntemlerine kıyasla çok kısa sürede ve yüksek detay zenginliğinde üç boyutlu olarak elde edilebilmesidir (Aydar ve diğ., 2011).

Lazer tarama cihazları ile yapılan ölçümlerde insanlardan kaynaklanan hatalar klasik ölçme yöntemlerine göre daha az olduğu için ölçüm sonuçları da klasik yöntemlere göre çok daha hassas olmaktadır. Ayrıca bu yöntem geleneksel ölçme teknikleri ile kıyaslandığı zaman 3 boyutlu nokta bilgilerinin çok yüksek hızla elde edilebildiği bir ölçme tekniğidir. Ölçme alanının 3 boyutlu nokta bilgileri, nokta dizileri şeklinde yüksek doğrulukla ölçülebilmektedir. Yersel lazer tarayıcılar pek çok ölçme uygulamasında giderek artan bir oranla kullanılmaktadır (Altuntaş ve Yıldız, 2008).

Lazer teknolojisi, özellikle jeodezik ve inşaat mühendisliği ile ilgili çalışmalarda, elektronik uzunluk ölçümlerinde, tünellerde, madenlerde, ulaşım ve altyapı çalışmaları gibi çalışmalarda yaygın olarak kullanılmaktadır. Ayrıca, obje veya alanların deformasyonlarının belirlenmesi, mimarlık gibi alanlarda ve tarihi ve kültürel objelerin üç boyutlu modellenmesi çalışmalarında da yaygın olarak kullanılmaktadır.

Yapılan çalışmada, test alanına farklı açılar verdirilerek topcon yersel lazer tarayıcı ile tarama işlemi yapılmış ve bu açılara bağlı olarak yersel lazer tarayıcının konum doğruluğu araştırılmıştır.

MATERYAL ve YÖNTEM (MATERIAL and METHOD)

Test Alanı (Test Area)

Yapılan çalışmada kullanmak amacıyla öncelikle sanayide 2.10 metre ve 2.80 metre boyutlarında bir test alanı yaptırılmıştır. Bu test alanının içi çelik dış yüzeyi ise sunta kaplama olup Şekil 1′ de görüldüğü gibi özel demir ayaklar üzerine oturtulmuş sabit, sallanmayan bir özelliktedir.

Şekil 1. Test alanı
Figure 1.*The test area*

Test alanının tam düşey olmasını sağlamak amacıyla ayakları ve arka kısmında düzeç vidaları ve üzerinde düzeçler bulunmaktadır. Bunlar yardımıyla test alanı düşey hale getirilmiştir. Üzerindeki sunta kaplama yüzey, ışığı en fazla yansıtan renk olduğundan beyaz olarak seçilmiştir.

Topcon Yersel Lazer Tarayıcı (Topcon Terrestrial Laser Scanner)

Yapılan çalışmada Şekil 2' de görülen "Topcon GLS-1000" marka yersel lazer tarayıcı kullanılmıştır. Topcon yersel lazer tarayıcı hızlı bir şekilde veri toplama ve saklama özelliğine sahiptir. Hassas tarama teknolojisi, 2 megapiksel dijital kamera, saniyede 3000 nokta tarama hızı, 330 metre menzile kadar %90 yansıtma, 1 metreden 150 metreye kadar 4 mm doğruluk sağlama, yatayda ve düşeyde 6'' açı doğruluğu, yatay ve düşeyde hareket edebilme özelliklerine sahiptir.

Topcon yersel lazer tarayıcı ile yapılan taramalarda nokta bulutlarında daha az gürültü meydana gelmektedir ve 100 metrenin üzerindeki mesafelerde bile yeterli doğruluğa sahiptir.

Şekil 2. Topcon yersel lazer tarayıcı
Figure 2. *Topcon Terrestrial laser scanner*

Yöntem (Method)

Yapılan çalışmada amaç test alanına farklı açılar verilerek topcon yersel lazer tarayıcının tarama doğruluğunun belirlenmesidir. Bu amaç için oluşturulan test alanının farklı tarama açılarında yapılan taramalarından elde edilen nokta bulutları yardımıyla test alanının yatay konuma getirildikten sonra oluşacak hacimlerini hesaplayarak bilinen hacimleri ile karşılaştırmalarını yapmak ve en uygun tarama açısını belirlemektir. Bunun için ayakları ve arka kısmında bulunan düzeçler yardımıyla düşeyliği sağlanan test alanının düşeyliğinin tekrar kontrol edilmesi için jeodezik ölçme aleti total station ile test alanı üzerinde lokal sistemde 2.70×2.00 metre boyutundaki alanda boyutu 10 cm olan kare grid ağı oluşturularak Şekil 3′ de görüldüğü gibi elde edilen 588 noktanın koordinatları okunmuştur. Y ve Z koordinatları yer değiştirilerek test alanının üç boyutlu görüntüsü elde edilmiştir ve Şekil 4′ de sunulmuştur.

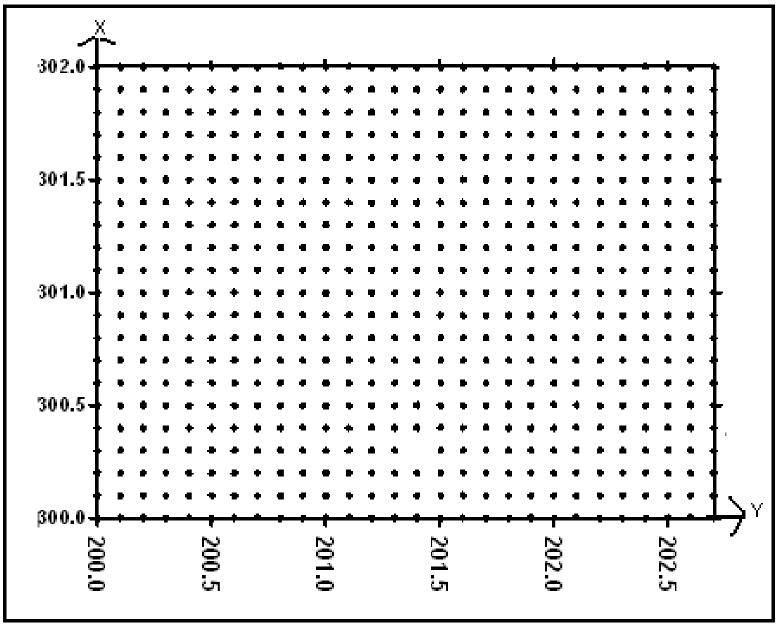

Şekil 3. Test alanı üzerinde oluşturulan grid ağı
Figure 3. *The grid network created on test area*

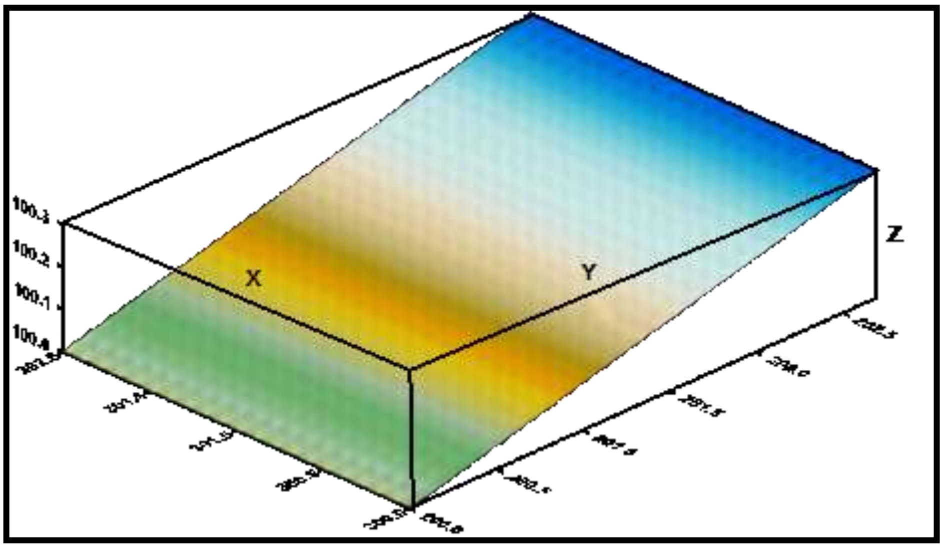

Şekil 4. Test alanındaki grid ağının üç boyutlu görüntüsü
Figure 4. *Three dimensional image of the grid network on the test area*

Grid ağının koordinatlandırılmasında tanımlanan koordinat sistemi test alanına dik olmadığından bir dikdörtgen prizmanın yarısı kadar bir yüzey elde edilmektedir. Bu yüzeyin olması gereken hacmi 0.8154 m^3, elde edilen koordinatlarla hesaplanan hacmi ise 0.8165 m^3 olarak dikdörtgen prizmanın hacim hesabı yöntemine göre hesaplanmıştır.

Sonuçların çok yakın olması test alanının düşeyliğinin sayısal olarak da sağlandığını göstermektedir. Ayrıca test alanı üzerinde okunan koordinatlarda bir sistematiğin olması da gerekmektedir. Bu durumda üç eksen boyunca görsel olarak da kontrol edildi. Eksenlere ait X, Y ve Z koordinatlarının kendi aralarındaki sistematik Şekil 5, Şekil 6 ve Şekil 7′ de görülmektedir.

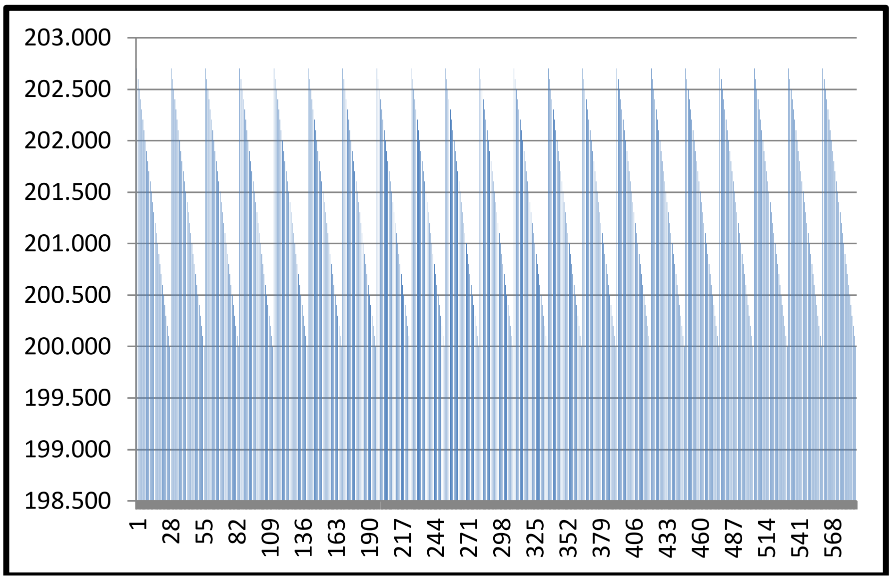

Şekil 5. X koordinatları arasındaki sistematiklik

Figure 5. *Systematicty between the x coordinates*

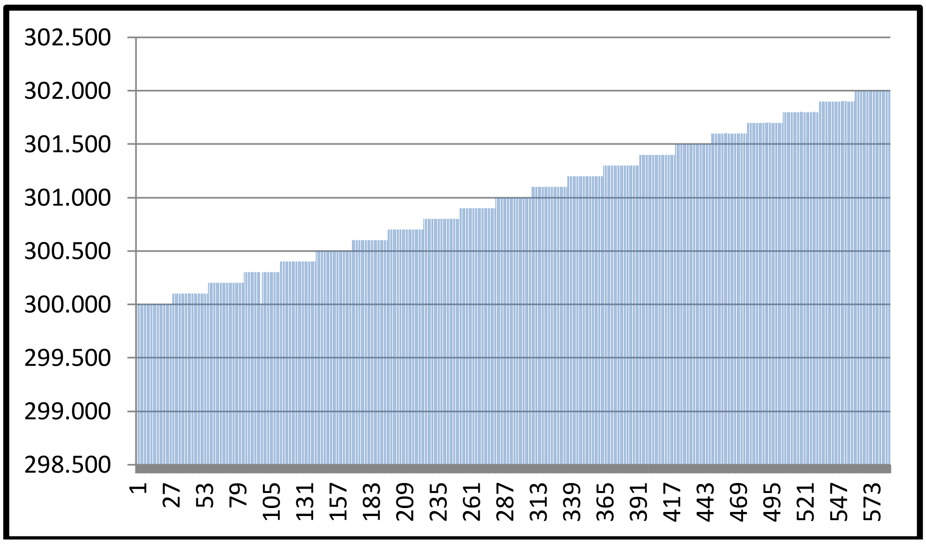

Şekil 6. Y koordinatları arasındaki sistematiklik

Figure 6. *Systematicty between the y coordinates*

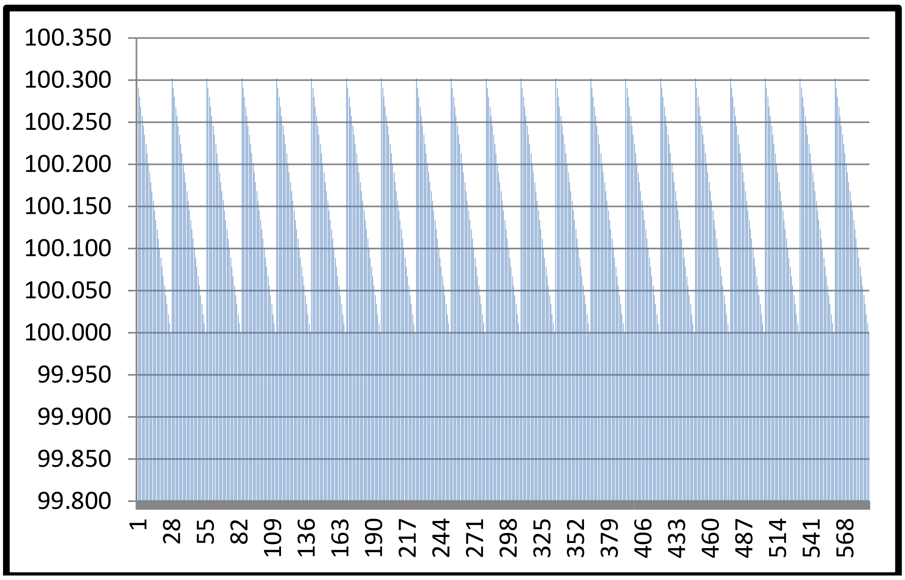

Şekil 7. Z koordinatları arasındaki sistematiklik

Figure 7. *Systematicty between the z coordinates*

Her tarama test alanından 35 metre uzaklıktan sabit noktadan yapılmıştır. Bunun için test alanı öncelikle şekil 8′ de görüldüğü gibi dik olarak taranmıştır.

Şekil 8. Test alanının dik olarak taratılması

Figure 8. *scanning the test area perpendicularly*

Taramalar dış ortamın etkilerini azaltmak için kapalı mekanda yapılmıştır. Tarama işlemi bittikten sonra veriler scanmaster programına yüklenmiş ve burada polyworks programında kullanılmak üzere ptx formatına dönüştürülmüştür. Daha sonra her tarama için ptx formatındaki veriler polyworks programında açılarak fazla nokta bulutları temizlenmiştir. Şekil 9′ da test alanının 30^{0}′ lik açı ile taranmış verisinin fazla nokta bulutlarından temizlenmiş görüntüsü, Şekil 10′ da ise test alanının 60^{0}′ lik açı ile taranmış verisinin fazla nokta bulutlarından temizlenmiş görüntüsü görülmektedir.

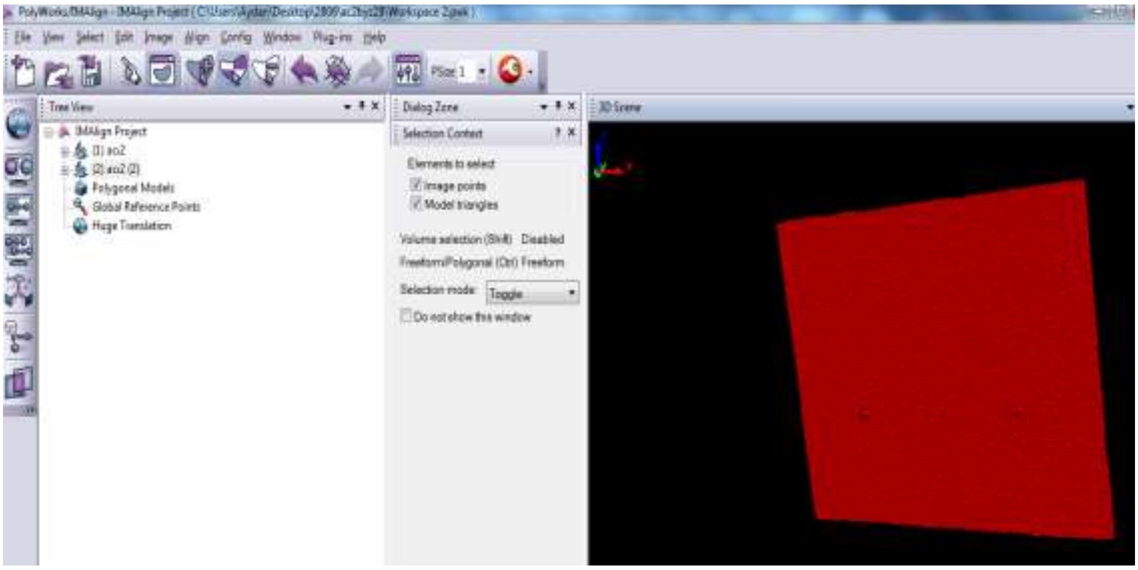

Şekil 9. 30⁰′ lik açı ile taranan test alanının gereksiz nokta bulutlarından temizlenmiş görüntüsü

Figure 9. *Image of the test area that was scanned from 30⁰ angle and cleaned unnecessery point clouds*

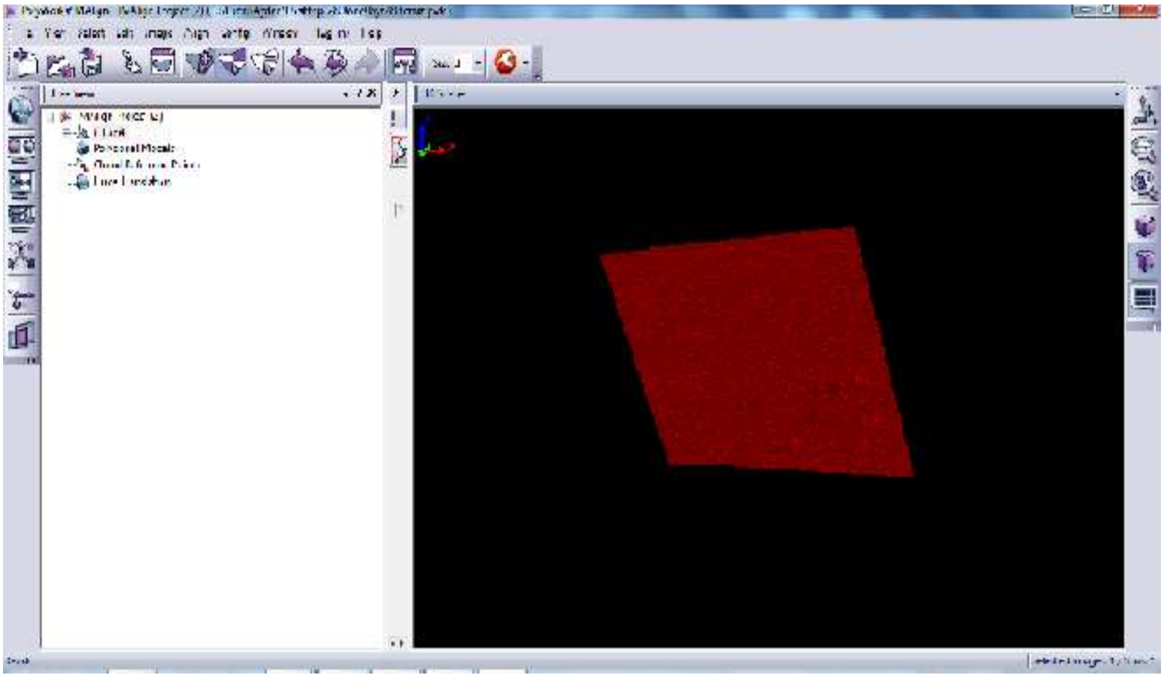

Şekil 10. 60⁰′ lik açı ile taranan test alanının gereksiz nokta bulutlarından temizlenmiş görüntüsü

Figure 10. *Image of the test area that was scanned from 60⁰ angle and cleaned unnecessery point clouds*

Gereksiz nokta bulutları silindikten sonra test alanı üzerinde kalan noktaların koordinatları Excel programına atılarak koordinatların minimum ve maksimum değerleri bulunmuştur. Muhtemel bir dönüşüm hatasından kaçınmak için tarayıcıdan elde edilen lokal koordinatlar doğrudan kullanılmıştır. Elde edilen koordinatlardan "Y" ve "Z" değerleri yer değiştirilerek test alanı yatay hale getirilmiştir. Eğer taramalar test alanına tam dik şekilde yapılmış olsaydı test alanının yatay hale gelmesi ile oluşacak dikdörtgen prizmanın hacminin sıfır olması gerekecekti. Ancak genel olarak yapılan taramalarda tarayıcı objeye tam dik olmadığından ve tarayıcı düzeçlenmediğinden bu mümkün olmamaktadır. Bu durumda tabanı taranan bölgenin kenarları yani minimum ve maksimum "X" koordinatları arasındaki fark, minimum ve maksimum "Y" koordinatları arasındaki fark ve yüksekliği minimum ve maksimum

"Z" koordinatları arasındaki fark olan bir yarım dikdörtgen prizma oluşacaktır. Burada bulunan fark değerleri çarpılarak (Taban alanı×yükseklik) ve bulunan sonuç ikiye bölünerek (yarım dikdörtgen prizma olduğu için) olması gereken hacim değerleri her istasyon için hesaplandı. Test alanının dik olarak taranması ile elde edilen olması gereken hacim değerinin hesaplanması Şekil 11' de gösterilmiştir.

	A	B	C	D
16822	-19.312101	-28.100002	1.299100	
16823	-19.312099	-27.845100	1.299100	
16824	-19.312099	-28.619101	1.299200	
16825	-19.312099	-28.320900	1.299200	
16826	-19.311998	-28.289799	1.299200	
16827	-19.311899	-28.028198	1.299200	
16828	-19.311802	-28.344200	1.299300	
16829	-19.311703	-28.357800	1.299400	
16830	-19.311701	-28.712000	1.299600	
16831	-19.311701	-28.564301	1.299800	
16832	-19.311701	-28.448502	1.299800	
16833	-19.311600	-28.569902	1.299900	
16834	-19.311600	-27.813400	1.299900	
16835				
16836				
16837	-20.468300	-28.995100	0.000100	MİN
16838	-19.311600	-27.813400	1.299900	MAK
16839				
16840	1.156700	1.181700	1.299800	FARK
16841				
16842			0.888330	HACİM
16843				

Şekil 11. Test alanının dik olarak taranması ile elde edilen olması gereken hacim değeri
Figure 11. *Volume value which is obtained by scanning the test area vertically*

5 adet tarama istasyonuna ait koordinat değerlerinin minimum ve maksimum değerleri arasındaki fark hesaplandıktan sonra koordinat değerleri "Surfer" programına aktarıldı ve her istasyon için hacim değerleri hesaplandı. Şekil 12' de test alanının dik olarak taranması ile elde edilen nokta bulutlarından hesaplanan hacim değeri gösterilmiştir.

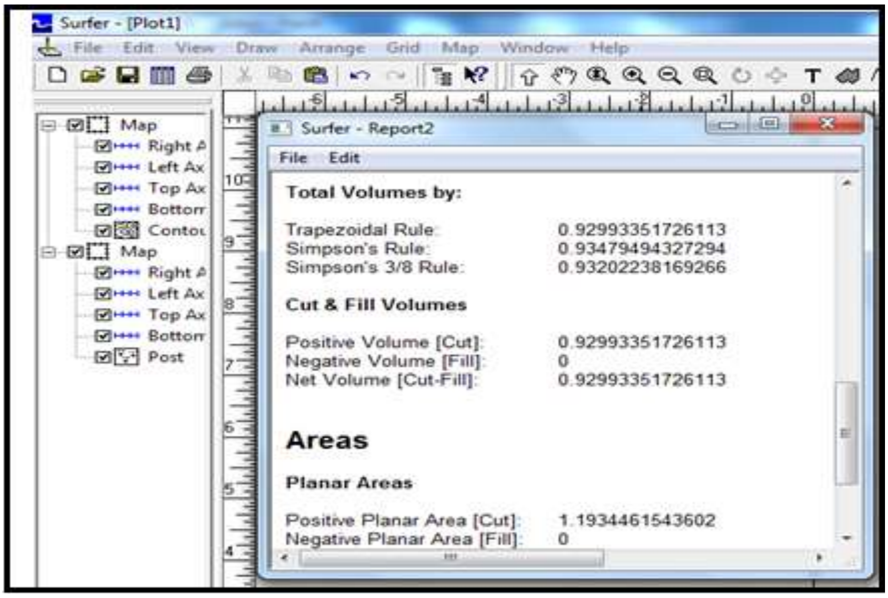

Şekil 12. Test alanının dik olarak taranması ile elde edilen nokta bulutlarından hesaplanan hacmi
Figure 12. *The volume is calculated from point clouds that is obtained from the test area scanned vertically*

Hacim hesaplamalarında obje yüzeyi düz olduğu için düz yüzeylerde en iyi sonucu veren lineer enterpolasyon yöntemi kullanıldı (Yılmaz, 2007). Ayrıca her istasyon noktası için koordinatlardan elde edilen hacim değerleri de hesaplandı. Böylece hacimler arasındaki farklar elde edildi.

BULGULAR (RESULTS)

Yapılan hesaplamalardan sonra her tarama için nokta bulutlarından hesaplanan hacimler ile olması gereken hacimler ve aradaki farklar toplu halde Çizelge 1′ de gösterilmiştir.

Çizelge 1. Hesaplanan hacim değerlerinin toplu olarak gösterilmesi ve aradaki farklar

Table 1. *Collectively show the calculated volume values and the differences*

OBJE YÜZEYİ EĞİKLİĞİ	NOKTA BULUTLARINDAN HESAPLANAN HACİMLER	OLMASI GEREKEN HACİMLER	FARKLAR(m^3)
DİK	0.9299	0.8883	0.0416
150	0.3245	0.3146	0.0099
300	0.6341	0.5420	0.0921
450	0.6103	0.6883	-0.0780
600	0.3066	0.3227	-0.0161

Çalışmada kullanılan test alanının 2.7 m x 2.0 m′ lik kısmı değerlendirmeye tabi tutulmuştur. Lazer tarayıcı test alanına tam dik olmayıp Y ekseninde 30 cm′ lik bir kayıklık bulunmaktadır. Daha öncede belirtildiği gibi bu durumda her tarama için boyutları 2.7x2.0x0.3 m′ den oluşan bir yarım dikdörtgen prizma elde edilmektedir. Bu yarım dikdörtgen prizmanın hacmi 0,810 m^3 olarak hesaplanmıştır. Bu yarım dikdörtgen prizmanın her bir kenarı 1 mm den 15 mm′ ye kadar arttırılarak hacimler tekrar hesaplandığında Çizelge 2′de verilen değerler elde edilmektedir.

Çizelge 2. Kenar uzunlukları 1 mm arttırılan prizmanın hacim ve fark değerleri

Table 2. *Edge length 1 mm increased prism′ s volume and the difference values.*

Y	X	Z	Hata (mm)	Hesaplanan hacim (m^3)	Olması gereken hacim (m^3)	Farklar (m^3)
0.301	2.701	2.001	1	0.81341		0.00341
0.302	2.702	2.002	2	0.81682		0.00682
0.303	2.703	2.003	3	0.82024		0.01024
0.304	2.704	2.004	4	0.82366		0.01366
0.305	2.705	2.005	5	0.82709	0.81000	0.01709
0.306	2.706	2.006	6	0.83052		0.02052
0.307	2.707	2.007	7	0.83396		0.02396
0.308	2.708	2.008	8	0.83740		0.02740
0.309	2.709	2.009	9	0.84085		0.03085
0.310	2.710	2.010	10	0.84430		0.03430
0.311	2.711	2.011	11	0.84776		0.03776
0.312	2.712	2.012	12	0.85122		0.04122
0.313	2.713	2.013	13	0.85469		0.04469
0.314	2.714	2.014	14	0.85816		0.04816
0.315	2.715	2.015	15	0.86164		0.05164

Bu çalışmadan elde edilen hacim farkları ile Çizelge 1′ de elde edilen farklar karşılaştırıldı. Çizelge 2′ ye göre eğer hacim farkı 0.02740 m^3 çıktıysa sekiz nolu satıra karşılık gelen hata miktarı ile taramanın yapıldığı varsayılmaktadır. Bu değer de Çizelge 2′ ye göre 8 mm′ dir. Buna göre yapılan 5 adet taramaya ait tarama hassasiyetleri çizelge 3′ de verilmiştir.

Çizelge 3. Obje yüzeyi eğikliği ve tarama hassasiyetleri
Table 3. *The inclination of the object surface and scanning precisions*

Obje Yüzeyi Eğikliği	Tarama Hassasiyeti (mm)
Dik	12.1
15^0	2.9
30^0	Hassasiyet sınırları içine girmemiştir.
45^0	Hassasiyet sınırları içine girmemiştir.
60^0	4.7

SONUÇ VE TARTIŞMALAR (RESULTS and DISCUSSIONS)

Son yıllarda yersel lazer tarayıcıların tarama hassasiyetleri ve kullanım alanları gittikçe artmaktadır. Birçok mühendislik uygulamalarında oldukça başarılı bir şekilde uygulanmaktadır. Bir objeye ait üç boyutlu konum verilerinin elde edilmesinde en önemli faktör bu verilerin hassasiyetidir. Aynı zamanda bu verilerin en kısa zaman diliminde elde edilmesi de diğer önemli bir faktördür. Yersel lazer tarama teknolojisinin en yaygın kullanım alanlarından biri olan üç boyutlu modellemenin yanında deformasyon ölçmeleri gibi veri hassasiyetlerinin oldukça önemli olduğu uygulamalarda bulunmaktadır.

Ulvi ve arkadaşları tarafından yapılan çalışmada Kızkalesi yüzeyindeki karakteristik noktalar Geomax ZTS 605 elektronik uzaklık ölçerle ölçülmüş ve genel sistemdeki koordinatları elde edilmiştir. Aynı zamanda yersel lazer tarayıcı ile de taramalar yapılmış ve bunun sonucunda manuel birleştirme ile elde edilen konumlandırılmış nokta bulutu kümeleri içerisinden aynı noktaların koordinatları belirlenmiş ve bu koordinatlar arasında karşılaştırma yapılmıştır. Elektronik uzaklık ölçerle yapılan ölçümler sonucu elde edilen koordinatlar ile manuel yöntemde -16mm ile 17 mm arasında farklar bulunmuştur. Belirlenen karakteristik noktaların elektronik uzaklık ölçer ve lazer tarayıcı ile yapılan tarama sonucu elde edilen koordinatların farklarından yararlanarak her bir koordinat bileşeni için duyarlık ölçütleri belirlenmiştir. Bu sonuçlardan yararlanılarak da noktalardaki konum değişimleri belirlenmiştir. Ağırlıklı olarak manuel yöntemde nokta konum doğruluğu ± 19.7 mm bulunmuştur. Ağırlıklı olarak her nokta için konum doğruluğu ise ± 13.9 mm ile ± 26.4 mm arasında bulunmuştur. Koordinat farkları ve bunların standart sapmalarının hesaplandığı dikkate alınarak elektronik uzunluk ölçer ve lazer tarayıcıdan iki yöntemle elde edilen koordinat farklarının anlamlı olup olmadığının irdelenmesinde t-testi uygulanmıştır. T-testi sonuçları incelendiğinde bütün test değerlerinin sınır değerlerinin altında kaldığı görülmektedir (Ulvi ve Yakar, 2014).

Yersel lazer tarayıcılarda tarama aralığı tanımında aslında ışınsal çözünürlük tanımlanmaktadır. Bu çalışmada test alanına farklı açılar verilerek Topcon yersel lazer tarayıcının bu açılar altındaki konum doğruluğu araştırıldı. Yapılan çalışmada 35 metre mesafeden sabit noktadan test alanı dik ve 4 farklı açıyla taranmış ve 2.9 mm ile 12.1 mm aralığında bir tarama hassasiyetinin olduğu görülmüştür. 30^0 ve 45^0 lik açılarla yapılan taramalardan elde edilen hata miktarlarının tanımlanan hata aralığına girmediği görülmüştür. Tüm sonuçlar değerlendirildiğinde yapılacak en uygun taramanın 15^0 lik açı ile yapılan tarama olduğu görülmüştür. Bilindiği gibi her tarama için düşünülen 5 mm tarama aralığı her taramada bir miktar değişmektedir. Buna bağlı olarak da her tarama için elde edilen nokta sayıları da farklı olmaktadır. Nokta sayılarının farklılığı da sonuçları etkilemektedir. Diğer taraftan obje üzerinde belli bir bölgeye diğer bölgelerden daha fazla ışığın düşmesi bu bölgede veri eksikliğine sebep olmaktadır. Sonuç olarak bu çalışmada kullanılan Topcon lazer tarayıcının 35 metrelik mesafede yapılan taramalarda konumlama hassasiyetinin 2.9 mm ile 12.1 mm arasında değiştiği, 30^0 ve 45^0 lik açılarla yapılan taramalarda hata miktarının tanımlanan hata aralığına girmediği, taramaların 15^{0}lik açı ile yapılmasının daha uygun olduğu görülmüştür.

TEŞEKKÜR

Bu çalışma Aksaray Üniversitesi Bilimsel Araştırma Projeleri (BAP) Koordinatörlüğü tarafından 2015-063 nolu araştırma projesi kapsamında desteklenmiştir. Yazarlar Aksaray Üniversitesi BAP Koordinatörlüğüne teşekkür ederler.

KAYNAKLAR (REFERENCES)

Altuntaş, C., Yıldız, F., 2008, "Yersel Lazer Tarayıcı Ölçme Prensipleri ve Nokta Bulutlarının Birleştirilmesi", *Jeodezi, Jeoinformasyon ve Arazi Yönetimi Dergisi*, 1, Vol. 98, pp. 20-27.

Aydar, U., Avşar, Ö., Kaya, Ş., Bozkurtoğlu, E. ve Şeker, D.Z., "Yüzeylerin Pürüzlülük Açılarının Lazer Tarayıcılar Yardımıyla Belirlenmesi", *13. Türkiye Harita Bilimsel ve Teknik Kurultayı, Ankara*, 18-22 Nisan 2011.

Gümüş, K. ve Erkaya, H., "Mühendislik Uygulamalarında Kullanılan Yersel Lazer Tarayıcı Sistemler", *11. Türkiye Harita Bilimsel ve Teknik Kurultayı*, Ankara, 2-6 Nisan 2007.

Karşıdağ, G., 2011, *Yersel Lazer Tarama Ölçmelerinde Doğruluk Analizi*, Yüksek Lisans Tezi, İstanbul Teknik Üniversitesi, Fen Bilimleri Enstitüsü, İstanbul.

Ulvi, A. ve Yakar, M., 2014. "Yersel Lazer Tarama Tekniği Kullanarak Kızkalesi' nin Nokta Bulutunun Elde Edilmesi ve Lazer Tarama Noktalarının Hassasiyet Araştırması", *Harita Teknolojileri Elektronik Dergisi*, Vol. 6(1), pp. 25-36.

Yılmaz, H. M., 2007, "The Effect of Interpolation Methods in Surface Definition: An Experimental Study", *Earth Surface Processes and Landforms*, Vol. 32, pp. 1346-1361.

SUJEST, c.5, s.1, 2017
SUJEST, v.5, n.1, 2017
ISSN: 2147-9364 (Electronic)

A WEB BASED SERVICE APPLICATION FOR VISUAL SINKHOLE INVENTORY INFORMATION SYSTEM; CASE STUDY OF KONYA CLOSED BASIN

[1]Osman ORHAN, [2]Murat YAKAR, [3]Osman Sami KIRTILOGLU

[1,2,3]*Selcuk University, Department of Geomatics Engineering, Campus, Selcuklu, Konya, TURKEY*
[1]osmanorhan44@gmail.com, [2]yakar@selcuk.edu.tr, [3]okirtiloglu@selcuk.edu.tr

(Geliş/Received: 06.10.2016; Kabul/Accepted in Revised Form: 07.12.2016)

ABSTRACT: Sinkholes are commonly defined as deep pits giving the appearance of a chimney or well resulting by collapsing of underground rivers in horizontal or near-bedded lime stones or active cave ceilings. Sinkholes appear as deep pits in the so-called karst land, usually on limestones and carbonates that are easily rinsed with water. The sinkhole occurrences in our country are very often seen on the Obruk Plateau in the Konya Closed Basin. In Karapinar region and its surroundings located in this plateau, especially in recent years surface deformations and sinkhole formations are frequent. The resulting sinkholes in the field of agriculture and occurred in areas close to residential areas is to upset the locals.
Several studies have been carried out about the formation of sinkholes in Konya Closed Basin and especially around Karapinar. As a result of the literature survey, different information about the number of sinkholes in the region has been reached. Therefore, an inventory information system that is as up-to-date as daily, accurate, and rich in attribute information (position information, shape, diameter, depth, distance to settlements, year of formation, region etc.), has been created as a result of detailed field work, analyzing satellite images, and examining digital terrain model. The inventory information of the 283 objects created within the scope of the study will be used as support data in the future hazard, risk and planning studies. In addition, the inventory data will be shared through a Web-based system with the relevant people and institutions. The Geoinformation System-like Web application is built using Google Maps and Fusion Tables services for data storage and management, both are free services from Google Inc. The web application's infrastructure includes HTML5, CSS3, JavaScript, Google Maps API V3, and Google Fusion Tables API technologies. Using these technologies, it is possible to create effective map "Mash-Up" applications by adding Google maps to a Web page, where spatial data is stored in Fusion Tables and can be displayed as a layer on Google maps. The sinkhole inventory information system presented with web-based application is handled in detail in this article.

Key Words: *Karapınar, Sinkhole, Inventory, Google API, Mash-Up*

Görsel Obruk Envanter Bilgi Sistemi için Web Tabanlı Servis Uygulaması; Konya Kapalı Havzası Örnek Çalışması

ÖZ: Obruk, yatay veya yataya yakın tabakalı kireç taşlarında bulunan yeraltı nehirlerinin veya aktif mağara tavanlarının çökmesi sonucu oluşmuş, baca veya kuyu görüntüsü veren derin çukurluklara verilen isimdir. Obruklar karst arazi denilen, genelde suyun kolayca eritebildiği kireçtaşları ve karbonatlar içeren düzlüklerde bulunan derin çukurlar şeklinde görünürler. Ülkemizde obruk oluşumları, Konya Kapalı Havzası'nda yer alan Obruk Platosunda çok sıklıkla görülmektedir. Bu

DOI: 10.15317/Scitech.2017.71

platoda yer alan Karapınar ve çevresinde, özellikle son yıllarda sıklıkla yüzey deformasyonları ve obruklar meydana gelmektedir. Oluşan obrukların tarım alanlarında ve yerleşim alanlarına yakın bölgelerde meydana gelmesi bölge halkını tedirgin etmektedir.
Konya Kapalı Havzası ve özellikle Karapınar civarında, obruk oluşumları ile ilgili bazı çalışmalar gerçekleştirilmiştir. Literatür araştırması sonucunda, bölgedeki Obruk sayısı ile ilgili farklı bilgilere ulaşılmıştır. Bu yüzden günümüze kadar güncel, doğru ve öznitelik bilgisi bakımından zengin (konum bilgisi, şekil, çap, derinlik, yerleşim yerlerine mesafe, oluşum yılı, bölgesi, vb.) bir envanter bilgi sistemi, detaylı arazi çalışması, uydu görüntüleri ve bölgeye ait yüksek çözünürlüklü sayısal arazi modelinin incelenmesi sonucunda oluşturulmuştur. Çalışma kapsamında oluşturulan 283 obruğa ait envanter bilgisi gelecekte gerçekleştirilecek tehlike, risk ve planlama çalışmalarında destek veri olarak kullanılacaktır. Ek olarak, bu envanter verisi ilgili kişi ve kurumlar ile Web tabanlı bir sistem vasıtasıyla paylaşılacaktır. Coğrafi Bilgi Sistemi benzeri Web uygulaması, Google firmasının ücretsiz hizmetleri olan Google Maps ve veri depolama ve yönetimi için oluşturduğu Fusion Tables hizmetleri kullanılarak oluşturulmuştur. Web uygulamasının altyapısı HTML5, CSS3, JavaScript, Google Maps API V3 ve Google Fusion Tables API teknolojilerini içermektedir. Bu teknolojilerin kullanılmasıyla, bir Web sayfası içerisine Google haritaları eklenerek, mekânsal verilerin Fusion Tables içerisinde depolandığı ve Google haritalar üzerinde bir katman olarak görüntülenebildiği etkili harita “Mash-Up” uygulamaları oluşturulması mümkün olmaktadır. Web-tabanlı uygulama ile sunulan obruk envanter bilgi sistemi, bu makalede detaylı olarak ele alınmaktadır.

Anahtar Kelimeler: *Karapınar, Obruk, Envanter, Google API, Mash-Up.*

INTRODUCTION

Disaster, largely or entirely occurring naturally, exactly unpredictable, occurring suddenly, causing loss of life and property, is defined as a result of climatic events, biological, meteorological, hydrological, and geological origin (Sipahioğlu, 2003; Hoyois *et al*., 2006; Akıncı *et al*., 2010).

In recent years, damage reduction studies done in order to minimize the effects of disasters are one of the most studied topics and funded. Nowadays, "Risk Identification" and "planning" concepts are the basis of the damage reduction (Safeland, 2010; Bilgilioğlu, 2014; Ozturk, 2016). Determination of disaster risk areas and preparation of their plans depend on the existing accurate and timely inventory information, which exist, about disasters. In this context, essential spatial information must be determined for disasters such as sinkholes, earthquakes, landslides, floods etc. in risk assessment and planning studies. This information must be collected and presented to the stakeholders in a GIS environment at immediately or soon after the disaster.

The formation of sinkholes, which is one of the types of geological disasters, involves natural processes of erosion or gradual removal of slightly soluble bedrock (such as limestone) by percolating water, the collapse of a cave roof, or a lowering of the water table. Sinkholes often form through the process of suffusion. For example, groundwater may dissolve the carbonate cement holding the sandstone particles together and then carry away the lax particles, gradually forming a void (Friend, 2002). Sinkhole formations are very often seen in the Obruk Plateau located in Konya Closed Basin in our country.

Sinkhole formation is a natural disaster that occurred as a result of land use and excessive groundwater usage. Sinkhole formations usually seen in Konya Closed Basin (KCB) in general (Ustun et al., 2010). The majority of sinkholes are to be found in Karapınar located in KCB. In recent years, sinkholes, which create space under soluble limestone in time and formed by the collapse of the ground, has created large negative effects on socio-economic development of the region and damaged the cultivated area. Also, it has become a threat for residential area and folk's safety.

Over the past two decades, developments in Internet and technology have brought the concept of Web-mapping. Web mapping is the process of implementing and visualizing maps on the World Wide Web (WWW or commonly just Web). Since the birth of the Web in 1989 (Tim Berners-Lee, 2016), invented at CERN for the exchange of research documents and shortly after the emergence of the first map server Xerox PARC Map Viewer (Putz, 1994), Web-based maps (or Web maps) have raised widespread use and have evolved to Rich Internet Applications (RIA) at the present. Web maps are often used to display overlays to bring information to users via the Internet. These overlays may contain information from other Web sources (i.e. RSS feeds) and/or users own external data. Getting an overlay onto a Web map varies depending upon the mapping API (Application Programming Interface). In computer programming, an application programming interface (API) is a set of routines, protocols, and tools for building software and applications (Wikipedia, 2016). An API may be for a Web-based system, operating system, or database system, and it provides facilities to develop applications for that system using a given programming language. Of course the way of delivering Web maps substantially changed in 2005 when Google introduced its tile-based mapping system based on AJAX that facilitated interactive zooming and panning (Peterson, 2012). Just 6 months after the release of the Google Maps, Google has launched Google Maps API which makes it possible to embed a Google Map on any Website or Web page free of charge and provides overlaying information from other Web sources or users own external data. Other online map providers like Microsoft Bing Map, MapQuest, Yahoo! Maps, OpenStreetMap and ESRI include an API. Almost all of these services support adding geometric primitives like point (marker), polyline and polygons as an overlay and creating info windows, putting image overlays on top of the map and external data layer support for common types as KML, JSON or GeoRSS. Some providers like Google, also have advanced tools such as Fusion Tables for data storage, management and overlay as a layer on the map.

There are a lot of alternatives to create a Web map that fulfills basic mapping functions and almost all of these are free of charge except some usage limits. Even the majority of them allow creating powerful heatmaps automatically.

Therefore, the aims of this study are the creation a sinkhole inventory information system, which shows their spatial distributions, features and relationship between environmental factors, and to make reachable these information systems for people on the subject with the help of a visual Web-based service application for sinkhole inventory system for Konya Closed Basin.

MATERIAL AND METHOD

Study Region

The KCB is located in the Central Anatolian Plateau (Turkey) at latitude 36^{0} 51'–39^{0} 29'N and longitude 31^{0} 36'–34^{0} 52'E and at an altitude of about 1,000 m (Figure 1). KCB covers a 5,426,480-ha surface area (nearly 7% of Turkey's total area) larger than that of The Netherlands. Within the basin, there are 11 watery regions (lakes, reed beds) named as Lakes Samsam, Kozanlı, Kulu, Beyşehir, Suğla, Bolluk, Tersakan, Tuz and Reed Beds Ereğli, Reed Bed and Hotamış. A smooth plane at 900–1,050 m altitude has formed the main part of the Central Anatolia Plateau in KCB, Turkey's largest closed basin in which three million people live, 45% in rural areas and 55% in urban areas. The agricultural revenue provided by KCB was due to grains (9.2%), beans (6.2%), and industrial crops including sugar beet (8.5%). As a result of insufficient drainage, the soils of the region usually have the alluvial and salty characteristics due to high groundwater level, watering, and terrestrial semiarid mild climate conditions dominant in the basin. The water of the basin comes to an end in stagnant water, marshy places, or semimarshy places. The lack of a river in this wide basin, limited rainfall, and high evaporation ratios have formed a favorable water balance that is rarely met in closed basins. The shallow lake and reed beds at the center of the basin are fed by many rivers flowing to the region. The climate characteristics of the basin present the Mediterranean climate (mild and rainy winters, hot and dry summers) at the south, the terrestrial climate (cold winters, hot and dry summers) at the center and north of the basin, and the desert climate in Karapınar and its vicinity. The rainfalls were mostly observed in winter and spring seasons. The natural richness and the lakes of the basin provide significant living places for the migratory birds (Durduran, 2010; Doğdu *et al*., 2007). In scope of this study, boundary of Konya Closed Basin has been selected as a study area in general. However, more studies have been carried out in Karapınar having more sinkholes formation.

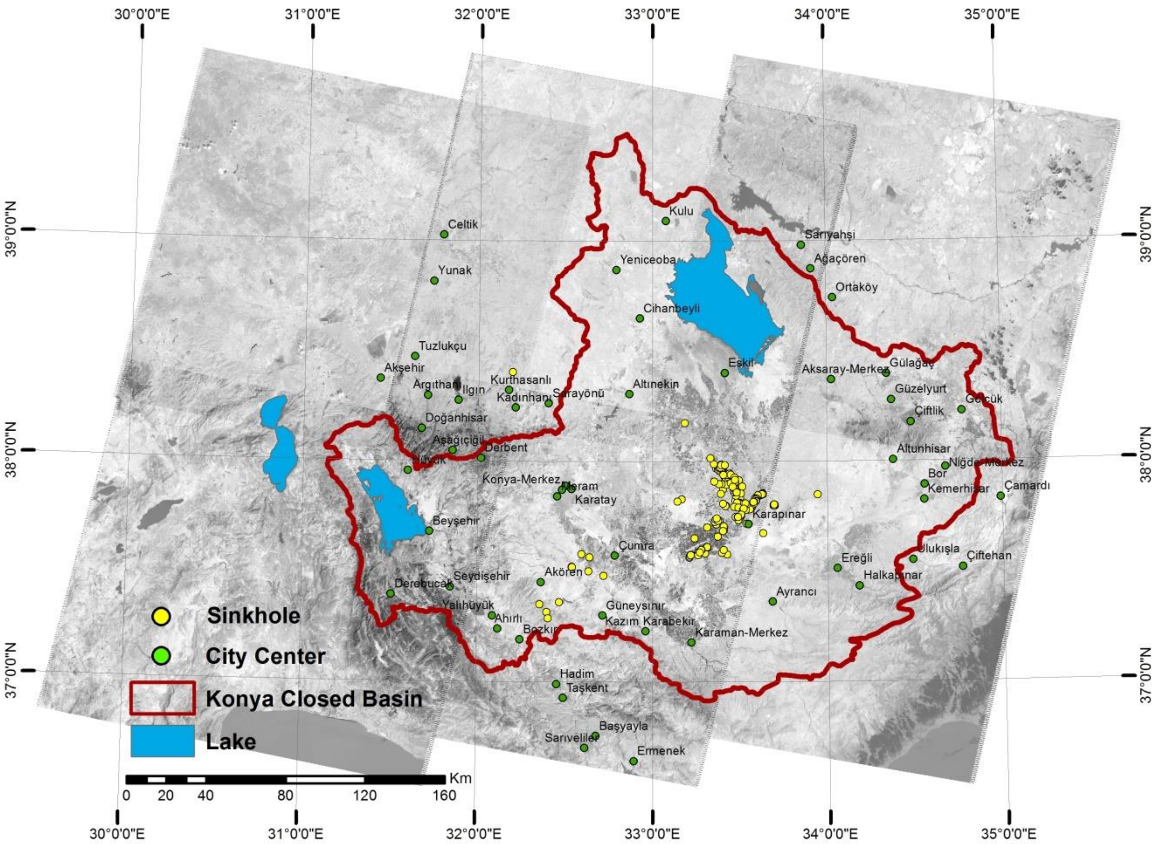

Figure 1. Study Area

Fieldwork

Fieldwork was conducted in Karapinar and its surroundings. First of all, a comprehensive literature review was performed without doing field work. Information about some sinkholes in Karapınar, was collected from previous studies carried out in this area.

(a) Çıralı Sinkhole (b) Meyil (Eğimli) Sinkhole (c) Osmanoğlu Sinkhole

(d) A new ly formed sinkhole In the spring of 2015 (Diameter 80 m, depth 60 m)

(e) A new sinkhole formed in the region close to settlements in the spring of 2015 (Diameter 60 m, depth 70 m)

(f) A sinkhole formed in the beet field on 23 Aug 2016 (g) A sinkhole in the settlement in Nasuhpinar region

(h) A new sinkhole formed within the settlement in 2014 (Diameter: 50 m)

Figure 2. Images from field work in Karapınar and its surroundings

As a result of the literature review, the spatial and attribute information about around 100 sinkholes, was obtained (Bozyigit and Tapur, 2009; Yılmaz, 2010; Dogan and Yılmaz, 2011; Bozyigit and Tapur, 2013). High-resolution satellite images and aerial photography were used in the determination of the other sinkholes in this area.

Sinkhole locations and potential sinkhole locations have been marked by examining satellite images and aerial photography. Moreover, sinkhole locations easily determined by using the Digital Elevation Model (DEM) which were produced using images of Cosmo-SkyMed satellite data. Before starting the fieldwork, 398 point was determined using DEM, satellite images and aerial photography. Later, Fieldwork carried out with GPS, Total Station etc. in order to determine whether these specified points are sinkholes and to collect geometric and attribute information in Karapınar and its surroundings. Sinkhole No, Sinkhole Name, Town, Region, Year, Distance from Residential Area, Sinkhole Shape, Sinkhole Depth, , Sinkhole Diameter, Elevation, Groundwater Stiation, Information, Lat-Long have been collected for each sinkholes as a result of both filedwork and interviews with the people. 283 Sinkholes were found as a result of this fieldwork.

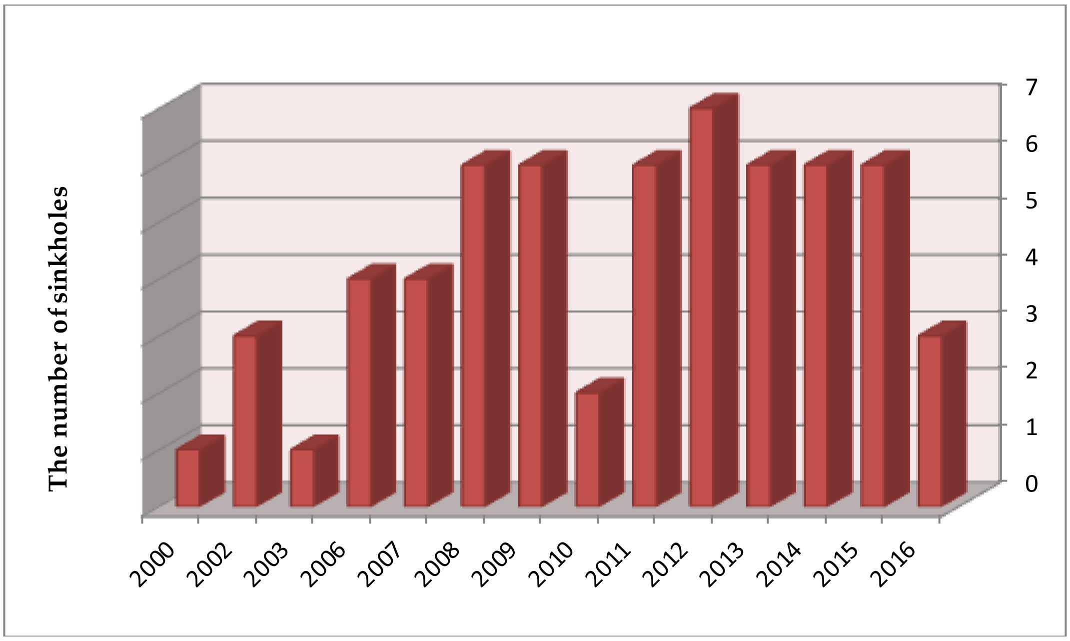

Figure 3. The number of sinkholes formed between 2000 and 2016

After the field work in Karapinar and its surrounding area, it has been determined that from the year 2000 until today, 61 sinkholes were formed. Figure 3 shows that sinkholes regularly have formed every year since 2000 and An average of 6 sinkholes formed for each year in the last six year. Morover, it is observed that sinkholes, formed in the region of Karapinar, are located in the settlement area and its surrounding.

Web-Based Application

For the purpose of visualizing and sharing the results, a Web based application has been established by using Google Maps and its useful data storage and manipulating product Fusion Tables which are all Google's free of charge Web service elements. The infrastructure of Web application includes HTML5, CSS3, JavaScript, Google Maps API V3 and Google Fusion Tables API technologies. These technologies make it possible to make effective Web-based applications involving an embedded Google Map in a Web page, storing the spatial or tabular data in Fusion Tables and add this data as a map layer on embedded map. A useful option with Google Maps is the support of using Fusion Tables as layers on the map application. Google Fusion Tables is a cloud-based service for data management and integration. Fusion Tables enables users to upload tabular data files (spreadsheets, CSV, KML), currently up to 100MB. The system provides several ways of visualizing the data (i.e., charts, maps, and timelines) and the ability to filter and aggregate the data. It supports the integration of data from multiple sources by performing joins across tables that may belong to different users. Users can keep the data private, share it with a select set of collaborators, or make it public and thus crawlable by search engines.

The service launched in June 2009. By the Fusion Tables API, users can copy a small fragment of JavaScript code into the source of their page (e.g., a blog entry) and the visualization will be displayed there, with a live link to the data. That is, when the data is updated in Fusion Tables, the visualization is also updated (Gonzales et al., 2010). It provides client-side visualizations through the Google Visualization API. This is a well-established framework for visualizing data on the client. The visualization is rendered on the browser using JavaScript or Flash, and the data required by the visualization is obtained from a data source interface. The sinkhole attribute files were produced as KML (Keyhole Markup Language) files and added on the map as Fusion Tables layers. Also the sinkhole images were produced as raster image files and added on each sinkhole attribute and their infowindow. Fusion Tables are also have the ability of heatmap function. Heatmaps display colors on the map to represent the density of points from a table. Figure 4 illustrates the distribution of sinkhole point locations.

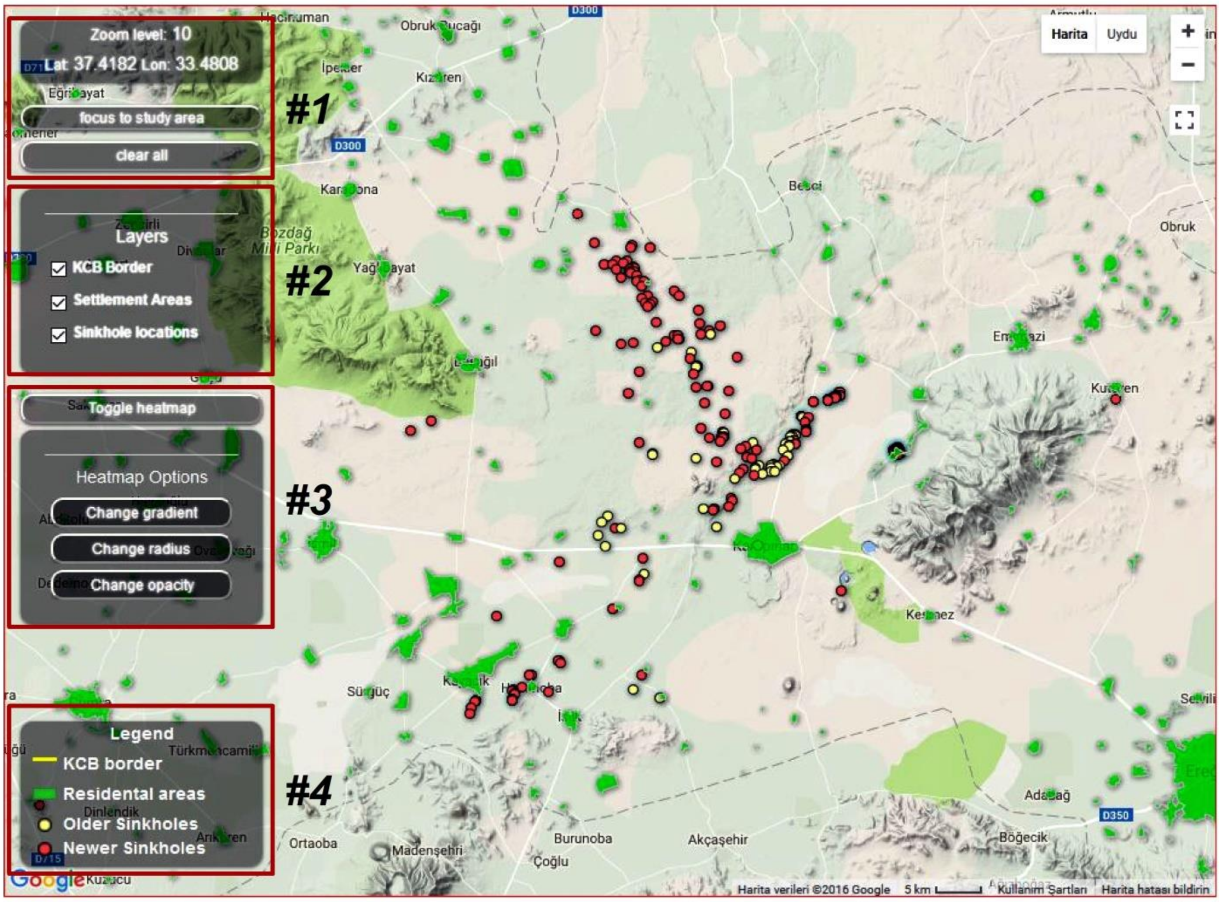

Figure 4. Distribution of sinkholes as point locations

In figure 4, focus to study area button, to clear all layer button, coordinate and zoom level information is cantained in box 1, buttons to open and close the layers is cantained in box 2, toogle heatmap screen located in box 3 located in figure 4, and legend located in box 4. Figure 5 illustrates heatmap display of same points. Moreover, heatmap buttons provide three different display option such as; change gradient, change radius, change opacity.

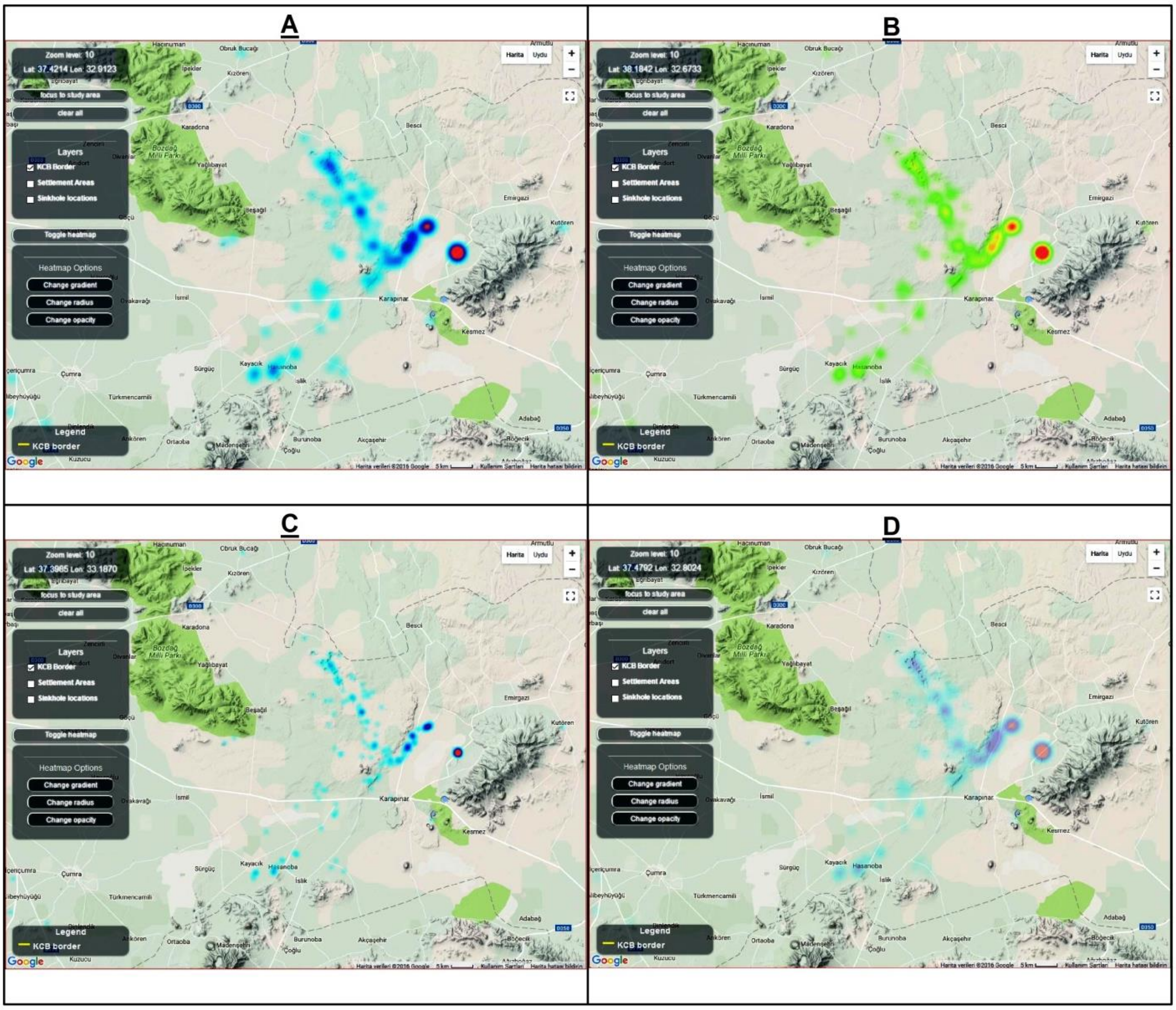

Figure 5. A: Heatmap display of sinkholes; B: Effect of the change gradient for heatmap; C: Effect of the change radius for heatmap; D: Effect of the change opacity for heatmap

The main idea of produced Web-based application is to display the determined sinkhole locations as points in an interactive Web-based map and provide attributes of sinkholes to users as infowindows. It comes from the idea of simplest way to keeping up to date information and sharing with concerned clients. Figure 6 shows an infowindow of a sinkhole when clicked on the map.

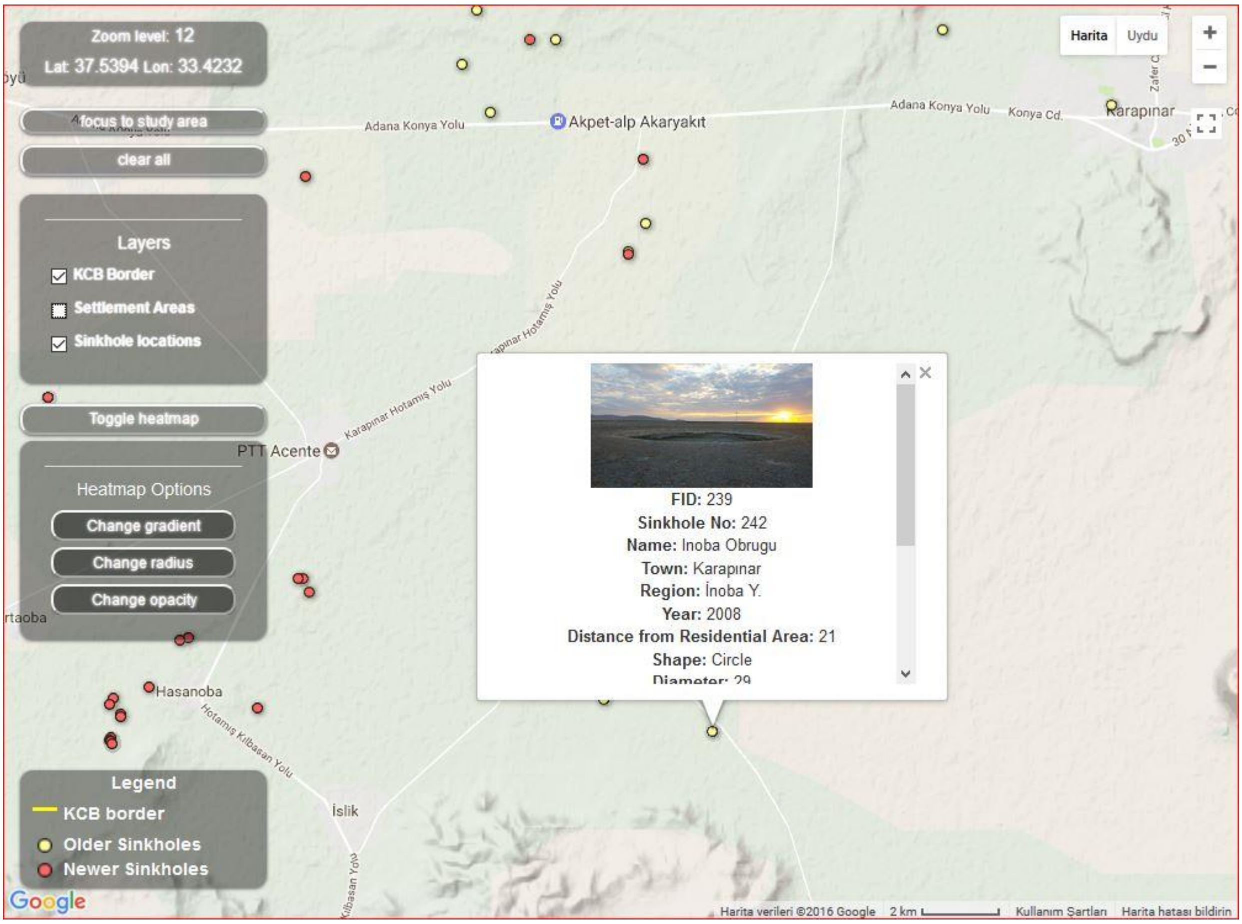

Figure 6. An infowindow of a sinkhole

CONCLUSION

In this study, it was studied to complete for the inventory data of sinkhole one of the most important problems in Konya closed basin and sinkhole inventory information (geometric and attribute information), one of the base needed of disaster management, has been completed In order to reduce the effects of this disaster. One of the base maps was prepared to demonstrate the profiles of the disaster in this region with disaster databases kept the inventory data.

283 sinkholes have been identified by examining satellite images, aerial photography and interviews with the people living in this study area in Karapınar and its surroundings in scope of the creation of sinkholes inventory information system. Three sinkholes (64/15/25m in diameter and 30/ 0.6/ 6 m in depth) formed in this region until august 2016. As a result of literature research and interviews with the people living there 61 of 283 sinkholes have occurred in this area since 2000. 21of 283 sinkholes were filled in order to prevent the decline in estate values and continue the agricultural activity.

Sinkhole inventory maps are the basis of the input parameters of regional scale sinkhole susceptibility, potential hazards and risks assessments. Appropriate use of produced Sinkhole inventory maps is expected to create a favorable impact in sinkhole risk management and mitigation activities in Konya Closed Basin.

A Web-based application produced to provide interactive maps for delivering sinkhole information to concerned clients which uses Google Maps infrastructure. We used Google Fusion Tables to store, manage and manipulate data, because it is free (except some limitations), easy to create interactive maps and share via a link or embed your own Web page, and easy to keep up to date. Our application is a Web page including an embedded Google Map window and a Fusion Table layer on this map. As a future work, we are planning to improve this application as a GIS (Geographic Information System) like environment which clients are capable of performing spatial queries or permitted ones can edit the database.

REFERENCES

Akıncı H., Doğan S., Kılıçoğlu C., Keçeci S. B., 2010, "Production of The Landslide Susceptibility Map of Samsun City Center", *Electronic Journal of Map Technologies*, Vol. 2(3), pp. 13-27. (in Turkish)

Berners-Lee, T., 2016, Frequently Asked Questions-Start of the Web. https://www.w3.org/People/Berners-Lee/FAQ.html [26.04.2016]

Bilgilioğlu, S., 2014, *Developing Geographic Data Model To Create Landslide Maps And Its Use In Disaster Management*, Master Thesis, Aksaray University, Graduate School of Natural and Applied Sciences, Aksaray.

Bozyiğit, R., Tapur, T., 2013, *Sinkhole Invebtory for Konya*. 8 th.Regional Directorate of Nature Conservation and National Parks, Konya Branch Directorate Project.

Bozyiğit, R., Tapur, T., 2009, "The Effect of Ground Waters for Formation of Obruk in Konya Plain and Around", *Selçuk University Journal of Social Sciences Institute*, Vol. 21, pp. 137-155.

Doğan, U., Yılmaz, M., 2011, "Natural and Induced Sinkholes of The Obruk Plateau and Karapınar-Hotamış Plain, Turkey" *Journal of Asian Earth Sciences*, Vol. 40(2), 20 January 2011, pp. 496-508, ISSN 1367-9120,

Doğdu, M. S., M. M. Toklu, C., Sağnak, 2007, "Examination of Precipitation and Groundwater Level Values in Konya Closed Basin", First Turkish Climate Change Congress, (in Turkish), pp. 394–401. 11-12 April 2007, İstanbul.

Durduran, S. S., 2010, "Coastline Change Assessment on Water Reservoirs Located in The Konya Basin Area, Turkey, Using Multitemporal Landsat Imagery". *Environmental Monitoring and Assessment*, Vol. 164, pp. 453-461.

Friend, S., 2002, *Sinkholes*. Pineapple Press Inc. p. 11. ISBN 1-56164-258-4. Retrieved 7 June 2010, USA.

Gonzalez, H., Halevy, A., Jensen, C.S., Langen, A., Madhavan, J., Shapley, R., Shen, W., "Google Fusion Tables: Data Management, Integration and Collaboration in The Cloud". In Proceedings of the 1st ACM Symposium on Cloud Computing (pp. 175-180). 10 – 11 June 2010, Indianapolis, IN, USA

Hoyois, ,P., Below, R., Scheuren, J-M., Guha-Sapir, D., 2006. *Annual Disaster Statistical Rewiew Numbers And Trend,* Univeriste Catholique De Louvain-Brussels-Belgium, Brussels.

Öztürk, O., 2016, *Developing Geographic Data Model to Create Landslide Hazard Maps and Its Use in Disaster Management,* Master Thesis, Aksaray University, Graduate School of Natural and Applied Sciences, Aksaray.

Peterson, M. P., 2012, *Online Mapping With APIs, In: Online Maps with APIs and WebServices*, Eds: Springer, pp. 3-12.

Putz, S., 1994, "Interactive Information Services Using World-Wide Web hypertext", *Computer Networks and ISDN Systems,* Vol. 27 (2), pp. 273-280.

Safeland, 2010, *Living With Landslide Risk in Europe: Assessment, Effects of Global Change, and Risk Management Strategies*, Grant Agreement Project No. 226479, 7th Framework Programme of the European Commission.

Sipahioğlu, Ş., 2003, *Location and Evaluation of Natural Disasters in Geography Curriculum.*, s.96-101. Ankara: Gazi Publications.

Ustun, A., Tusat, E., & Yalvac, S., 2010, "Preliminary Results of Land Subsidence Monitoring Project in Konya Closed Basin Between 2006–2009 by Means of GNSS observations", *Natural Hazards and Earth System Sciences,* Vol. 10(6), pp. 1151-1157.

Wikipedia Contrubitors, 2016, The Definition of Application Programming Interface, https://en.wikipedia.org/ wiki/Application_programming_interface [26.04.2016]

Yılmaz, M., 2010, "Environmental Problems Caused by Ground Water Level Changes around Karapinar", *Ankara University Journal of Environmental Sciences,* Vol. 2(2), pp. 145-163.

SUJEST, c.5, s.1, 2017
SUJEST, v.5, n.1, 2017
ISSN: 2147-9364 (Electronic)

INVESTIGATING IMPACTS OF LARGE DAMS ON AGRICULTURAL LANDS AND DETERMINING ALTERNATIVE ARABLE AREAS USING GIS AND AHP IN ARTVIN, TURKEY

[1]Halil AKINCI, [2]Ayse Yavuz ÖZALP, [3]Mehmet ÖZALP

[1,2]Artvin Çoruh University, Engineering Faculty, Department of Geomatics Engineering, Artvin, TURKEY
[3]Artvin Çoruh University, Faculty of Forestry, Department of Forest Engineering, Artvin, TURKEY
[1]hakinci@artvin.edu.tr, [2]ayavuzozalp@artvin.edu.tr, [3]mozalp@artvin.edu.tr

(Geliş/Received: 07.11.2016; Kabul/Accepted in Revised Form: 12.12.2016)

ABSTRACT: Large dams are generally built for the purposes of providing drinking or irrigation water, flood control, and producing hydroelectric power, but their constructions also result in some negative outcomes such as decreasing in flora and fauna diversity, inundation of arable lands, forest areas, cultural sites and involuntary displacement of people. The city of Artvin has been facing almost all of those negative effects since five large dams have being constructed on the section of the Çoruh River flowing within the city boundary. Three of those large dams completed submerged 795.60 ha of fertile agricultural land under the reservoir waters. The objective of this study was to determine potential suitable agricultural areas in substitution for those inundated due to these five dams. For this, the Analytic Hierarchy Process (AHP) method was used in this study. In the application, parameters including great soil groups, land use capability class, land use capability sub-class, soil depth, erosion degree, slope, aspect, elevation and other soil properties were used. A suitability map was created and separated into 5 categories according to the land suitability classification provided by the FAO. After deducting the forests, pastures, and reservoir areas, newly classified suitability map showed that 2.08% (11603.25 ha) of the study area was highly suitable, while 3.43% (19132.84 ha) was moderately suitable and 4.30% (23989.99 ha) was marginally suitable for agricultural production. It was interpreted that high slope, insufficient soil depth for agricultural production, and high erosion degree of the study area were effective factors in these findings.

Key Words: *GIS, AHP, Agriculture, Land use suitability analysis, Artvin*

Artvin İlinde Büyük Barajların Tarım Arazileri Üzerindeki Etkilerinin İncelenmesi ve CBS ve AHP Kullanılarak Alternatif Ekilebilir Alanların Belirlenmesi

ÖZ: Büyük barajlar, genellikle içme veya sulama suyu sağlama, taşkın kontrolü ve hidroelektrik enerji üretimi amaçlı inşa edilirler. Fakat büyük barajların inşası, flora ve fauna çeşitliliğinin azalması, ekilebilir arazilerin, orman alanlarının, tarihi ve kültürel alanların su altında kalması ve insanların isteksiz olarak yer değiştirmesi gibi bazı olumsuz sonuçlara neden olmaktadır. Artvin ili, Çoruh nehrinin şehrin sınırları içinde akan bölümünde inşa edilen beş büyük baraj nedeniyle tüm bu olumsuz etkilerle karşı karşıya kalmıştır. Tamamlanan üç büyük baraj, 795.60 ha verimli tarım arazisini rezervuar suları altında bırakmıştır. Bu çalışmanın amacı, bu beş büyük baraj nedeniyle sular altında kalan tarım arazilerinin yerine potansiyel tarım alanlarını belirlemektir. Bunun için çalışmada, Analitik Hiyerarşi

Note: This paper has been presented at the Selcuk International Scientific Conference on Applied Sciences (ISCAS 2016) held in Antalya (Turkey), September 27-30, 2016.

DOI: 10.15317/Scitech.2017.72

Proses (AHP) yöntemi kullanılmıştır. Uygulamada, büyük toprak grupları, arazi kullanım kabiliyeti sınıfı, arazi kullanım kabiliyeti alt sınıfı, toprak derinliği, erozyon derecesi, eğim, bakı, yükseklik ve diğer toprak özellikleri parametreleri kullanılmıştır. Oluşturulan uygunluk haritası, FAO tarafından sağlanan arazi uygunluk sınıflamasına göre 5 kategoriye ayrılmıştır. Ormanlar, meralar ve rezervuar alanları çıkarıldıktan sonra yeniden sınıflandırılan uygunluk haritası, çalışma alanının %2.08'inin (11.603,25 ha) yüksek derecede, %3.43'ünün (19.132,84 ha) orta derecede ve %4.30'unun (23.989,99 ha) tarımsal üretim için düşük derecede uygun olduğunu göstermiştir. Bu sonuçlara ulaşılmasında, çalışma alanındaki eğimin yüksek olmasının, toprak derinliğinin tarımsal üretim için yeterli olmamasının ve çalışma alanının yüksek erozyon derecesine sahip olmasının etkili olduğu değerlendirilmiştir.

Anahtar Kelimeler: *CBS, AHP, Tarım, Arazi kullanımı uygunluk analizi, Artvin.*

INTRODUCTION

It is known fact that rapid population growth and migration require new areas in order to meet vital requirements particularly in cities. This situation leads to severe pressure on natural resources and inappropriate use of natural resources such as forests, pastures, wetland, agricultural lands, etc. against their potentials. Likewise, large investment projects such as roads, bridges, airports and dams destroy particularly agricultural lands and leads to their misuse. Therefore, protecting the nature and the land on which we live, taking maximum advantage of their existing potential, developing and presenting them to the use of the next generations can be possible only by developing land use plans by examining the usage options not conflicting with each other (Akten *et al.*, 2009).

The prerequisite of land usage plan is to evaluate the land suitability. The mentioned evaluation provides guidance to the optimal usage of lands by providing information about opportunities and limits of land usage (Mokarram and Aminzadeh, 2010) and involves the decision to use the existing resources according to the their evaluated potential (Bandyopadhyay *et al.*, 2009). For this, first of all the most suitable land use type is determined with the suitability analyses considering the land features and the user requirements (Akbulak, 2010; Amiri and Shariff, 2012). The land use suitability analysis is the determination of the suitability and the suitability level of a land for a particular use (agriculture, forest, recreation, etc.), and an important step of this determination process is to define the criteria affecting the suitability of the land (Al-Shalabi *et al.*, 2006). The fact that there are many criteria considerably complicates the land use suitability analysis. This is because in order to support the long-lasting use, without damage, of a particular land, it is also required to consider the criteria such as natural features of that land as well as its socioeconomic and environmental costs and results (Duc, 2006; Bandyopadhyay *et al.*, 2009).

In addition to these, it is observed that there is not a certain standard for the parameters required to be considered for the evaluation of the land suitability potential for agriculture, and that the researches generally use the parameters that they can reach during their studies. When the mentioned studies are examined, it is observed that the topographic and soil characteristics of lands are commonly used. For example; during the agricultural land suitability analysis, Perveen *et al.* (2007) used the parameters of soil texture, soil moisture, soil consistency, pH, soil drainage, organic matter content and slope. During their evaluation of arable lands, while Zengin and Yilmaz (2008) considered the parameters of land use capability classification (LUCC), soil depth, restrictive soil characteristics, drainage, erosion, slope, aspect, water existence, rainfall, temperature, vegetation cover and access; Akbulak (2010) used the parameters of slope, erosion, soil depth, restrictive soil characteristics, elevation and distance to road. During the land suitability analysis they conducted in Tabriz, Iran for agricultural production, Feizizadeh and Blaschke (2012) used 8 factors (altitude, slope, aspect, soil fertility, soil pH, temperature, rainfall and groundwater) included in four main groups as topography, climate, soil characteristics and water resources. Finally, during their studies where they determined the arable areas in Yusufeli district of Artvin, Akinci *et al.* (2013) used the parameters of great soil group, land use capability class, land use capability sub-class, soil depth, slope, aspect, elevation, erosion degree and other soil properties.

In the light of this information, the evaluation of the suitability of a certain land part for agricultural production requires the consideration of many criteria. Due to the fact that the criteria affecting the land suitability do not have the same importance levels, various methods were used for the determination of their importance and sub-criteria scores (Parakach, 2003). For example; in their study aiming to determine the physical land suitability for rice production, Perveen *et al.* (2007) used the Analytical Hierarchy Process (AHP) method. In addition, in their study integrating GIS and AHP methods, Mustafa *et al.* (2011) evaluated the suitability of the agricultural lands for some crops to be grown during summer and winter in Kheragarh Tehsil area of India. Moreover, in a similar study for searching the optimal use of land resources for agricultural production, Feizizadeh and Blaschke (2012) conducted a land suitability analysis based on GIS and AHP method. Akinci *et al.* (2013) also used GIS and AHP methods in order to determine the alternative agricultural lands for Yusufeli (Artvin) district since the current agricultural lands to be inundated by the reservoir water of Yusufeli Dam. Therefore, when reviewing the current literature, it can be clearly seen that many researchers such as Mishra *et al.* (2015); Bozdağ *et al.* (2016); Romeijn *et al.* (2016); Yalew *et al.* (2016), and Pramanik (2016) used GIS and AHP methods in respect to both analyzing the suitability of agricultural land and producing related maps.

On the other hand, as is known; mostly constructed to provide potable and/or irrigation water, to prevent flood and to produce hydroelectric power, the large dams have negative influences such as forcing people to migration, destroy of cultural and historical heritage, submerging agricultural and forest lands and decrease of flora and fauna diversities. Artvin city was affected all of these negative influences due to the five large dams of which four were completed and one is under construction on Çoruh River. In the districts having the mentioned dams, the fertile agricultural lands and many villages were partially or totally submerged and this led the people to migrate to city centers or other cities.

For this reason, this study aimed to determine the lands suitable for agriculture to be alternatives for the agricultural lands submerged/to be submerged due to the dams in the region including Murgul, Borçka, Ardanuç, Yusufeli and Central districts having the five dams whose constructions were completed and who are under construction on Çoruh River. In order to realize this objective, AHP method integrated with GIS was applied since it is considered as one of the most commonly used multi-criteria decision-making approaches in the literature for analyzing the suitability of agricultural lands. As a result of this study, the distribution and the sizes of the lands suitable for agriculture were determined in the mentioned districts.

MATERIAL AND METHOD

Study Area

The study was carried out in area covering the administrative borders of Murgul, Borçka, Central, Ardanuç and Yusufeli districts and the lower part of Çoruh River where a total of five large dams, of which three of them (Muratlı, Borçka, Deriner) were completed and two of them (Artvin and Yusufeli) are still under construction. The research area is located between the northern latitudes of 40o 34′ 20″ – 41o 31′ 30″ and the eastern longitudes of 41° 9′ 25″ – 42° 22′ 46″ and it covers a surface area of approximately 557819.20 ha (Figure 1).

Out of all the dams projected on Çoruh River, the reservoirs of the already completed Muratlı, Borçka and Deriner Dams started to be filled with water in 2005, 2006 and 2012, respectively. These dams have inundated 795.60 ha agricultural area along with impacting 49 villages and 1 neighborhood totally and/or partially. On the other hand, Artvin and Yusufeli Dams are being constructed and the former one has started to collect water in its reservoir in 2015. These two dams have left a total of 1164.40 ha arable land under inundated (Yıldırımer, 2013), making up about 9% of the whole surface area of the Artvin province. The arable lands in the province generally consist of small family-run establishments and thus, the agricultural production model is completely based on manpower with almost no mechanical operations. Plant production is mostly done in the arable lands found along the valley plains formed by Çoruh River and its tributaries while animal production is carried out in upper sections of the valley (Yavuz Özalp *et al.*, 2013).

Parameters Used in the Land Suitability Analyses

For identifying parameters and the method in determining lands suitable for agriculture, the study done by Akıncı et al (2013) in Artvin was followed. In this respect, in order to analyze the research area for lands suitable for agriculture, nine parameters including great soil group (GSG), land use capability class (LUCC), land use capability sub-class (LUCS), soil depth, slope, aspect, elevation, erosion level and other soil properties (OSP) were used.

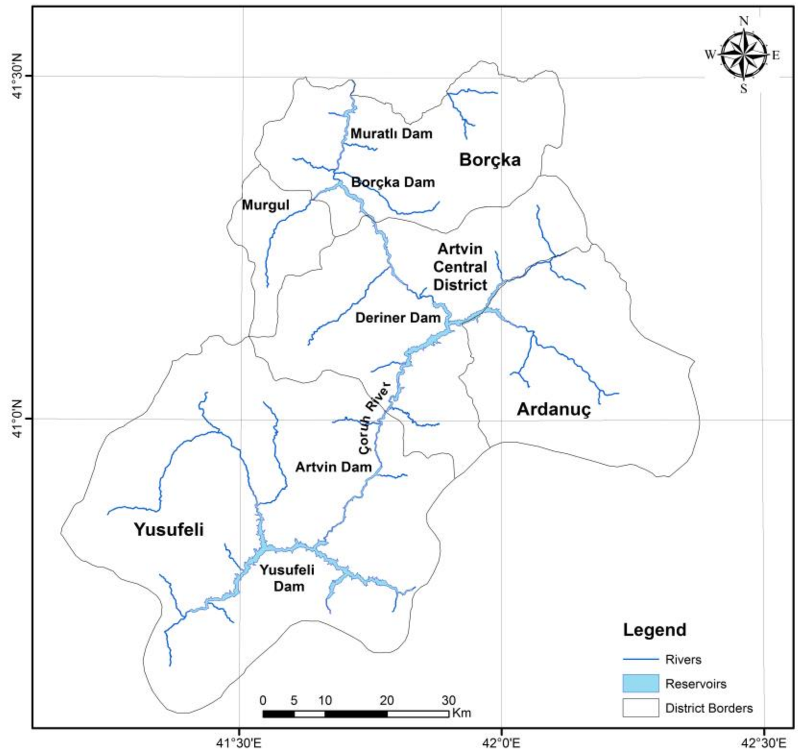

Figure 1. Study area map

Great Soil Group: Soil classification systems were created to help determining both the conditions for soil formation process and the behaviours of the soils providing contribution in estimating the soil performance for agricultural production. Thus, it is crucial to know the dominant soil class when deciding on the suitability of land for agricultural production (Akıncı *et al.*, 2013). In this respect, the dominant soil group in the study area is classified as brown forest soil with 50.57% (Table 1).

Land use capability class: Land use capability class (LUCC), in general, demonstrates the suitability of a given soil for the cultivated plants. In forming LUCCs, soils are grouped based on the constraints they bring to the agricultural products to be cultivated on them, the risk for loss of the crops in case the soils are used for cultivation and the reactions the soils will give to management applications (Akıncı *et al.*, 2013). In the study area, the prevalent LUCC is class VII with 66.02% while the classes of I, II, III and IV known as suitable for agricultural production only consists of 3.62% (Table 1).

Land use capability sub-class: Land use capability sub-class (LUCS) represents the prevalent constraints determining the capability class (Akıncı *et al.*, 2013). The problems of soil inadequacy, slope and erosion damage related to the steepness exist in 76.39% of the study area (Table 1). In addition, there are issues of inadequate drainage, wetness, and flood damage observed in the area.

Soil depth: Soil depth is the most important soil characteristic affecting the hydrologic properties of soils and its behaviors against erosion. Changes in soil depth is connected with processes of soil formation including chemical weathering of parent rock, loss of material formed through this weathering and transportation of soil by means of erosion (Fu *et al.*, 2011). Besides the age pf soil formation, soil depth is also directly associated with topography, parent material, living organisms and climate (Gessler *et al.*, 2000). The great degree of steepness in the study area caused soil depth to be low. As shown in Table 1, approximately 75% of the study area is classified as shallow or very shallow while the percentage of deep and medium-deep soils regarded as more suitable for plant cultivation is determined to be 10.99% (Table 1) in respect to soil depth.

Erosion: Erosion is an important criteria reducing soil fertility by negatively affecting the physical, chemical and biological properties of soils. Erosion reduces the soil depth required for the development of plant roots and the amount of water needed by plants, decreases the content of nutritional elements and organic matter and consequently leads to the formation of poor soil that is unsuitable for cultivation of plants (Lobo *et al.*, 2005). With this respect, in about 64.01% and 21.92% of the study area suffers from severe and moderate erosion, respectively (Table 1).

Other soil properties: Among the other soil properties limiting plant production in the study area is the rockiness with 44.30 %. Moreover, there are problems of stoniness and inadequate drainage (Table 1). These mentioned problems are thought to be occurred as a result of erosion damage.

Elevation: Elevation is a crucial factor playing a part in variation of vegetation cover by affecting temperatures to change, particularly in highlands. As known, temperatures fall by about 0.5 Co vertically for every 100 m within the first 4 km of the troposphere whereas it drops by 0.6 Co after 4 km and by 0.7–0.8 Co near the tropopause. As a general rule, for each 100 m increase in elevation on mountains, it corresponds to 100 m of divergence from south to north or from lower latitudes to higher latitudes. In other words, when going up about 100 m on the mountains, the vegetation periods and blooming of plants expected to be delayed by 4 to 6 days (Atalay, 2006). This, in turn, negatively impacts the diversity of plants to be selected for agricultural production. It was found that the elevation ranges from 50 m to 3930 m in the study area and approximately 55% of the research area has elevation over 1500 m.

Slope: Both the thickness of the soil layer (Atalay, 2006) and control of erosion are greatly affected by slope degree (Koulouri and Giourga, 2007) of an area. With the increase in degree of slope, the sediment amount transported with erosion rises while the thickness of soil layers drops. This, in turn, negatively affects soil properties, causing decrease in production and fertility of soils. The slope was over 30% for about 85% of the lands in the study area, indicating that the most of the research site lies within the classes of very steep and rugged (Table 1).

Aspect: In order to keep their physiological activities, plants require sun exposure at certain amounts and intervals. In this respect, it is a general fact that most cultivated plants show optimum growth in the aspects of southern and western because these two receive sunlight for a considerable part of the day.

For this reason, the aspect should be considered as a criterion for determining suitable lands for agricultural production (Akıncı *et al.*, 2013). When considering the study site for this parameter, it was determined that almost 62% of the area properly receives sunlight (Table 1).

The Analytic Hierarchy Process (AHP)

Developed as a model to solve problems of multi-criteria decision-making, the Analytic Hierarchy Process (AHP) was introduced by Thomas L. Saaty in 1997 (Kavas, 2009). The AHP method helps users to define the weights of the parameters for solving multi-criteria problems and thus it is one of the most widely known and used model. In the AHP method, for every problem, there is a hierarchical model having objectives, criteria, sub-criteria and alternatives are used (Saaty, 1990). When the problem is set on a hierarchical frame, the weights of the criteria forming the hierarchy are estimated (Öztürk and Batuk, 2010). In order to evaluate the criteria found in a level compared with other criteria included in the next hierarchy level, scoring is done by utilizing the preference scale according to Saaty (1980) and a pairwise comparison matrix is formed (Saaty, 1980; Saaty, 2004). The pairwise comparison matrix consists of n*(n-1)/2 comparisons for n number of elements (Malczewski, 1999; Öztürk and Batuk, 2010).

Table 1. Areal and percentile distributions of the main and sub-criteria parameters in the study area

Main criteria	Weight	Sub-criteria	Area (ha)	Area (%)	Score
GSG	0.278	A (alluvial)	1375.25	0.25	10
		Y (high mountain meadow soils)	69006.39	12.37	10
		M (brown forest soils)	282114.49	50.57	8
		P (red-yellow podzolic soils)	66068.47	11.84	7
		K (colluvial soils)	357.69	0,07	7
		X (basaltic soils)	3279.63	0.59	7
		N (non-calcic brown forest soils)	71900.93	12.89	5
		CE (chestnut soils)	853.08	0.15	3
		Other (water bodies, urban fabric etc.)	62863.27	11.27	0
LUCC	0.233	I, II, III	3452.25	0.62	10
		IV	16716.65	3.00	8
		VI	106483.32	19.09	2
		VII	368303.72	66.02	1
		VIII	57878.61	10.38	0
		Other (water bodies, urban fabric etc.)	4984.65	0.89	0
LUCS	0.162	e (slope and erosion damage)	53467.43	9.59	3
		es (slope and erosion damage, soil inadequacy)	359697.59	64.48	2
		se (soil inadequacy, slope and erosion damage)	12954.30	2.32	2
		sw (soil inadequacy, wetness, inadequate drainage)	67555.09	12.11	3
		w (wetness, inadequate drainage or flood losses)	1206.57	0.22	5
		Other (water bodies, urban fabric etc.)	62938.22	11.28	0
Soil depth (cm)	0.116	Deep (>90)	563.90	0.11	10
		Medium-deep (90-50)	60673.93	10,88	8
		Shallow (50-20)	195356.60	35.02	6
		Very shallow (20-0)	225050.78	40.34	2
		Litosolic	14075.76	2.52	1
		Other (water bodies, urban fabric etc.)	62098.23	11.13	0
Slope (%)	0.096	0-2	2053.98	0,37	10
		2-6	3649.77	0,65	8
		6-12	12133.17	2.18	6
		12-20	25548.48	4,58	4
		20-30	41782.50	7.49	3
		> 30	472651.30	84.73	1
Aspect	0.040	Flat, S,SE, SW	209179.00	37.51	8
		E, W	135959.22	24.37	7
		NE, NW	141149.61	25.30	5
		N	71531.37	12.82	2
Elevation (m)	0.032	50-250	5109.84	0.92	10
		250-500	18870.84	3.38	9
		500-1000	91128.33	16.34	8
		1000-1500	136853.99	24.53	7
		1500-2000	136893.15	24.54	5
		> 2000	168963.05	30.29	2
Erosion degree	0.025	1 (very weak)	1375.25	0.25	10
		2 (moderate)	122290.80	21.92	8
		3 (severe)	357055.44	64.01	6
		4 (very severe)	14234.45	2.55	4
		Other (water bodies, urban fabric etc.)	62863.26	11.27	0
OSP	0.018	y (inadequate drainage)	1300.29	0.23	6
		t (stony)	69697.51	12.49	4
		r (rocky)	247103.57	44.30	2
		Other (water bodies, urban fabric etc.)	239717.83	42.98	0

Solving a problem with AHP is carried out using the weights or priorities of the criteria determined by normalizing the pairwise comparison matrix. For this normalization, a ''normalized pairwise comparison matrix'' is generated by dividing the column elements of the matrix by the sum of each column. The elements in the rows of the obtained matrix are summed and the total value is divided by the number of elements in the row. At this point, a vector of priority or weight is obtained (Tombus, 2005). Weights are within the range of 0–1, and the sum of them is equal to 1 (Malczewski, 1999; Öztürk and Batuk, 2010).

There can be some level of inconsistencies occurring during the performing pairwise comparisons of criteria with the AHP. Thus, the logical consistency of these pairwise comparisons have to be tested (Öztürk and Batuk, 2010). For this, the consistency ratio developed by Saaty (1980) can be used in order to estimate the consistency of pairwise comparison judgments and it is calculated for the pairwise comparison matrix. As suggested by Saaty (1980), the upper limit for this ratio is ''0.10'', indicating that the judgments exhibit a sufficient degree of consistency if it is below 0.10 and the assessment can be continued. However, if it is over 0.10, then the judgments are seen as inconsistent and the quality of the judgments should to be improved. The consistency rate may be reduced through reviewing the judgments one more time (Öztürk and Batuk, 2007).

Data sets and methodology

The data regarding the topographical parameters such as slope, aspect and elevation were gathered from digitally-formatted standard topographical maps (1/25.000 scale). Firstly, the Digital Elevation Model (DEM) of the research area was generated using ArcGIS 10.2 software and then the maps of slope, aspect and elevation were created after this DEM was converted into the ESRI GRID format with a 30x30 m cell size.

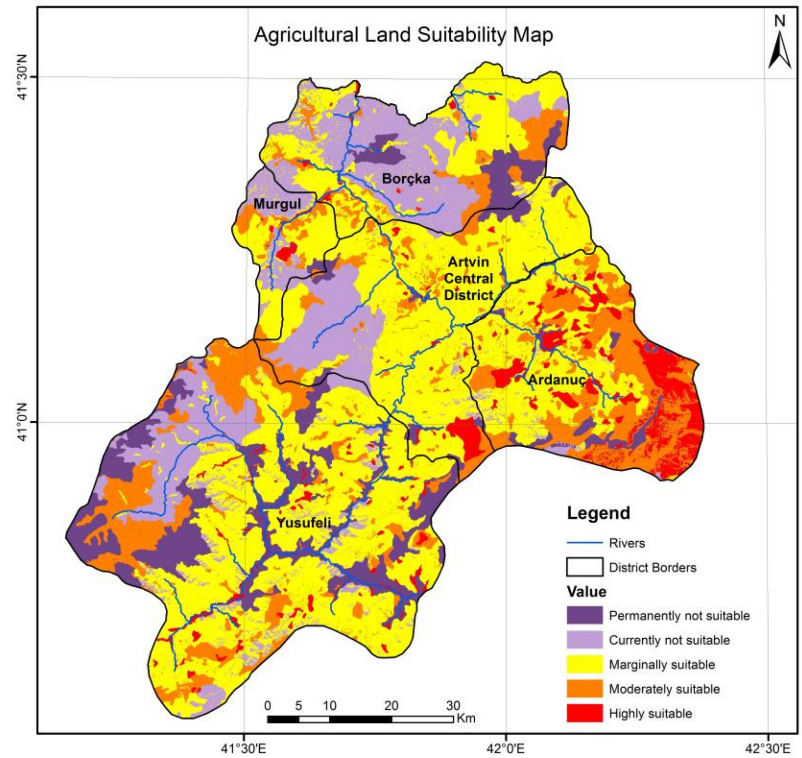

Figure 2. Agricultural land use suitability map

As for obtaining data in respect to soil properties, the 1/25.000 scaled digital soil maps provided by the General Directorate of Agricultural Reform were used. Maps of soil properties such as GSG, LUCC, LUCS, soil depth, erosion degree and OSP for the study area (in 30x30 m cell size ESRI GRID format) were generated soil maps in ESRI Shape format through considering the entity parameters found in the national soil database.

Current data of agricultural land, forest area and pasturelands in the study area were gathered from forest management plans created by the Artvin Regional Directorate of Forestry in the ESRI Shape format (in 1/25.000 scale). The areal coverage of the reservoirs was estimated using DEM after obtaining the coordinates and elevations of highest water-level for Yusufeli, Artvin and Deriner Dams thanks to the Artvin Regional Directorate of State Hydraulic Works.

In the next step, the weights of parameters and points of sub-parameters were obtained from the study by Akıncı et al (2013) completed in Artvin's Yusufeli district. After the weights of parameters and the points of sub-parameters were assigned to the related layer, the raster maps of nine parameters were overlaid using both weighted sum and overlay analysis and land suitability maps of agricultural land use were created. Changing between 0.24 and 8.974, the suitability index for agricultural land use was classified into five classes according to the land suitability classification of FAO (1976) using classification method of natural breaks (Figure 2).

Finally, the suitability map for agricultural land use in the study area was generated by subtracting areas of forest, rangeland and dam reservoirs from the re-classified suitability map (Figure 3).

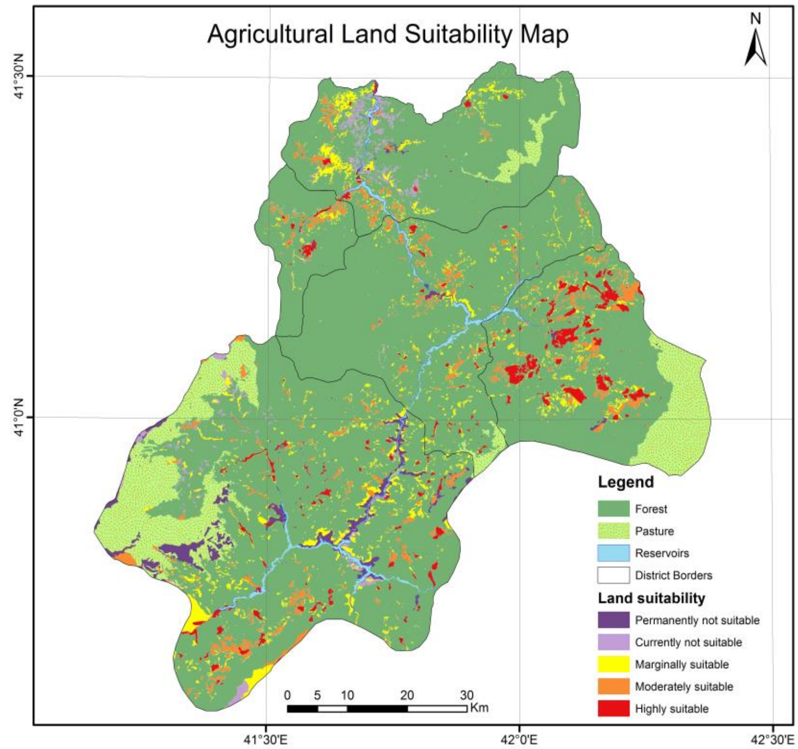

Figure 3. Suitability map obtained after removing pasture, forest lands and reservoirs

RESULT AND DISCUSSION

Considering the agricultural land use suitability map produced (Figure 3) and the data of Table 2, it was determined that the rate of the land permanently not suitable for agriculture was 11.41% (63659.62 ha); that the rate of the land currently not being suitable for agriculture was 18.14% (101210.63 ha); that the rate of the land marginally suitable for agriculture was 47.85% (266890.49 ha); that the rate of the land moderately suitable for agriculture was 17.42% (97174.62 ha); and that the rate of the land highly suitable for agriculture was 5.18% (28883.53 ha) (Table 2).

9.95% (55504.72 ha) of the study area is covered with pasture and 75.67% (422099.27 ha) of it is covered with land having forest (Table 2). 90.03% (240287.02 ha) of the lands that is marginally suitable for agricultural use, 79.8% (77548.88 ha) of the lands that is moderately suitable for agricultural use and 54.91% (15861.18 ha) of the lands that is highly suitable for agricultural use coincide with forest and pasture lands.

These lands were excluded from the suitability map as agricultural activities cannot be conducted on forest and pasture lands in accordance with the statutory legislation in force in Turkey.

Table 2. The distribution of agricultural land suitability analysis results based on area and percentage

Suitability degree	Total area classified by the suitability analysis		Areas to be inundated by the reservoirs (ha)	Area within forestlands (ha)	Area within pasturelands (ha)	Suitable for agricultural production	
	(ha)	(%)				(ha)	(%)
Permanently not suitable	63659,92	11,41	3406,55	33859,80	16504,05	9889,52	1,77
Currently not suitable	101210,63	18,14	296,12	89450,71	4092,35	7371,45	1,32
Marginally suitable	266890,49	47,85	2613,48	238485,26	1801,76	23989,99	4,30
Moderately suitable	97174,62	17,42	492,90	52900,85	24648,03	19132,84	3,43
Highly suitable	28883,53	5,18	1419,10	7402,65	8458,53	11603,25	2,08
Total	557819,19	100	8228,15	422099,27	55504,72	71987,06	12,90

The total size of the reservoir areas of the dams constructed on Çoruh River is 8228.15 ha. Considering the reservoir areas, it was calculated that a total part of 1912 ha of the lands being suitable for agriculture with moderate and high level was going to be submerged in to the water of 5 large dams (Table 2). The similar results were achieved also during the study of Yildirimer (2013). Yildirimer (2013) indicated that according to the forest management plans, the agricultural land of 159 ha was going to be submerged into Muratli Dam, the agricultural land of 167 ha into Borçka Dam, the agricultural land of 469 ha into Deriner Dam, the agricultural land of 60 ha into Artvin Dam and the agricultural land of 1104 ha into Yusufeli Dam (a total agricultural land of 1959 ha). During the study conducted by Toker (2010), the sizes of the agricultural lands submerged into the reservoir areas of Muratli, Borçka and Deriner Dams were determined. Accordingly, it was indicated that the agricultural land of 824 ha in total was submerged into the water of these three dams. Likewise, considering the expropriation data, it was calculated that 3800 parcels were expropriated due to Artvin Dam and that the agricultural land of 83 ha was submerged into the water of Artvin Dam. As the expropriation process of Yusufeli Dam continues, the data could not be obtained related to the expropriated agricultural lands due to this dam.

In conclusion, when the pasture, forest and reservoir areas were excluded from the land of 126058.15 ha that was particularly determined as suitable for agriculture with moderate and high level, it was determined that only an area of 30736.09 ha could be used for agricultural purpose. The low rate of highly suitable agricultural land found in this study can be associated with the factors of the severe slope, the high erosion degrees and the shallow soil depth of the research. Similarly, a study conducted in Ispir, Erzurum (Turkey) to assess the suitability of agricultural lands has also resulted in low rate (0.9%) of highly suitable agricultural lands (Demir et al., 2011) and the authors related these outcomes to the high average slope rate in the region of Ispir, limiting potential areas suitable for agriculture practices. Moreover, in a research completed in Darjeeling district of India, it was determined that only 5.31% of the study area was highly suitable for agricultural production, mostly due to the facts that the majority of the land use type was forest (with 65%) besides the high slope degrees of the district (Pramanik, 2016).

CONCLUSION

In this study aiming to determine the alternative lands suitable for agriculture on the scale of Borçka, Murgul, Central, Ardanuç and Yusufeli districts of Artvin; GIS and AHP method, being one of the multi-criteria decision making analysis methods, were utilized. The study was realized by using 9 criteria reflecting the topographic characteristics and the soil structure of the area. As a result of the evaluation, it was determined that 9.8% of the study area is suitable for agricultural production. In addition, considering the forest and pasture areas within the borders of the study area and the areas within the reservoir areas of the dams, it was determined that about 85% of the lands being suitable for agricultural production coincides with these areas and accordingly that they could not be used for agricultural purpose.

It was determined that there were two main reasons for the fact that the rate of land being suitable for agriculture was such low. The main and the most influential reason is that the majority of the lands determined as being suitable for agriculture in the study area coincides with the current forest and pasture areas. The forest and pasture legislation in force in Turkey does not allow the forest and pasture areas to be used for any other purpose, including agricultural production, in order to protect these areas. Therefore, these areas corresponding to about 85% of the study area were excluded from the evaluation. The second reason is the problems arising from the geomorphologic characteristics of the study area. Corresponding to the dominant great soil group in the study area, the brown forest soil does not have any inconvenience in terms of plant production other than its slight acidic characteristics. However, the problems arising from the geomorphologic situation of the area such as high slope degree had negative impacts on the erosion severity, the rate of bare rock areas, the soil depth and the land use capability classification. All of these inconveniences caused a low rate of land, on the study area, where plant production could be performed.

REFERENCES

Akbulak, C., 2010, "Analitik Hiyerarşi Süreci ve Coğrafi Bilgi Sistemleri ile Yukarı Kara Menderes Havzası'nın Arazi Kullanımı Uygunluk Analizi", *Uluslararası İnsan Bilimleri Dergisi*, Vol. 7(2), pp. 557-576.

Akıncı, H., Yavuz Özalp, A., Turgut, B., 2013, "Agricultural Land Use Suitability Analysis Using GIS and AHP Technique", *Computer and Electronics in Agriculture*, Vol. 97 (2013), pp. 71-82.

Akten, M., Yılmaz, O., Gül, A., 2009, "Alan Kullanım Planlamasında Rekreasyonel Alan Kullanım Ölçütlerinin Belirlenmesi: Isparta Ovası Örneği", *Süleyman Demirel Üniversitesi Orman Fakültesi Dergisi*, Vol. 2 (2009), pp. 119-133.

Al-Shalabi, M.A., Mansor, S.B., Ahmed, N.B., Shiriff, R., "GIS Based Multicriteria Approaches to Housing Site Suitability Assessment", *XXIII FIG Congress*, 8-13 October 2006, Germany.

Amiri, F., Shariff, A.R.B.M., 2012, "Application of Geographic Information Systems in Landuse Suitability Evaluation for Beekeeping: A Case Study of Vahregan Watershed (Iran)", *African Journal of Agricultural Research*, Vol. 7(1), pp. 89-97.

Atalay, İ., 2006, *Toprak Oluşumu, Sınıflandırılması ve Coğrafyası*, Meta Basım Matbaacılık, İzmir.

Bandyopadhyay, S., Jaiswal, R.K., Hegde, V.S., Jayaraman, V., 2009, "Assessment of Land Suitability Potentials for Agriculture Using A Remote Sensing and GIS Based Approach", *International Journal of Remote Sensing*, Vol. 30(4), pp. 879-895.

Bozdağ, A., Yavuz, F., Günay, A.S., 2016, "AHP and GIS Based Land Suitability Analysis for Cihanbeyli (Turkey) County", *Environmental Earth Sciences*, (2016) 75:813, DOI 10.1007/s12665-016-5558-9.

Demir, M., Demircioglu Yıldız, N., Bulut, Y., Yılmaz, S., Özer, S., 2011, "Alan Kullanım Planlamasında Potansiyel Tarım Alanlarının Ölçütlerinin Coğrafi Bilgi Sistemleri (CBS) Yöntemi ile Belirlenmesi (Ispir Örneği)", *Iğdır Üniversitesi Fen Bilimleri Enstitüsü Dergisi*, Vol. 1 (3), pp. 77–86.

Duc, T.T., 2006, "Using GIS and AHP Technique for Land-use Suitability Analysis", *International Symposium on Geoinformatics for Spatial Infrastructure Development in Earth and Allied Sciences (GIS-IDEAS 2006)*, 9-11 November 2006, Ho Chi Minh City, Vietnam.

FAO, 1976, *A Framework for Land Evaluation, Soils Bulletin 32*, FAO and Agriculture Organization of the United Nations, Rome.

Feizizadeh, B., Blaschke, T., 2013, "Land Suitability Analysis for Tabriz County, Iran: A Multi-Criteria Evaluation Approach Using GIS", *Journal of Environmental Planning and Management*, Vol. 56(1), pp. 1-23.

Fu, Z., Li, Z., Zai, C., Shi, Z., Xu, Q., Wang, X., 2011, "Soil Thickness Effect on Hydrological and Erosion Characteristics Under Sloping Lands: A Hydropedological Perspective", *Geoderma*, Vol. 167, pp. 41-53.

Gessler, P.E., Chadwick, O.A., Chamran, F., Althouse, L., Holmes, K., 2000, "Modeling Soil-landscape and Ecosystem Properties Using Terrain Attributes", *Soil Science Society of America Journal*, Vol. 64, pp. 2046–2056.

Kavas, E., 2009, "Analitik Hiyerarşik Süreç Yöntemiyle İzmir İlinde Heyelan Duyarlılığının Coğrafi Bilgi Sistemleri Tabanlı İncelenmesi", *TMMOB Coğrafi Bilgi Sistemleri Kongresi (CBS2009)*, 02-06 Kasım 2009, İzmir.

Koulouri, M., Giourga, C., 2007, "Land Abandonment and Slope Gradient as Key Factors of Soil Erosion in Mediterranean Terraced Lands", *Catena*, Vol. 69(3), pp. 274–281.

Lobo, D., Lozano, Z., Delgado, F., 2005, "Water Erosion Risk Assessment and Impact on Productivity of A Venezuelan Soil", *Catena*, Vol. 64(2-3), pp. 297–306.

Malczewski, J., 1999, *GIS and Multicriteria Decision Analysis*, John Wiley and Sons, New York.

Mishra, A.K., Deep, S., Choudhary, A., 2015, "Identification Of Suitable Sites for Organic Farming Using AHP & GIS", *The Egyptian Journal of Remote Sensing and Space Sciences,* Vol. 18, pp. 181–193.

Mokarram, M., Aminzadeh, F., 2010, "GIS-based Multicriteria Land Suitability Evaluation Using Ordered Weight Averaging with Fuzzy Quantifier: A Case Study in Shavur Plain, Iran", *The International Archives of the Photogrammetry, Remote Sensing and Spatial Information Sciences*, Vol. 38(II), pp. 508-512.

Mustafa, A.A., Singh, M., Sahoo, R.N., Ahmed, N., Khanna, M., Sarangi, A., Mishra, A.K., 2011, "Land Suitability Analysis For Different Crops: A Multi Criteria Decision Making Approach Using Remote Sensing and GIS", *Researcher,* Vol. 3(12), pp. 61-84.

Öztürk, D., Batuk, F., 2007, "Çok Sayıda Kriter ile Karar Vermede Kriter Ağırlıkları", *Yıldız Teknik Üniversitesi Sigma Mühendislik ve Fen Bilimleri Dergisi*, Vol. 25(1), pp. 86-98.

Öztürk, D., Batuk, F., 2010, "Konumsal Karar Problemlerinde Analitik Hiyerarşi Yönteminin Kullanılması", *Yıldız Teknik Üniversitesi Sigma Mühendislik ve Fen Bilimleri Dergisi*, Vol. 28, pp. 124-137.

Parakash, T.N., 2003, *Land Suitability Analysis for Agricultural Crops: A Fuzzy Multicriteria Decision Making Approach*, Msc Thesis, The International Institute for Geo-information Science and Earth Observation (ITC), Enschede, The Netherlands.

Perveen, M.F., Nagasawa, R., Uddin, M.I., Delowar, H.K.M., 2007, "Crop-Land Suitability Analysis Using A Multicriteria Evaluation & GIS Approach", *5th International Symposium on Digital Earth (ISDE5)*, 5-9 June 2007, University of California, Berkeley, USA.

Pramanik, M.K., 2016, "Site Suitability Analysis for Agricultural Land Use of Darjeeling District Using AHP and GIS techniques", *Modeling Earth Systems and Environment,* Vol. 2(2), pp. 1-22, DOI 10.1007/s40808-016-0116-8.

Romeijn, H., Faggian, R., Diogo, V., Sposito, V., 2016, "Evaluation of Deterministic and Complex Analytical Hierarchy Process Methods for Agricultural Land Suitability Analysis in a Changing Climate", *ISPRS International Journal of Geo-Information*, Vol. 5(6), 99; doi:10.3390/ijgi5060099.

Saaty, T.L., 1980, *The Analytic Hierarchy Process: Planning, Priority Setting, Resource Allocation*, McGraw-Hill International, New York, NY, U.S.A.

Saaty, T.L., 1990, "An Exposition of the AHP in Reply to The Paper 'remarks on The Analytic Hierarchy Process", *Management Science,* Vol. 36, pp. 259-268.

Saaty, T.L., 2004, "Mathematical Methods of Operations Research", Dover Publications, Mineola, 415–447.

Toker, E., 2010, *Borçka ve Deriner Barajlarının Çoruh Havzasında Neden Olduğu Arazi Kullanım Değişiminin ve Arazi Tahribatının İrdelenmesi*, Msc Thesis, Artvin Çoruh Üniversitesi Fen Bilimleri Enstitüsü, Orman Mühendisliği Anabilim Dalı, Artvin.

Tombuş, F.E., 2005, *Uzaktan Algılama ve Coğrafi Bilgi Sistemleri Kullanılarak Erozyon Risk Belirlemesine Yeni Bir Yaklaşım, Çorum İli Örneği*, Msc Thesis, Anadolu Üniversitesi, Fen Bilimleri Enstitüsü, Uzaktan Algılama ve Coğrafi Bilgi Sistemleri Anabilim Dalı, Eskişehir.

Yavuz Özalp, A., Akıncı, H., Temuçin Kılıçer, S., 2013, "Artvin Ili Arazisinin Topografik ve Bazı Fiziksel Özelliklerinin Tespiti ve Bu Özelliklerin Arazi Örtüsü Ile Ilişkisinin Incelenmesi", *Artvin Çoruh Üniversitesi Orman Fakültesi Dergisi*, Vol. 14, pp. 292-309.

Yalew, S.G., van Griensven, A., Mul, M.L., van der Zaag, P., 2016, "Land Suitability Analysis for Agriculture in The Abbay Basin Using Remote Sensing, GIS and AHP Techniques", *Modeling Earth Systems and Environment*, Vol. 2(2) 2:101, DOI 10.1007/s40808-016-0167-x.

Yıldırımer, S., 2013, *Çoruh Nehri Üzerinde Tamamlanan, İnşası Devam Eden ve Planlanan Büyük Barajların Neden Olduğu ve Olacağı Arazi Kullanım Değişimlerinin Belirlenmesi*, Msc Thesis, Artvin Çoruh Üniversitesi Fen Bilimleri Enstitüsü, Orman Mühendisliği Anabilim Dalı, Artvin.

Zengin, M., Yılmaz, S., 2008, "Ardahan Kura Nehri Ve Yakın Çevresi Alan Kullanımlarının Belirlenmesi ve Optimal Alan Kullanım Önerileri", *Atatürk Üniversitesi Ziraat Fakültesi Dergisi*, Vol. 39(1), pp. 43-54.

SUJEST, c.5, s.1, 2017
SUJEST, v.5, n.1, 2017
ISSN: 2147-9364 (Electronic)

REAL ESTATE VALUATION IN URBAN REGENERATION APPLICATION; CASE STUDY OF KONYA

[1]Sukran YALPIR, [2]Eda BAYRAK

[1,2] *Selcuk University, Department of Geomatics Engineering, Campus, Selcuklu, Konya, TURKEY*
sarici@selcuk.edu.tr, [2] edabayrak006@hotmail.com

(Geliş/Received: 07.11.2016; Kabul/Accepted in Revised Form: 29.01.2017)

ABSTRACT: The land valuation is a field that must be done with scientific, right and independent perspective. The land valuation is not only in the estimation of marketing value, additionally it finds usage areas like mortgaged sales, expropriation, urban renewal etc.

This study is about the expropriation and how the land valuation must be done in this area. In this study, the application area was chosen as the premises of the expropriation in the district of Uluirmak in Meram, KONYA, and the valuation before the application was done with the Cobb - Douglas Hybrid regression method. Twenty three criterion's that belong to the number of 1078 constructed and unconstructed premises were utilized. In consequence of the nonlinear regression modeling it succeeded about 98%. The land valuation does not only depend on the area index, it can be done in a short time while a lot of criterion's are considered, by this way the proprietors are able to get their rights with this developed mathematical model.

Key Words: *Real estate valuation, Urban regeneration, Regression, Cobb-Douglas.*

Kentsel Dönüşüm Uygulamalarında Taşınmaz Değerleme; Konya Örneği

ÖZ: Taşınmaz değerlemesi bilimsel, doğru ve bağımsız olarak yapılması gereken bir alandır. Taşınmaz değerleme sadece piyasa değerini tahmin etmede değil ipotekli satışlarda, kamulaştırmada, imar uygulamalarında, kentsel dönüşüm ve birçok konuda kullanım alanı bulunmaktadır.

Bu çalışmada, kentsel dönüşüm ve kentsel dönüşüm alanında yapılan taşınmaz değerlemenin nasıl olması gerektiği konusundadır. Çalışmada uygulama alanı olarak seçilen Konya ili Meram ilçesinde bulunan Uluırmak mahallesindeki kentsel dönüşüm uygulamasındaki taşınmazların, uygulama öncesi değerlemesi Cobb Douglass hibrit regresyon yöntemi ile yapılmıştır. Çalışma alanında 1078 adet yapılı ve yapısız taşınmaza ait 23 kriter kullanılmıştır. 23 kriterin 17 tanesi arsaya 6 tanesi yapıya ait özellikleri içermektedir. Nonlineer regresyon modellemesi sonucunda yaklaşık %98 başarı elde edilmiştir. Taşınmazların, sadece taşınmaz alan endeksli değil çok sayıda kriter göz önünde bulundurarak kısa sürede yapılabileceği ve mülk sahiplerinin haklarının eşit olarak verilebileceği geliştirilen matematiksel model ile ortaya konmaya çalışılmıştır.

Anahtar Kelimeler: *Taşınmaz değerleme, Kentsel dönüşüm, Regresyon, Cobb-Douglas*

Note: This paper has been presented at the Selcuk International Scientific Conference on Applied Sciences (ISCAS 2016) held in Antalya (Turkey), September 27-30, 2016.

DOI: 10.15317/Scitech.2017.73

INTRODUCTION

Urban renewal involves a partial or total renewal of a city through suitable projects and strategic plans that provide options for solving urban problems and seek for permanent solutions for physical, social and environmental problems in a specific area. Urban renewal aims to create sustainable, habitable, healthy and contemporary cities (Ucar, 2009). Urban renewal works involve highly critical phases such as identification of the renewal site appraisal of the value of a real estate based on its prior and subsequent condition. In order to avoid doing injustice to the property owners, it is essential that the real estates be appraised as per their original and new conditions. Today, this is done by municipalities based on their own arrangements. Previous urban renewal works mostly involved comparative appraisal efforts based on the locations of the real estates. Today, the significance of this particular aspect has come to be appreciated and the municipalities spend more efforts for bringing about arrangements to tackle this complicated issue.

The determination of real-estate value is today’s one of the most popular labor branch. The factors like the difficulty in finding real-estate similar to the considered estate, having many factors affecting the value, variability due to local regions and preferences and the difficulty in defining the situation with common mathematical equations necessitate the new searches for the determination of values. Nowadays, reconstruction and urban renewal works require fair, accurate and quick real estate valuation just as the case in the more commonly known practices such as sale, purchase, taxation and expropriation. Owing to the fact that there are vast number of factors that determine the value of the real estates and that mass appraisal have to be valued all at the same time, traditional valuation methods may not be fit to be applied in the case of such applications. For this reason, a mathematical model should be developed to be used in the valuation of mass appraisal.

Multiple regression analysis that is frequently found in the literature is regarded as a valid and widely accepted method (Yalpir et al., 2002; Rossini, 1998; Stephen et al., 2010). It is calculated based on purchase and sale values and involves a number of real estate values, the accuracy of the method is further improved. Despite practical hardships, it is nevertheless a preferable method in terms of its close approximation to the purchase and sale values. Regression analysis for real estates can be described as a statistical technique that allows a real estate to be evaluated with the relevant characteristics in order to identify the significant determinants of the real estate value and the numbers thereof.

In the absence of linearity between independent variables and dependent variables, nonlinear regression method –being a stochastic method- can be applied. In the multiple regression model, there is a number of independent variables that affect the dependent variable and the general purpose for such studies is twofold:

1. Find out which independent variable/variables affect the dependent variable the most.
2. Estimate the value of the dependent variable through the variables that are known to affect the dependent variable. The purpose of the study may be to find one or both of them (Alpar, 1997).

With respect to the both purposes, regression method can be regarded as the right method for real estate valuation. However, due to the fact that there is a wide variety of real estate available, the method is required to be modeled separately based on the type of the property. Whereas, valuation of both land and buildings can be performed at the same time through Cobb-Douglas hybrid modeling without necessarily relying on separate modeling for property type (Ozkan and Yalpir., 2005).

The implementation area for this study is Uluirmak District in Meram county, Konya province, which is one of the urban renewal areas. This study employs a regression analysis called Cobb-Douglas Hybrid method instead of traditional methods. A data set, consisting of 23 criteria, -17 for land, 6 for buildings- was established for the study area, which is composed of 1078 real estates with and without buildings on them, and the values obtained through the model thus established were compared with the existing values.

REGRESSION ANALYSIS

Regression analysis involves expressing the relationship between a variable with one or more than variable through a mathematical function. Depending on the type of mathematical functions it is divided into two methods, namely:

- Linear regression method
- Non linear regression method (Orhunbilge, 2002).

While linear models are estimated to be impartial, normally distributed and with minimum variance, non linear regression models mostly apply when the sample size is fairly big (Kutner et al., 1996).

Linear regression studies can be commonly encountered in most real estate valuation studies in the literature (Din, et al., 2001; Isakson, 2001). It is well known that there are many factors affecting the valuation of real-estates each of which has different effect on the value. The value estimation considering many criteria can be made with multi-regression methods. In the real estate market, the values pertaining to the items being sold and purchased (dependent variables) and the criteria that affect the property value (independent variables) are summed up and subjected to a mathematical model that is capable of making value estimations using multiple regression method.

In the linear regression model, the dependent variable is assumed to be a linear function of one or more independent variables plus an error introduced to account for all other factors (Equation 1):

$$y_i = \beta_0 + \beta_1 x_{i1} + \beta_2 x_{i2} \ldots\ldots \beta_k x_{ik} + u_i \qquad (1)$$

In the above *regression equation,*

y_i : the *dependent variable, (the value of the real-estate),*

$x_{i1}, \ldots, x_{iK}$: the *independent or explanatory variables, (number of room, age, etc.)* and

u_i : the *disturbance* or *error term.* The goal of the regression analysis is to obtain the estimations of the unknown parameters.

$\beta_1, \ldots, \beta_k$ indicates how a change in one of the independent variables affects the values taken by the dependent variable.

Non linear regression models can also be demonstrated in a simple form like linear models (Equation 2):

$$y_i = f(x_i, \gamma) + \varepsilon_i \qquad (2)$$

In non linear regression models, the number of regression parameters is not directly correlated with the number of explanatory variables therein. The γ in equation 2 is the non-correlated error term for the unknown parameters in the form of n $p\times1$ vector, ε , $E(e) = 0$ and $Var(e) = \sigma2$; $f(x_i, \gamma)$, on the other hand, is described as the expectation function for the non linear regression model (Ratkowsky, 1983).

Cobb-Douglas Hybrid Modeling

Regression method is more commonly found in the product market than nonlinear mathematical models. The Cobb-Douglas hybrid modeling has been developed based on the linear and non-linear models in the appraisal of real estate values. This model is called the hybrid model as it incorporates the elements from both linear and non-linear models. Since this model can be used in the appraisal of real estates with or without a building, it allows one to identify the value of the land in the absence of a building. As shown in the example below, the first part of the model –the one with the A variable-demonstrates the land characteristics, while the other part -the one with the Y variable- reveals the building characteristics.

$$Pi = \beta_0 A_{1,i}{}^{\beta 1} A_{2,i}{}^{\beta 2} A_{3,i}{}^{\beta 3} \ldots + \theta_0 Y_{1,i}{}^{\theta 1} Y_{2,i}{}^{\theta 2} Y_{3,i}{}^{\theta 3} \ldots \quad (3)$$

$A_{j,i}$: Land characteristics (the study includes a total of 17 variables) (17 criteria in the study)

$Y_{j,i}$: Building characteristics (the study includes a total of 6 variables) (6 criteria in the study)

$B_{0,(i-1)}$ and $\theta_{0,\ (i-1)}$ denote the fixed parameters pertaining to the land and building (McCain et all, 2003; Rossini and Kershaw, 2005).

APPLICATION

Study Area

It comprises the urban renewal area that is being developed around Uluirmak Distrcit and its vicinity in Meram county, Konya province. According to the data obtained from the Urban Renewal Department of Meram Municipality, the study area contains a total of 1078 real estates, 372 of which have no buildings on them (land) and 706 have construction on them. A total of 23 criteria have been established with respect to the said real estates, 17 of which are concerning to the land and 6 to the buildings and facilities erected on them. The real estates with construction include domiciles with and without garden, detached properties, apartment blocks, reinforced concrete buildings, adobe houses and warehouses. In terms of ownership, however, 666 of them belong to private persons, 2 to associations, 1 to public, 2 to Konya Metropolitan Municipality, 15 to Meram Municipality, 8 to corporations and 8 to foundations. While the total surface area of the project is 266.843 m², the cadastre project area, including current derelicts areas, is 232.990 m². The project was allocated an area of 20.760 m² for developing schools, squares, social facilities, green areas, car parks etc. The illustrative value set in the project for the urban renewal site is 1,80 rate. The implementation plan for the area is presented in Figure 1.

Figure 1. The map of implementation plan for Uluirmak area

Quantification of the data and normalization procedure

The data set obtained from Meram Municipality is arranged in the form of columns allocated to lands and buildings by using Excel. Since the data we had composed of both digital and verbal contents, a scoring procedure was conducted to convert the verbal data into the digital form. The study conducted by Yomralioglu (1997) was used while scoring each criterion separately in itself. Scoring procedure was conducted solely for the purposes of converting the verbal data into the digital one. The digital values contained in the data set were maintained.

Due to the differences observed between the units and value gaps in each criterion, it became necessary to conduct a normalization procedure following the arrangement of the data set. A normalization procedure was conducted for the values contained in each criterion within the value gap ranging from min to max. The Equation 4 was employed for the said criteria by setting the maximum value at 2 and minimum value at 1.

$$Xnorm = (Xi - Xmin)/(Xmax-Xmin) + 1 \quad (4)$$

RESULTS

The nonlinear regression model (Equation 3) was applied to the arranged and normalized data set by using the SPSS 15 software package, as a result of which the values of the fixed variables were found as presented in the Table 1. The conformity of the mathematical model thus created was tested with the aforementioned software package. To this end, 23 criteria found through the normalization procedure and the values of 1078 real estates, as of 2015, were input to the program and the relationship between the data was studied in the program using a correlation method.

Of such coefficients, the ones specified as 'β' were concerned with the characteristics associated with lands, while the ones specified as 'θ' were concerned with the characteristics associated with buildings. It was established that the criteria that affected the value of the land the most were β_{12} (Allotment area), β_{17} (Partnership arrangement to share the flooded areas) and β_{11} (Parcel multiplier coefficient), while the ones that affected it the least were β_4 (Construction license status) and β_5 (Area of use license status). As for the characteristics associated with buildings, the criteria that affected the value the most were θ_1 (The gross building area) and θ_6 (Floors condition of real estate), the one that affected the least was θ_3 (Outbuildings area) type. While the criteria of θ_4 (Garden wall length) and θ_5 (Number of trees) had an equal effect on the value (Table 1).

According to this model, the number of characteristics associated with the buildings and other inventories erected on the land are more than the effects of the criteria associated with the land. The Cobb-Douglas Hybrid regression model established for the purposes of this study was found to be highly successful. The results of the model are presented in the Table 2.

According to the Table 2; R^2 = 1-(Residual Sum of Squares)/ (Corrected Sum of Squares) = 0,941. By applying the model created through the coefficients obtained from the SPSS program to the data set, we have identified the model values for the real estates covered within the scope of the urban renewal study. Following the modeling obtained through the real estates in the data set, (estimated values) were compared. As a result of this comparison, the absolute error was found as 2,05%.

Table 1. Cobb-Douglas Hybrid regression coefficients

Criteria	Parameters of the criteria	Estimate Lower Bound	Criteria	Parameters of criteria	Estimate Lower Bound
Constant	β_0	0,320	Total abandonment	β_{13}	0,070
Location	β_1	-0,270	Total area of parcels	β_{14}	-0,158
Parcel type	β_2	-0,045	Excluding commercial space	β_{15}	-0,073
Land status	β_3	-0,185	Share falling area	β_{16}	-0,041
Construction license status	β_4	-0,025	Partnership arrangement to share the flooded areas	β_{17}	0,772
Area of use license status	β_5	-0,029	Constant	θ_0	0,660
Causing to settle in	β_6	0,163	The gross building area	θ_1	0,306
Marketing authorization	β_7	0,233	Common area of use	θ_2	0,124
Type of soil	β_8	-0,046	Outbuildings of area	θ_3	0,020
Independent part total	β_9	-0,737	Garden wall length	θ_4	0,052
Independent part quality	β_{10}	-0,254	Number of trees	θ_5	0,052
Parcel multiplier factor	β_{11}	0,767	Floors condition of real	θ_6	0,229
Allotment area	β_{12}	1,515			

Table 2. Results obtained for the Cobb-Douglas Hybrid model

Source	Sum of Squares	df	Mean Squares
Regression	1447,221	25	57,889
Residual	1,090	1052	0,001
Uncorrected Total	1448,311	1077	
Corrected Total	18,392	1076	

The R^2 and linear equations obtained as per the trend line which was established based on the real estate values found through the nonlinear regression model as well as the distribution and scattering of the values in the data set- were studied (Figure 2). The proximity of the R^2 point distributions obtained as a result of the graphical distribution- to the line is that of the specified value. Success increases as it comes near the point 1. If the model results are found to be 100% and as the line will be established as y=x in the equation, the success of the study will increase when the coefficient of x is 1 or thereabouts. The fact that, as a result of the study, the R^2 and equation have been established as 0,9986 and y=0,9369x respectively suggests that Cobb-Douglas Hybrid model is a successful and usable model for value estimations as shown in the case of the present urban renewal study.

CONCLUSIONS

Performance of sample urban renewal matching based on only the area related criteria in the previous urban renewal studies resulted in a number of unjust and unfair implementations. That approach led to financial grievances on the part of the citizens and devaluation of the properties by losing sight of the characteristics that actually affect the value of real estate. In order to eliminate such injustice, it is essential that the legal and physical characteristics of each real estate are determined and the valuation is done based on such characteristics and that the calculated value is matched with real estate to present after urban renewal project. For this reason, the urban renewal area located at Uluirmak District in Meram/Konya county was calculated in terms of real estate values using Cobb-Douglas Hybrid model and the success of the mentioned model was examined. As a result of the study, the model was found to be highly successful at the point of accurate value estimation.

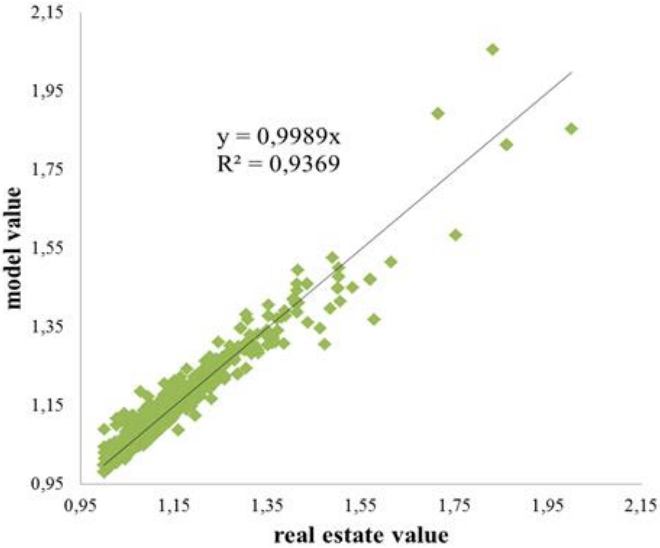

Figure 2. Comparing Cobb-Douglas Hybrid model with model and market values

Time is of the essence in urban renewal projects. It becomes more and more difficult and time consuming to appraise the value of the real estates as the number of characteristics associated with them increase. For this reason, increasing the number of criteria is no longer a preferred method in value appraisal. The model developed in this study is highly beneficial in terms of time and cost saving. By using this method, it is anticipated that the real values of real estates can be established in a short space of time and an equal valuation. So it can be maintained through fixed points of the criteria that apply to everybody. This way, the more characteristics of real estate has the more accurate and easier to determine its value. Through this study, unobjective real estate valuation will be avoided, and the one sided view and opinion of the real estate appraiser will be eliminated.

Moreover, the fact that the land and buildings are available at the same time will not make any difference in the model in terms of establishing the values of the land and the buildings and other inventories thereon on a separate basis nor will it require a remodeling. The model will be able to use in both circumstances. The model thus created will also be efficient in terms of identifying the criteria that are not compulsory to be addressed.

ACKNOWLEDGEMENT

We appreciate the support of Meram Municipality for this study. This publication was presented as oral presentation in ISCAS-2016 Antalya/TURKEY.

REFERENCES

Alpar, R., 1997, *Uygulamalı Çok Değişkenli İstatiksel Yöntemlere Giriş-1*, Kültür Ofset, Ankara.

Din, A., Martin H., Andre B., 2001, "Environmental Variables and Real Estate Prices", *Urban Studies*, Vol. 38(11), pp. 1989–2000.

Isakson, H. R. 2001, "Using Multiple Regression Analysis in Real Estate Appraisal Excerpt from Papers and Proceedings", *Appraisal Journal*, Vol. 69(4), pp 424-430.

Kutner M. H., Neter J., Nachtsheim C.J., Wasserman W., 1996, *Applied Linear Statistical Models*, McGraw Hill.

McCain, R. A., Jensen, P., Meyer, S., 2003, *Research on Valuation of Land and Improvements in Philadelphia*, Department of Economics and International Business, LeBow College of Business Administration, Drexel University, Philadelphia, 1-24.

Orhunbilge, N., 2002, *Applied Regression and Correlation Analysis*, Istanbul University Publication, Istanbul, ISBN, 975-404.

Ozkan, G., Yalpir S., "Taşınmaza Ekonomik Bakış ve Değerlendirmesi", *10. Türkiye Harita Bilimsel ve Teknik Kurultayı*, Ankara, 28 Mart – 1 Nisan 2005.

Ratkowsky, D. A., 1983, *Nonlinear Regression Analysis*, Marcel Decker Inc., New York.

Rossini, P., Kershaw, P., 2005, "Using a Hybrid Automated Valuation Model to Estimate Capital and Site Values" (Doctoral dissertation, Pacific Rim Real Estate Society (online)).

Rossini, P., 1998, "Improving the Results of Artificial Neural Network Models for Residential Valuation", *Fourth Annual Pacific-Rim Real Estate Society Conference*, Perth, Western Australia, 19-21 January 1998.

Stephen M., Lennon C., Winky H., 2010, "Quantile Regression Estimates of Hong Kong Real Estate Prices", *Urban Studies*, Vol. 47(11), pp. 2461–2472.

Ucar, C., 2009, *Kentsel Dönüşümün Uygulama Bölgesi Dinamiklerine ve Taşınmaz Değerine Etkileri,* Master Thesis, Institute of Science and Technology, ITU University, Istanbul.

Yalpir, S., Ozkan, G., Erdi, A., 2002, "Kentsel Alanlarda Taşınmaz Değerlerinin Belirlenmesi ve Konya Örneği", *Selçuk Üniversitesi Jeodezi ve Fotogrametri Mühendisliği 30. Yıl Sempozyumu*, Konya, 16-18 Ekim 2002.

Yomralioglu, T., 1997, *Kentsel Alan Düzenlemelerinde İmar Planı Uygulama Teknikleri*, Jeodezi ve Fotogrametri Derneği (JEFOD) Yayın no:1, Trabzon.